GEMS & GEMOLOGY

SPRING 2015
VOLUME LI

THE QUARTERLY JOURNAL OF THE GEMOLOGICAL INSTITUTE OF AMERICA

Vietnamese Blue Spinel

Chinese Tradition in Modern Jewelry Design

Moroccan Amethyst and Mozambique Ruby

2015 Tucson Gem Shows

GEMS & GEMOLOGY

Spring 2015
VOLUME 51, No. 1


pg. 3


pg. 20


pg. 37


pg. 86

Editorial

Feature Articles

Notes and New Techniques

Field Reports

Regular Features

GEMS & GEMOLOGY

gia.edu/gems-gemology

Subscriptions
Copies of the current issue may be purchased for $29.95 plus shipping. Subscriptions are $79.99 for one year (4 issues) in the U.S. and $99.99 elsewhere. Canadian subscribers should add GST. Discounts are available for group subscriptions, GIA alumni, and current GIA students. To purchase print subscriptions, visit store.gia.edu or contact Customer Service. For institutional rates, contact Customer Service.

Database Coverage
Gems & Gemology's impact factor is 0.778, according to the 2013 Thomson Reuters Journal Citation Reports (issued July 2014). *G&G* is abstracted in Thomson Reuters products (Current Contents: Physical, Chemical & Earth Sciences and Science Citation Index—Expanded, including the Web of Knowledge) and other databases. For a complete list of sources abstracting *G&G*, go to gia.edu/gems-gemology, and click on "Publication Information."

Manuscript Submissions
Gems & Gemology, a peer-reviewed journal, welcomes the submission of articles on all aspects of the field. Please see the Guidelines for Authors at gia.edu/gandg or contact the Managing Editor. Letters on articles published in *G&G* are also welcome. Please note that Field Reports, Lab Notes, and Gem News International entries are not peer-reviewed sections but do undergo technical and editorial review.

Gems & Gemology is published quarterly by the Gemological Institute of America, a nonprofit educational organization for the gem and jewelry industry.

Postmaster: Return undeliverable copies of *Gems & Gemology* to GIA, The Robert Mouawad Campus, 5345 Armada Drive, Carlsbad, CA 92008.

Our Canadian goods and service registration number is 126142892RT.

About the Cover

The lead article in this issue examines the geological and gemological characteristics of blue spinel from Luc Yen, Vietnam. The centerpiece of the 18k yellow gold ring from the Love Doves collection is a 4.95 ct marquise-cut spinel, framed on either side by doves with ruby eyes. Photo by Robert Weldon/GIA, courtesy of Loretta Castoro. The gem-quality blue spinel octahedron associated with olivine in marble matrix was seen at a mine in the Luc Yen district. Photo by Vincent Pardieu/GIA. Composite image by Kevin Schumacher.

Printing is by L+L Printers, Carlsbad, CA.
GIA World Headquarters The Robert Mouawad Campus 5345 Armada Drive Carlsbad, CA 92008 USA

ISSN 0016-626X

Colored Gems, Chinese Jewelry Designers, and Colored Diamond Spectra

Welcome to the first *Gems & Gemology* of 2015!

Spring is always an especially busy time, because our first issue comes hard on the heels of the annual Tucson gem shows. This event always provides an illuminating window into the world of colored gem supply and demand. Indeed, articles in this *G&G* provide a flavor of that worldview, featuring Vietnamese blue spinel, Moroccan amethyst, ruby from Mozambique, and a survey of contemporary Chinese jewelry designs featuring a wealth of colored gemstones.

Our lead article, by French researcher Boris Chauviré and his coauthors, offers geological context and a gemological characterization of the vivid blue spinel from Luc Yen, northern Vietnam, which owes its remarkable color to traces of cobalt.

Next, GIA's Andrew Lucas and Merilee Chapin partner with Chinese coauthors Moqing Lin and Xiaodan Jia to survey the tremendous progress this country's jewelry designers have made in the last decade. Informed by their civilization's rich cultural roots and driven by the power of a rapidly growing domestic consumer market, the artistic prowess of Chinese designers is increasingly evident on the global stage.

"An illuminating window into the world of colored gem supply and demand..."

Our third article, by a joint Moroccan-Italian team headed by lead author Fabrizio Troilo, provides an introduction to amethysts from Boudi, Morocco. Their study outlines the geology, mining, and the internal and external features of this attractive material.

Our fourth paper, by GIA's Dr. Jim Shigley and Dr. Mike Breeding, bucks this issue's colored-gem trend. Their article provides a review of colored diamond spectra, including a foldout chart, which we trust many practicing gemologists will find illuminating.

In addition, we're delighted to present *G&G*'s third field report. GIA authors Merilee Chapin, Vincent Pardieu, and Andrew Lucas report on the geology and mining practices at Mozambique's Montepuez ruby deposit, currently the world's most important commercial source of ruby.

After these five feature articles, you'll find our regular Lab Notes and Gem News sections. This issue contains in-depth coverage of the February 2015 Tucson Gem and Mineral shows, along with reports on the recent Gemstone Industry & Laboratory Conference (GILC) and the GIA-sponsored International Diamond School for natural diamond researchers held late January in Brixen, Italy.

We're also delighted to present the results of the 2014 Dr. Edward J. Gubelin Most Valuable Article Award. Our sincere thanks to everyone who participated—we had an excellent response this year. Please see the results on page 31. Also, please don't forget to take the *G&G* Challenge, our annual multiple-choice quiz!

Finally, as many longtime contributors know, Stuart Overlin has been the editorial backbone of our journal for a number of years. I'm very pleased to announce Stuart's promotion to *G&G*'s managing editor. I'd also like to thank former managing editor Justin Hunter for his contribution. Justin is moving to an important new role at GIA.

We hope you enjoy this edition!

Duncan Pay | Editor-in-Chief | dpay@gia.edu

Blue Spinel from the Luc Yen District of Vietnam

Boris Chauviré, Benjamin Rondeau, Emmanuel Fritsch, Phillipe Ressigeac, and Jean-Luc Devidal

The Luc Yen district of northern Vietnam is a very productive gem province and the leading source of vivid blue spinel. This study characterizes the origin and gemological properties of these spinels, especially the cause of their unusually bright color, which is directly related to their value. Chemical and spectroscopic analyses indicated that the blue color is due to cobalt (Co^{2+}), with some iron contribution. Petrographic examination identified the context of the gem's formation, which appears to be linked to intense metamorphism during successive orogenies. The carbonate platforms in the ancient Paleo-Tethys Ocean were sandwiched and highly deformed during this orogeny, leading to marble and spinel formation. The authors propose that the cobalt (and to a lesser extent the iron) necessary for the blue color were transported by fluids during metamorphism of the sedimentary sequence.

Blue spinels are mined in Sri Lanka, Tanzania, Myanmar, Pakistan, and Vietnam (Shigley and Stockton, 1984; Delaunay, 2008; Pardieu and Hughes, 2008). Vietnam's two major spinel deposits, Luc Yen and Quy Chau, were discovered at the end of the 1980s. The Luc Yen deposits have mostly been mined since the 1990s (Pardieu and Hughes, 2008; Senoble, 2010). This area, known for its gem-quality ruby, red spinel, and sapphire (Webster, 1994; Hauzenberger et al., 2003; Long et al., 2004; Senoble, 2010; Huong et al., 2012), has also been a notable producer of vivid blue spinels since the 2000s (figure 1). Bright, saturated blue gems are very popular, as evidenced by the classic appeal of sapphire and the more recent trend of Paraíba tourmaline and bright blue apatite in the same color range. Therefore, the bright blue color of some spinels has increased the popularity of this gem overall (Delaunay, 2008; Senoble, 2010). In this article, we investigate the gemological characteristics of Vietnamese blue spinels and the geology of the deposits to gain a better understanding of this gem source.

See end of article for About the Authors and Acknowledgments.
Gems & Gemology, Vol. 51, No. 1, pp. 2–17,
http://dx.doi.org/10.5741/GEMS.51.1.2.

LOCATION AND ACCESS

The Luc Yen district is located in the Yen Bai province, in the north of Vietnam. Luc Yen's capital of Yen The (22°6′38.84″ N, 104°45′57.80″ E) is a five- or six-hour drive from Hanoi on a 160 km expanse of good road. All of the district's blue spinel mining sites lie within 20 km of Yen The. Several hours of walking or biking are needed to access these mines.

In Brief

- Over the past two decades, Luc Yen, Vietnam has become a notable source for blue spinel.
- Vietnamese blue spinel may have resulted from the involvement of evaporitic rocks during post-collision metamorphism.
- Cobalt (Co^{2+}) is the main chromophoric element in blue spinel, though iron (Fe^{2+}) is also a factor.

The blue spinel deposits are Bai Gou, May Trung, Bai Son, Bah Linh Mot, Khe Khi, Kuoi Ngan, Khao Ka, Lung Thin, Lung Day, Khin Khang, and Chuong Tran (figure 2). Of these, only May Trung, Bai Son, and Bah Linh Mot are primary deposits; the others are secondary placer deposits. Bai Son, reported by Senoble

Figure 1. The Luc Yen district of Vietnam has become a major source of top-quality blue spinel, including these two rough crystals (45 and 70 ct) and the 5 ct faceted stone. Photo by J.B Senoble; © Senoble & Bryl.

(2010), was no longer being mined as a primary deposit during our visit in February and March 2012. May Trung is divided into two sites located about 150 meters from each other: a marble cliff that is mined for red and lavender spinels, and a second site that is mined for blue spinel from a vein in marble.

GEOLOGY

The rich tectonic history of Southeast Asia is inherited from several deformation episodes related to the closure of the Paleo-Tethys Ocean and, later, to the Himalayan orogeny. The geology of northern Vietnam is dominated by metamorphic rocks inherited from these two major orogenic events. The first one, the Indosinian orogeny, led to the collision of the main shields (Yangtze and Indochina) during the Permo-Triassic at about 240–245 Ma (Kušnír, 2000; Lepvrier et al., 2008; Huong et al., 2012). In the later orogeny, the Himalayan collision during the Tertiary period, the terrains were strongly reworked. These terrains are primarily composed of metamorphic rocks, mainly medium-grade mica schist, marble, and granulitic gneisses (Kušnír, 2000; Leloup et al., 2001; Hauzenberger et al., 2003).

Northern Vietnam has been studied extensively to understand how a continental collision (in this case, between India and Eurasia) induced crustal wedges to extrude laterally into the surrounding

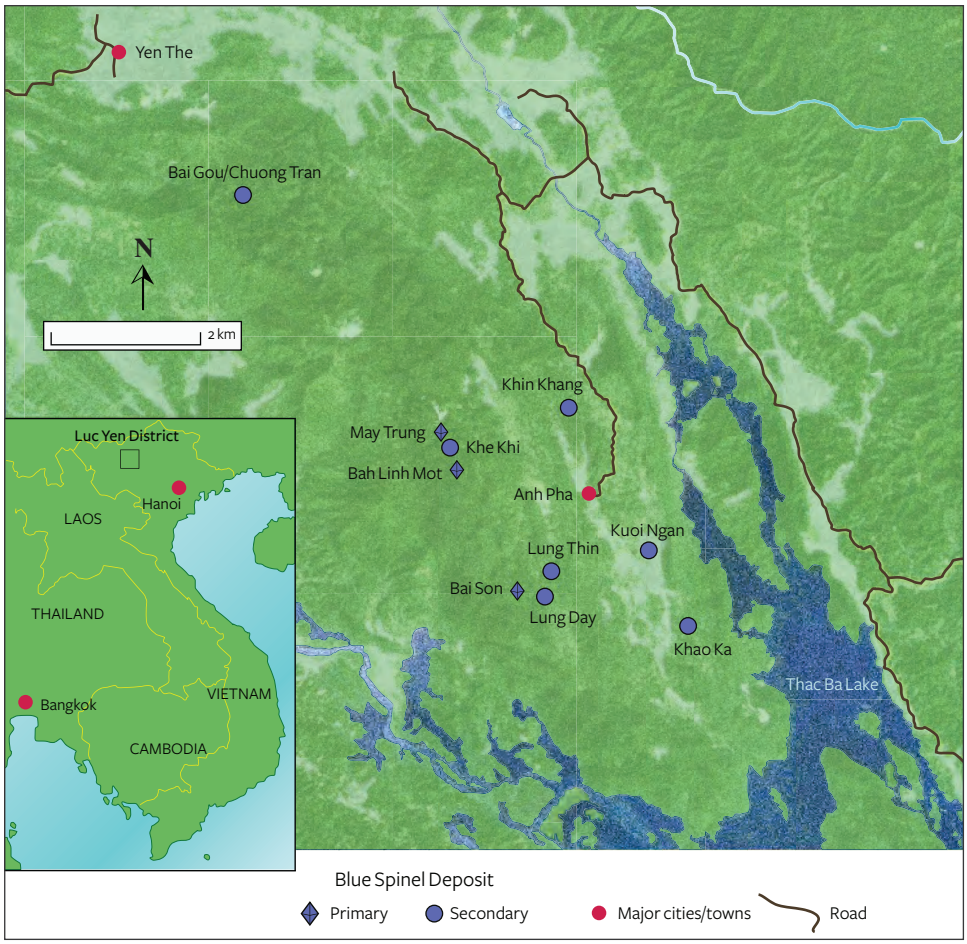

Figure 2. Most Vietnamese blue spinel deposits are confined to a 30 km² area in the Luc Yen district of northern Vietnam. The circles represent placer deposits, while diamonds indicate primary deposits in marble.

plates. (Tapponnier et al., 1982, 1990; Leloup et al., 1995, 2001; Jolivet et al., 2001; Anckiewicz et al., 2007). During the Oligo-Miocene (from 35 to 17 Ma), the Indo-Eurasian collision induced strong rock deformation over all of Southeast Asia. The Indochinese block was extruded toward the southeast, and this induced the Red River Shear Zone, extending from the Tibetan plateaus to the China Sea for more than 1,000 km (Jolivet et al., 2001; Leloup et al., 2001; Hauzenberger et al., 2003; Anckiewicz et al., 2007). The Yen Bai province is formed by two different geological units separated by a fault that is part of the Red River shear zone. To the northeast lies the Lo Gam zone, and to the southwest the Day Nui Con Voi range (figure 3).

All of Luc Yen's gem deposits are located in the Lo Gam zone (again, see figure 3). The structure of this unit results from the deformation of the Himalayan orogenesis superimposed on the preexisting Indosinian structure (Garnier et al., 2002, 2005). The Lo Gam formation consists of a sedimentary series metamorphosed into marble, gneiss, calc-silicates, micaschist, and amphibolite. These metamorphic rocks are sometimes intruded by granitic and pegmatitic dykes (Leloup et al., 2001; Garnier et al., 2005, 2008). The marbles are mainly calcitic and interlayered with Al-, V-, and Cr-rich amphibolites.

Blue spinel is found in a layer of marble more than 500 meters thick. It occurs in discontinuous series of lenses, tens of millimeters thick and meter-sized in length, roughly following the regional foliation. These marble lenses are remarkably rich in forsterite (magnesian olivine). The gem is often associated with calcite, forsterite, pargasite (sodi-calcic amphibole), sulfides, and chlorites (magnesian chlorite and clinochlore). Remarkably, blue spinel in these primary deposits is not associated with ruby or red spinel.

MINING

The three primary deposits at May Trung (22°1′48.9″ N, 104°48′42.7″ E), Bai Son (21°59′47.3″ N, 104°40′9.9″ E), and Bah Linh Mot (22°1′23.7″ N, 104°48′42.8″ E) are located on a mountain range composed of marble, standing about 600 meters high. Each site is mined by

a handful of locals, mainly farmers trying to earn extra income. The blue spinel is extracted from the marble using hand tools (figure 4, top) and a jackhammer.

Secondary deposits (figure 4, bottom left and bottom right) yield most of the blue spinel production. Some lie in the valley to the east of the spinel-rich mountain range. These include Kuoi Ngan (22°0′7.8″ N, 104°50′41.1″ E); Khao Ka (21°59′6.5″ N, 104°50′52.5″ E); Lung Thin (22°0′12.8″ N, 104°49′31.5″ E); Lung Day (21°59′51.3″ N, 104°49′23.3″ E); and Khin Khang (22°1′46.7″ N, 104°50′9.3″ E). Khe Khi (22°1′36.8″ N, 104°48′41.2″ E) and Bai Gou (22°4′43.2″ N, 104°47′5.5″ E) are located in the mountain in a small secondary basin. Miners use a water hose and a sluice to sort the gem-bearing gravels (figure 4, bottom left). Some secondary deposits are localized in karst caves inside marble (figure 4, bottom right). Heavy gravels are washed and sorted inside the cave and brought up to the surface, where they are sorted under daylight. In secondary deposits, blue spinel is found together with ruby, red spinel, sapphire, tourmaline, and occasionally gold.

PRODUCTION AND DISTRIBUTION

In secondary deposits, blue spinel is a by-product of ruby and red spinel mining. Even so, some large parcels contain more than a thousand carats of millimeter-sized, very saturated blue spinel (see Pardieu, 2012). Some dark grayish blue stones weighing approximately 5 ct have been faceted, but far fewer than ruby and red spinel.

Blue spinels from primary deposits are found in two different forms. Usually miners encounter them in "pockets" as centimeter-sized crystals, occasionally with a pleasing, well-defined octahedral shape

Figure 3. This geological map of Luc Yen shows two different geological formations: the Day Nui Con Voi Range in the southwest and the Lo Gam zone in the northeast. The blue spinel deposits are located in the Lo Gam zone. Adapted from Garnier (2003) and Long et al. (2004).

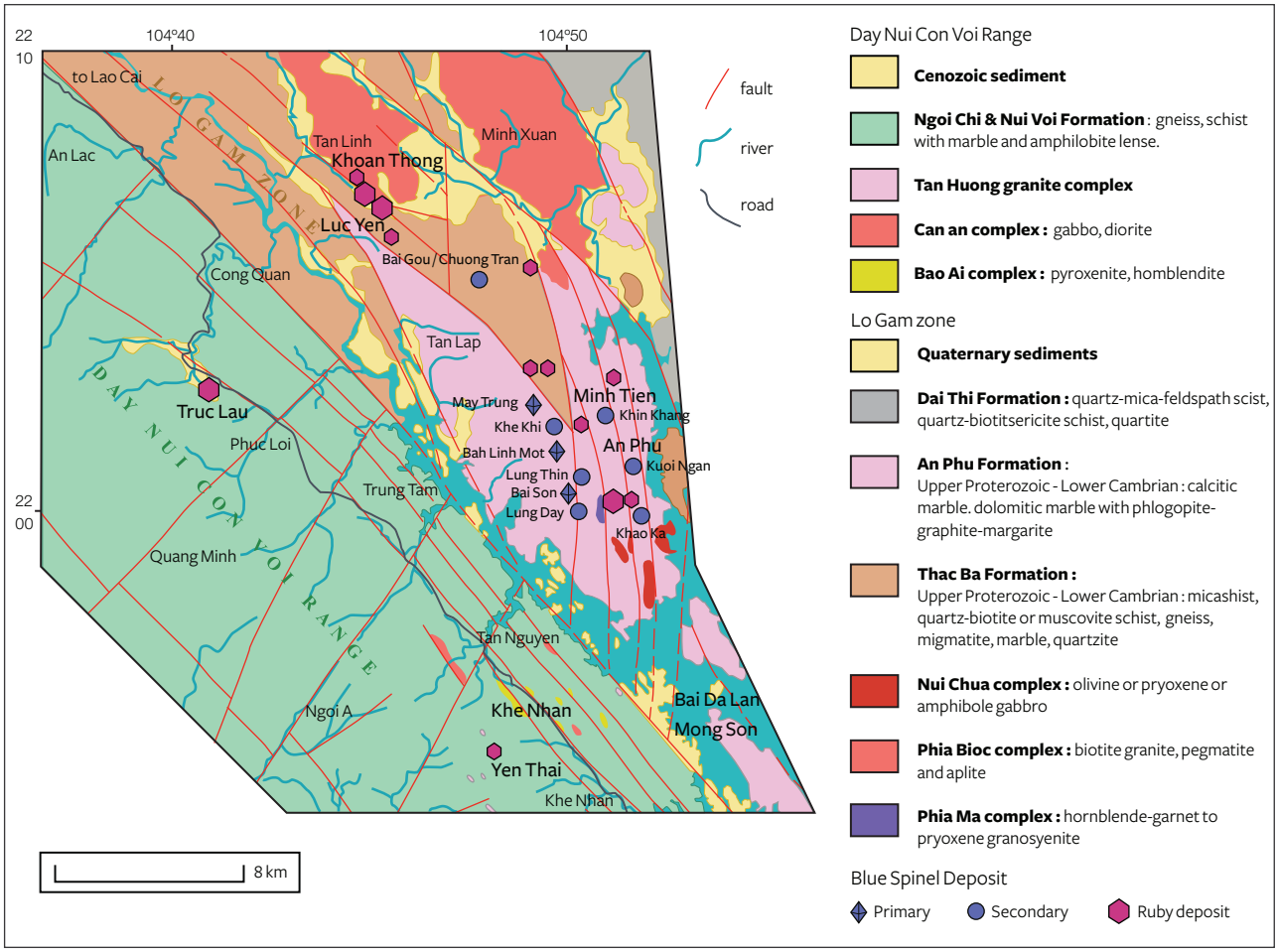

Figure 4. Gem-quality blue spinels are extracted from primary deposits by locals using hand tools, as shown in Bai Nua Doi (top). Secondary deposits are exploited in the valley with a sluice box to sort the minerals according to their density (bottom left). In the karstic environment, caves trap the gem-rich gravel (bottom right). These special secondary deposits are also processed with sluice boxes. Photos by Boris Chauviré.

with some portion containing gem material, or as aggregates of small octahedral crystals of varying quality. These are broken down or cobbed by miners to extract a small amount of gem spinel. These gem blue spinel can reach 5 ct, but they are often fractured. Spinels are also found as millimeter-sized octahedra or twins in the marble.

The blue spinel's hue, tone, and saturation vary from one deposit to the next. In the secondary Bai Gou deposit, the crystals have a very dark blue color and often reach 10 ct. In Chuong Tran and Bai Son, the spinel has a bright blue color (Senoble, 2010; Overton and Shen, 2011) and can reach 5 ct. Crystals from May Trung and Khe Khi have a very saturated cobalt blue color but are quite small (rarely larger than 1 ct).

Millimeter-sized blue spinels from the primary

deposits are often kept in marble so that the whole piece can be carved. This is done directly at the mining site, and the carvings are taken down to the valley to be sold as decorative pieces.

MATERIALS AND METHODS

Sample Collection. In early 2012, two field trips were organized to collect samples and map the main blue spinel deposits within the Luc Yen district. The first expedition enabled us to visit most of the corundum and spinel deposits and to understand the geology of this area. We also made contact with local merchants and miners for the second expedition just one month later. On the second field trip, we visited only blue spinel deposits and collected whole rock and gem-bearing samples. Most of the rock samples were collected at the mining site. Unfortunately, we did not observe gem samples at the mining sites. All gem blue spinels for spectroscopic and gemological measurements were procured from several local merchants in Yen The.

Materials. From the 55 carats of blue spinel we collected from local merchants, six representative rough crystals were selected and prepared in parallel-window plates for gemological and spectroscopic investigation. The least included and fractured samples were chosen for spectroscopic analysis. A polished window was prepared on each one to facilitate gemological and microscopic examination. One additional sample similar to SATBLU1 in color and saturation (labeled SATBLUchem) was prepared as a polished section for laser ablation–inductively coupled plasma–mass spectrometry (LA-ICP-MS) chemical analysis. Four additional samples from a later field trip by author EF were added to complete this study. These were also purchased from local merchants. The spinels were divided into three different parcels according to their color category (detailed in "Gemological Characteristics" below). The sample names consisted of the color category (GREBLU, SKYBLU and SATBLU) followed by a number; see table 1. Moreover, 73 rock samples were collected in the field from 11 different mining sites. From these, 19 thin sections were prepared for petrographic examination.

Methods. *Gemological Properties.* Specific gravity was measured hydrostatically with a Mettler Toledo JB703-c/FACT (with a precision of 0.001 ct). Internal features were observed with a standard gemological microscope. Refractive index was measured with a РФ-I refractometer with Rayner SVLS orange light. All spinel samples were observed under a 6 W A-Krüss Optronic 240 UV light, and we also tested their Chelsea filter reaction. Color was documented under normalized daylight (D65) and a normalized incandescent light (A).

Spectroscopic Measurements. UV-Vis-NIR absorption spectra of each sample (window plates) were taken with a Cary 5G Varian spectrophotometer in the 200–1500 nm range with a sampling interval of 1 nm and a spectral bandwidth of 1 nm maximum (sampling and spectral bandwidth were sometimes reduced to 0.25 nm to obtain better resolution). Raman spectra were collected on gem samples using both a Jobin-Yvon Labram with a 514 nm, 50 mW laser excitation, and a Jobin-Yvon Spex Horiba T64000 with a 647 nm, 50 mW laser excitation. The spectral range extended from 40 to 1500 cm^{-1} with a two-second exposure.

Chemical Composition. LA-ICP-MS chemical analysis was conducted at Blaise Pascal University (Clermont-Ferrand, France) using an Agilent 7500 spectrometer with a Resonetics M-50E laser (193 nm ablation wavelength, 5 Hz frequency with an energy between 10 and 12 J/cm^2). For these analyses, four indentations (about 73 µm in diameter) were ablated on each sample, and ^{27}Al was used as the internal standard. Data was processed with the GLITTER 4.4.2 software. To complement these analyses, we used a RIGAKU NEX CG energy-dispersive X-ray fluorescence (EDXRF) spectrometer operating at 25 kV and 0.10 mA. The detection limit for the major elements (Al, Mg) is about 0.1 wt.%, and below 0.01 wt.% for the minor elements. Each sample was measured for 90 seconds.

Petrographic Examination. Thin sections of rocks were observed with a standard Wild Makroscope M420 petrographic microscope, and a JEOL JSL-5800 LV scanning electron microscope (SEM) operating at 20 kV and 0.3 nA electron beam, with a 37° take-off angle of the detector. Mineral compositions of the samples and their inclusions were first determined by energy-dispersive spectroscopy (EDS) using an IMIX-PTS detector. This detector uses a high-resolution (115 eV) Ge crystal and an ultrathin polymer window, detecting elements ideally down to boron, if it is a major component of the material. The calibration standards used were either pure elements or simple compounds. The PGT software applies phi-rho-z data correction for the effect of X-ray absorp-

TABLE 1. Characteristics of gem blue spinels from Luc Yen, Vietnam.

Samples	SKYBLU1	SKYBLU2	SKYBLU3	SKYBLU4	GREBLU1	GREBLU2	GREBLU3	SATBLU1	SATBLU2	SATBLU3
Photo (normalized daylight)										
Photo (normalized incandescent light)										
Weight (ct)[1]	2.076	0.91	0.24	0.18	4.076	2.538	2.863	0.28	0.23	0.09
Dimensions (mm)[2]	10.8 x 5.2 x 4.3	7.6 x 4.6 x 2.7	3.8 x 2.7 x 1.5	2.9 x 2.4 x 0.5	14.9 x 7.1 x 4.1	9.8 x 5.4 x 2.8	9.7 x 5.5 x 3.1	2.8 x 1.1 x 2.1	3.9 x 2.7 x 1.4	3.1 x 1.9 x 1.4
Origin	Khao Ka	Khao Ka	Unknown	Unknown	Bai Son	Bai Son	Bai Son	Khe Khi	Unknown	Unknown
Refractive index	1.712	1.712	1.714	1.710	1.718	1.713	1.711	1.712	1.716	1.714
Specific gravity	3.583	3.584	3.594	3.596	3.578	3.598	3.583	3.410	3.673	3.645
Chelsea reaction	Pink-orange	Pink-orange	Red	Red	Pink-orange	Pink	Pink	Red	Red	Red

[1] *For SKYBLU4 and SATBLU1, the weight is the sum of the weights of the pieces from the sample.*
[2] *For SKYBLU4 and SATBLU1, the dimensions are an average of the measurements of each piece from the sample.*

tion in the analyzed material, taking into account all the matrix effects. Oxygen was calculated from the spectrum, not based on stoichiometry.

GEMOLOGICAL CHARACTERISTICS

Visual Appearance. We separated the spinel samples into three categories according to their color descriptions:

- SATBLU samples: medium to medium dark tone, strong to vivid saturation, and blue to violetish blue hue
- SKYBLU samples: medium light to very light tone, strong to very vivid saturation, and blue hue
- GREBLU samples: medium light to light tone, grayish to slightly grayish saturation, and blue to bluish violet hue

All of the rough samples were slightly fractured and contained very few inclusions. Color was homogeneous in each stone, and most showed a subtle color change from blue under daylight-equivalent normalized light (D65) to violetish blue under incandescent light (see table 1). The authors avoid the commonly used term "color shift" (Senoble, 2010), which Manson and Stockton (1984) defined in garnets while observing the combination of two color phenomena, nowadays identified separately: classical color change with lighting, and Usambara effect (change of color with thickness). We observed that the color change is more pronounced in stones with a more saturated color. While examining numerous parcels in Yen The, we observed that most of the grayish blue spinel—and some of the very saturated blue material, contrary to our other observations—did not show any color change.

Blue spinel from secondary deposits (except Khe Khi) is rounded and can reach several tens of carats. In Khe Khi, blue spinels are found as millimeter-sized octahedra.

Optical and Physical Properties. The samples' refractive index ranged from 1.711 to 1.718, and their specific gravity was from 3.578 to 3.673. They were isotropic, with no anomalous double refringence, and inert under both short- and long-wave UV light. Under the Chelsea filter, all the samples appeared pink to red (see table 1 for details). We observed that the darker the spinel, the redder the Chelsea filter reaction.

Microscopic Characteristics. Conchoidal fractures and "fingerprint" healed fractures were often present in our samples (figure 5, left). Some showed elongated tubes, while others contained groups of parallel tubes. We observed birefringence in some of these tubes,

Figure 5. Blue spinels (here, GREBLU3) often show healed fractures (fingerprints, left), and some samples contain irregular opaque black crystals associated with elongated tubes (center and right). Photos by Boris Chauviré; field of view 1 mm (under daylight equivalent light on the left, plane-polarized light in the center, and cross-polarized light on the right).

which suggested that they consisted of an anisotropic solid phase (figure 5, middle and right). Black, opaque, irregular to hexagonal crystal inclusions less than 1 mm, reminiscent of graphite, were also found in some samples (figure 5, middle and right). GREBLU1 was the only sample that had yellowish fractures covered by red crystals (probably ferric oxide hematite).

PETROGRAPHY AND CHEMISTRY OF HOST ROCKS

Minerals. The marble that hosts blue spinel is mainly composed of calcite (sometimes magnesian) and dolomite. The major additional phases are olivine and pargasite (figure 6). Several accessory phases were identified using the petrographic micro-

Figure 6. These views of thin sections from rocks bearing blue spinel (under plane-polarized light) show that blue spinel is always associated with olivine (forsterite) and pargasite in calcite matrix. Clinochlore surrounds all main minerals (left, field of view 1.5 mm). In the matrix, graphite and pyrrhothite are common accessory minerals (right, field of view 0.5 mm). Cc = calcite, Clh = clinochlore, Gph = graphite, Ol = olivine, Pg = pargasite, Pyr = pyrrhotite, Sp = spinel. Photomicrographs by Boris Chauviré.

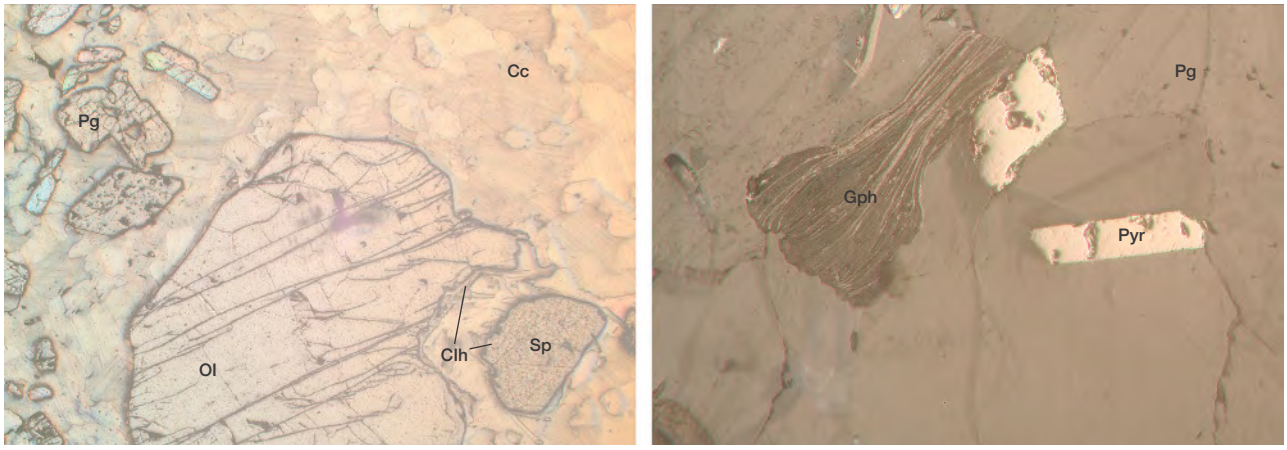

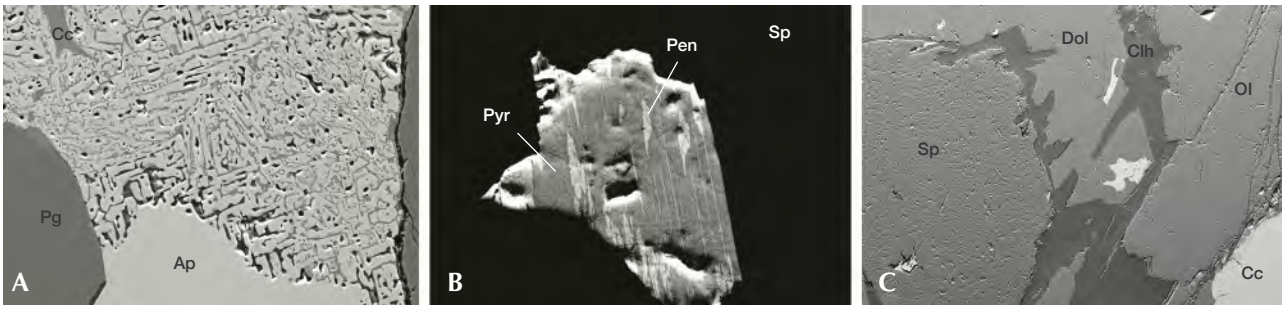

Figure 7. An inclusion of apatite in pargasite exhibits intergrowth with calcite (slightly magnesian; left, magnification 750×). In most cases, pyrrhotite inclusions have exsolutions of pentlandite, a sulfide with higher nickel content (center, magnified 1200×), which also contains cobalt. Using scanning electron microscopy with backscattered electron imaging, sensitive to the atomic number, a petrographic thin section of marble-bearing blue spinel shows that spinel and olivine are surrounded by clinochlore. The marble is composed of calcite and dolomite (right, magnified 65×). Ap = apatite, Cc = calcite, Clh = clinochlore, Dol = dolomite, Ol = olivine, Pen = pentlandite, Pg = pargasite, Pyr = pyrrhotite, Sp = spinel.

scope or EDS with SEM. These included titanite, rutile, zircon, graphite, apatite, several sulfide minerals (again, see figure 6), and phyllosilicates. The sulfides were mainly pyrrhotite ($Fe_{1-x}S$; monoclinic) with pentlandite exsolution lamellae ($(Fe,Ni)_9S_8$; cubic) and violarite ($FeNi_2S_4$; cubic). Raman spectroscopy helped to distinguish between different phyllosilicates, mainly clinochlore and phlogopite. Humite was not observed in the marble, although this mineral is associated with red or purple spinel, as well as ruby (Hauzenberger et al., 2003; Garnier et al, 2008).

Texture. The marble that hosts blue spinel has a granoblastic texture, with millimeter to centimeter grain size. SEM imaging with a backscattered electron detector showed exsolution features between calcite and dolomite, and intergrown apatite and calcite (figure 7a). Pentlandite lamellae in pyrrhotite present two different morphologies. The first consists of parallel flat lamellae less than 500 nm thick, crossing some pyrrhotite crystals from end to end. The second is lens-shaped, more than 1 µm thick and about 3 µm long, often associated with parallel flat lamellae (figure 7b).

Paragenesis. Blue spinel is observed only in olivine-rich lenses, associated with dolomite and calcite (figure 8). No blue spinel is observed in the marble when olivine is absent. The spinel-rich lenses are elongated nearly parallel to the regional foliation: roughly 45° toward the northeast. Spinel and pargasite show inclusions of apatite and sulfides similar in shape and composition for both host minerals. This suggests that apatite and sulfides preexisted spinel and pargasite. In some titanite crystals, SEM imaging revealed inclusions of zircon and pargasite. Therefore, titanite probably represents a later stage of mineralization. Clinochlore crystals surround all the other minerals (figure 7c), meaning it probably crystallized later during a hydration phase, and possibly during exhumation.

CHEMICAL COMPOSITION

Spinel. The composition of the three types of spinel crystals was measured in thin sections using EDS, and all rough samples were analyzed by EDXRF. These analyses identified them as spinel *sensu stricto* ($MgAl_2O_4$). Table 2 presents LA-ICP-MS chemical analyses on representative samples of the

TABLE 2. Trace-element composition of three spinel samples, measured by LA-ICP-MS.

Element (ppma)	Detection Limit (ppma)	SKYBLU1	GREBLU2	SATBLUchem
Li	4	2778	6030	2120
Be	10	552	946	32
Ti	2	3	3	202
V	1	11	6	362
Cr	3	16	8	1111
Mn	5	238	106	287
Fe	20	11,009	9362	12,794
Co	0.2	84	22	1236
Ni	1	85	29	2514
Cu	1	4	4	4
Zn	4	7242	4887	1047
Ga	0.2	299	1088	234

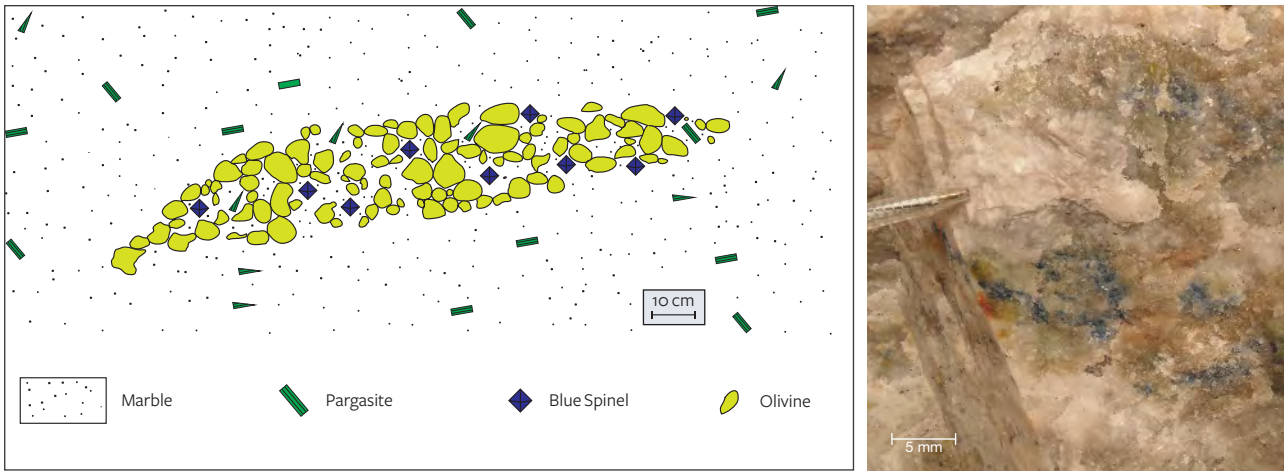

Figure 8. In Vietnam, primary blue spinel deposits appear as approximately lens-shaped bodies rich in olivine. These lenses are hosted in marble, and pargasite is found throughout the surrounding marble. Photo and drawing by Boris Chauviré.

three color categories. The main impurities detected were Li, Fe, and Zn. Significant traces of Be, Ti, V, Cr, Mn, Ga, Ni, and Co were also detected. All analyzed spinels had concentrations of Ga, Zn, and Li, consistent with those observed only in natural blue spinel (Muhlmeister et al., 1993; Krzemnicki, 2008; Saeseaw et al., 2009). All the samples presented nearly uniform concentration in iron and in copper: around 10,000 ppma (equal to 1 atomic percent) and 4 ppma, respectively. The other elements showed strong variation among samples. Sample SATBLUchem (saturated blue) was enriched in Ti, V, Cr, Mn, Co, and Ni compared to the other samples. Samples SKYBLU1 and GREBLU2 were enriched in Be and Zn compared to SATBLUchem. GREBLU2 is also enriched in Li and Ga compared to the two others.

Host Rocks. The chemical composition and characteristics of associated minerals were also examined with EDS analysis. Olivine is 99% pure forsterite (Mg_2SiO_4). Pargasite is rich in titanium, sodium, and chlorine. Apatites are fluorapatites with up to 20% chlorine in substitution of fluorine. In two thin sections, we analyzed one REE-rich unknown mineral and several molybdenum- and tungsten-rich unknown minerals. Cobalt was found in sulfides, as high as 1.5 wt.% in pentlandite and 3.5 wt.% in violarite.

SPECTROSCOPIC PROPERTIES OF BLUE SPINEL

UV-Vis Absorption Spectra. All UV-visible spectra showed a broad, intense absorption band between 500 and 670 nm composed of several narrower bands at about 545, 550, 560, 580, 590, and 625 nm (figure 9). Two transmission windows were seen in the visible part of the spectra, in the violet to blue region (400–500 nm) and in the red region (670–700 nm). We also observed several weak peaks between 300 and 500 nm at about 371, 386, 418, 427, 455, 460, and 480 nm. The bands at 427 and 460 nm are not visible on the spectra that show the most intense main band between 500 and 670 nm (samples SKYBLU2 and SATBLU1). Additionally, we noted a large, weak band centered at about 440 nm only on the SKYBLU samples. For samples GREBLU1 and SATBLU1, we also note an increasing absorption from 450 nm toward the UV.

Raman and Luminescence. The Raman spectra were typical of spinel, with weak peaks at 405, 665, and 766 cm^{-1} (figure 10a; Fraas et al., 1973). The 405 cm^{-1} peak was 9 cm^{-1} wide, evidence that the analyzed spinels were natural and unheated (Krzemnicki, 2008; Saeseaw et al., 2009). However, this Raman signal of spinel was overwhelmed by luminescence with the two available excitation wavelengths (514 or 647 nm). The luminescence band was centered at 107 cm^{-1} for the 647 nm excitation wavelength, corresponding to a 650 nm emission (figure 10b). In this case, the sample showed a strong red luminescence (figure 10b, inset) consistent with a broad band emission centered at 650 nm. In addition, many weak peaks between 673 and 710 nm, grouped in apparent triplets, were visible: 685, 687, and 689 nm; 696, 697, and 700 nm; and 704, 707, and 709 nm (figure 10b).

DISCUSSION

Primary Geological Origin. Red and blue spinels are always found in marble (figure 11). Garnier et al. (2008) proposed that this marble originated from an old car-

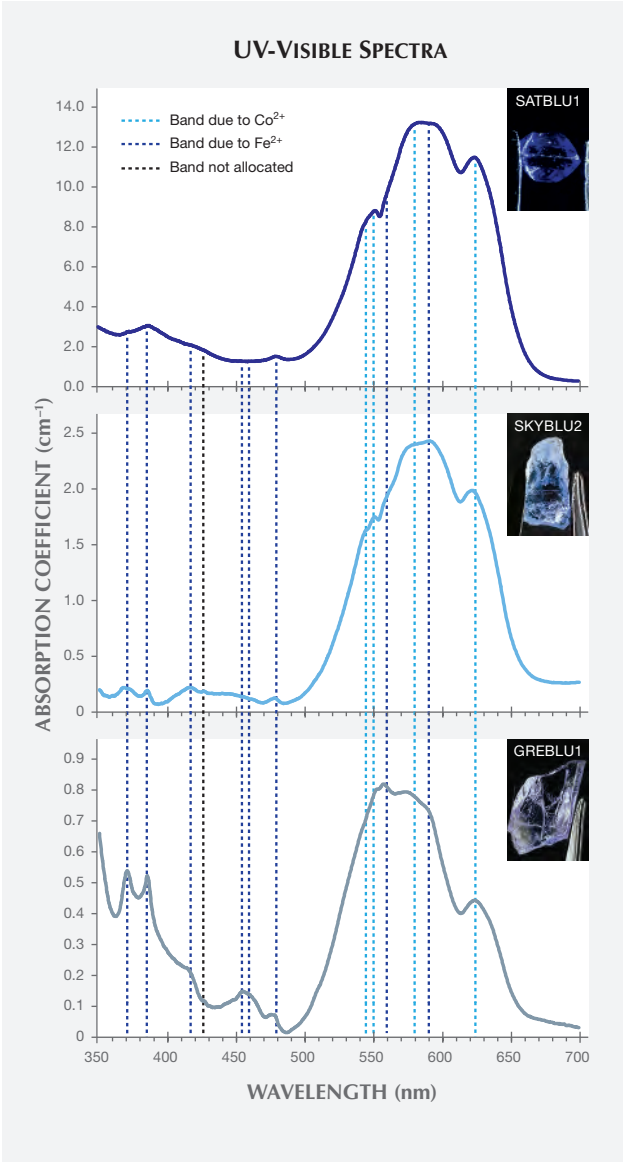

Figure 9. The UV-Visible spectra of typical blue spinels from Vietnam show a major composite absorption band between 500 and 650 nm, a large transmission window in the blue to violet region, and a smaller one in the red. The bands at 371, 386, 418, 455, 460, 480, 560, and 590 nm are due to Fe^{2+}.The bands at 545, 550, 580, and 625 nm are due to Co^{2+}. The band at 427 nm is not allocated.

bonate platform (considered Precambrian to Permo-Triassic), which later metamorphosed. Graphite crystals in these Vietnamese marbles likely derive from metamorphism of organic matter (Giuliani et al., 2003; Garnier et al., 2008). As already mentioned, blue spinels are always associated with olivine (nearly pure forsterite). This paragenesis is typical of the granulitic metamorphic facies (high temperature above 550°C for a CO_2-rich system; Bucher and Frey, 1994; Janardhan et al., 2001; Proyer et al., 2008). Pargasite is ubiquitous in marble, also representing a high-temperature phase. Pargasite, olivine, and spinel are nearly contemporaneous, and they may have crystallized from the destabilization of diopside with increasing pressure and temperature in a prograde reaction (Proyer et al., 2008; Ferry et al., 2011).

We detected some fluorine and chlorine in apatite and pargasite, and some sodium, lithium, and beryl-

Figure 10. The samples in this study displayed the typical Raman signal for spinel (top), with a strong continuum due to cobalt luminescence. But when the concentration in cobalt was too high, luminescence overwhelmed the signal for spinel. In some samples, spectra acquired using a 647 nm excitation showed additional luminescence peaks of chromium (the so-called organ pipe spectrum, bottom). Under green laser excitation (514 nm), the sample reacted with a red luminescence (bottom photo).

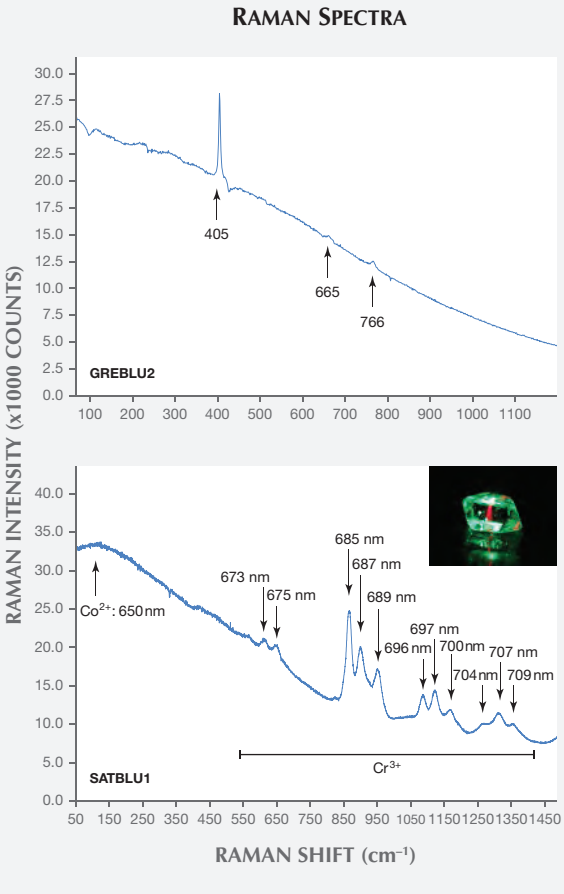

Figure 11. Blue spinel from Luc Yen in its marble host. Photo by Vincent Pardieu/GIA.

lium in blue spinel. These elements are indications that evaporitic rocks played a role during metamorphism (Proyer et al., 2008). Giuliani et al. (1993) and Garnier et al. (2005, 2008) also proposed this hypothesis from the study of fluid inclusions in gem ruby from the Luc Yen area.

Different areas yielding ruby and red or blue spinel show distinct characteristics. Red spinel and rubies have a very similar paragenesis. Forsterite is only associated with blue spinel, and clinohumite is only associated with red spinel. Clinohumite can also grow from diopside in a prograde reaction with dolomite and water (Proyer et al., 2008). Ruby-bearing rocks are very different from those containing blue spinel, as they underwent different metamorphic histories. Because of the intense tectonic activity in Luc Yen, it is possible that two rocks with very different geological histories have been brought in contact.

Garnier et al. (2008) did not observe evidence of a fluid circulating through the marble. They proposed that aluminum and chromium originally sedimented within the carbonate platform. These elements were mobilized due to the presence of halogen elements (fluorine and chlorine) from evaporitic rocks. We propose that the mobilization of Ni and Co happened through the same process. Another hypothesis is that Ni and Co were mobilized from amphibolitic rocks interlayered in the marble (observed by Garnier et al., 2006) via halogen-rich fluids. Fluids can be formed by the metamorphism of clay minerals, evaporate, and organic matter (Giuliani et al., 2003; Garnier et al., 2008).

Proposed Geological History. The ancient Paleo-Tethys Ocean (possibly Proterozoic to Permo-Triassic) separated the China (Yangtze) and Indochina cratons (now Vietnam, Laos, Cambodia, Thailand, and Myanmar). In this ocean, a carbonaceous platform developed by sedimentation. Tectonic movements caused the closing of this ocean, and evaporitic minerals were deposited. The two main blocks (Yangtze and Indochina) subsequently collided, and all the sedimentary and magmatic rocks of the oceanic crust underwent intense deformation and metamorphism. During the collision, the metamorphism of the mix of former carbonate platform minerals and some detritic material (such as clays) deposited with it may have led to the formation of diopside through the following reactions:

tremolite + calcite → diopside + dolomite
dolomite + quartz → diopside + carbon dioxide

By increasing metamorphism, diopside destabilized into olivine, spinel, and clinohumite. The reduction of evaporitic minerals such as sulfates formed chlorine- and fluorine-rich fluids. These fluids were involved in the mobilization of aluminum and other elements such as chromium (Giuliani et al., 2003; Garnier et al., 2008).

Some processes remain poorly understood. Why do some areas show clinohumite with red spinel while others show olivine and blue spinel? What is the main difference responsible for mobilizing more chromium (red spinel) or more cobalt (blue spinel) in the marble?

Origin of Blue Color and Color Change in Vietnamese Blue Spinels. The main absorption band between 500 and 670 nm, the dominant origin of color in these blue spinels, is composed of a series of bands at approximately 545, 550, 560, 580, 590, and 625 nm

Figure 12. A gem merchant examines a blue spinel from the Luc Yen district. Photo by Vincent Pardieu/GIA.

(again, see figure 9). Bands at 545, 550, 580, and 625 nm are due to cobalt (Co^{2+}) substituting for Mg^{2+} in tetrahedral sites of the spinel structure (Wherry, 1929; Pappalardo et al., 1961; Shigley and Stockton, 1984; Kuleshov et al., 1993; Muhlmeister et al., 1993; Delaunay et al., 2008; Duan et al., 2012; Bosi et al., 2012; D'Ippolito et al., 2015). The remaining absorption bands (at 371, 386, 418, 455, 460, 480, 560, and 590 nm) are allocated to iron (Fe^{2+}) in tetrahedral sites of the spinel structure (Gaffney, 1973; Dickson and Smith, 1976; Muhlmeister et al., 1993; Delaunay et al., 2008; D'Ippolito et al., 2015). A weak band observed at 427 nm is not attributed but may be linked with other measurable elements such as Ni. Consequently, the spectra show transmission windows between 300 and 500 nm and between 700 and 900 nm that explain the blue color. As expected, the spectra show that iron (Fe^{2+}) and cobalt (Co^{2+}) are the main chromophore elements. The other trace elements detected either do not give rise to absorption in the visible range or are much less efficient absorbers than cobalt. Chromium, which is the main chromophore for red and pink spinel, makes a significant contribution to color if the concentration is above 1000 ppma. (Muhlmeister et al., 1993; T. Häger, pers. comm., 2014). Cr concentration in SATBLU samples is borderline, but the Co concentration is higher, too. The contribution is considered negligible.

We observed that the SATBLU samples, which had the most saturated color, also had the most important cobalt optical absorption. In addition, the main band had an absorption coefficient greater than 10 cm^{-1}, and the iron optical absorptions observed were weak. For the parcel classified as SKYBLU, iron and cobalt optical absorption seemed to have a similar importance in the optical spectra, reaching a maximum of 2 cm^{-1} as compared to SATBLU samples. GREBLU samples had the most significant iron band, but the main absorption band only reached 0.5 cm^{-1}. We also observed a correlation between the cobalt absorption bands and the color saturation.

SATBLU2 had a Fe/Co value of approximately 10 (table 2), and the SATBLU samples had the most saturated color (table 1). GREBLUE2, with a Fe/Co ratio of about 425 (table 2), had a visible gray hue component (table 1). For intermediate Fe/Co ratios of about 130 (measured on SKYBLU1; see table 2), the spinel had a sky-blue color (table 1). Moreover, sample GREBLU1, which had the grayest color, showed more significant bands due to Fe^{2+}. We propose that the GREBLU samples are colored mainly by iron and the SATBLU samples by cobalt. The SKYBLU samples' colors arise from both iron and cobalt absorption. Hue differences are more significantly controlled by iron (with different species), while saturation is largely dictated by cobalt (D'Ippolito et al., 2015).

Using chemical and spectroscopic analysis from eight of our samples, we calculated the molar absorptivity of cobalt in spinel (*sensu stricto*) for three absorption bands. At wavelengths of 545, 580, and 625 nm, we took the apparent maximum of each band. We

determined a molar absorptivity of 530±29, 664 ±18, and 586±11 $L \cdot mol^{-1} \cdot cm^{-1}$, respectively. For the sake of comparison, we calculated the molar absorptivity of iron in spinel (*sensu stricto*) for bands 371, 386, 480, and 590 nm. These bands are attributed to ferrous iron (Fe^{2+}) in the tetrahedral site. Our chemical analysis measured only the total iron content. Assuming all iron was in the form Fe^{2+}, we propose that the molar absorptivity of ferrous iron in the tetrahedral site had an order of magnitude of about 30 $L \cdot mol^{-1} \cdot cm^{-1}$ for each band. With this method, values of molar absorptivity are not very accurate but provide a working assumption for our preliminary study. We recognize that further investigation is needed to fully understand the color in blue spinel. A Gaussian decomposition of spectra can improve the precision of these values. Nevertheless, it is apparent that in spinel, Co^{2+} is approximately 20 times more efficient at absorbing light, and thus creating color, than Fe^{2+} (consistent with D'Ippolito et al., 2015).

Spectra have two transmission windows between 350 and 500 nm (in the blue region) and between 670 and 900 nm (in the red region). This explains the pink to red reaction under the Chelsea filter and the color change. Indeed, the Chelsea filter probes a transmission window in the red. The color change is also explained when the spectral composition of the lighting environment is compared with the absorption spectra of spinel, although this change is not observed in every example. Compact fluorescent light emits more in the blue region than in the red, and therefore the spinel appears blue. Under incandescent light, which is richer in red, spinel displays a violetish blue color that is mostly blue with minor red.

Origin of Red Luminescence. Under laser excitation, our samples showed a strong red luminescence. In spectra acquired using a 647 nm excitation, we observed several peaks (in groups of three) between 673 and 710 nm (at about 673, 675, 685, 687, 689, 696, 697, 700, 704, 707, and 709 nm; see figure 10b). These peaks are known to be due to trivalent chromium (Cr^{3+}) substituting for aluminum in the octahedral site (Burns et al., 1965; Wood et al., 1968; Skvortsova et al., 2011). The broad band centered at 650 nm is allocated to divalent cobalt in the tetrahedral site of the spinel structure (Abritta and Blak, 1991; Kuleshov et al., 1993). These luminescence behaviors are consistent with our chemical analysis, as the strongest luminescence was observed in the SATBLU samples, which had higher concentrations of Cr^{3+} (1111 ppma) and Co^{2+} (1236 ppma).

CONCLUSION

We confirmed that the saturated "cobalt-blue" color of Vietnamese spinels (figures 12 and 13) is due predominantly to Co^{2+} substituting for Mg^{2+} in the tetrahedral site of the spinel structure. For the most saturated blue spinel, cobalt is the main coloring agent, even if iron is more abundant. Indeed, cobalt is a powerful coloring agent, with a molar absorptivity between 500 and 700 $L \cdot mol^{-1} \cdot cm^{-1}$ depending on wavelength, whereas iron (Fe^{2+} in the tetrahedral site) has a molar absorptivity of about 30 $L \cdot mol^{-1} \cdot cm^{-1}$. The higher the iron/cobalt ratio is, the grayer the color. The red transmission window of these gems explains both their pink to red Chelsea filter reaction and their slight change of color from blue to "lavender" with a change of lighting environment. The red luminescence is due to both Cr^{3+} and Co^{2+}, and it may have a minor influence on the perceived color.

This study offers clues to the definition of "cobalt-blue" spinel. Cobalt is actually the main chromophore, but the presence of iron is also significant. The term "cobalt-blue" can be clarified by further investigations on the significance of each chromophore elements (iron and cobalt). These investigations can propose a limit on the ratio of iron/cobalt above which the term "cobalt-blue" cannot be used.

Spinels from Luc Yen contain few inclusions. Fractures and fingerprints were the most common inclusions found. Sometimes, we observed parallel elongated tubes with black, irregular solid inclusions associated.

Figure 13. Vietnam's spinel production yielded this 2.59 ct cobalt blue gem. Photo by Robert Weldon/GIA, courtesy of Palagems.com.

From a geological standpoint, gem-quality blue spinels are associated with intense metamorphism. Their marble host results from the metamorphism of an ancient carbonaceous platform. This platform was located in the Paleo-Tethys Ocean, which separated Indochina and China. During the convergence of these "paleo-continents," the ocean closed off, accompanied by the formation of evaporitic rocks. The ocean crust, associated with the carbonaceous platform and evaporitic platform, was sandwiched between the two continents. The collision led to the metamorphism of the evaporite rocks, in turn producing fluids mobilizing some elements, possibly including cobalt. Spinel grew in the marble during this intense metamorphism. These processes of metamorphism and fluid interaction led to the crystallization of attractive blue spinels in the marble mountains of Luc Yen.

ABOUT THE AUTHORS

Mr. Chauviré (boris.chauvire@univ-nantes.fr) is a PhD student at the Laboratoire de Planétologie et Géodynamique de Nantes, France, and Dr. Rondeau is an assistant professor at the same laboratory (CNRS Team 6112). Dr. Fritsch (CNRS Team 6502) is a professor of physics at the University of Nantes, Institut des Matériaux Jean Rouxel. Mr. Ressigeac is product manager for Montepuez Ruby Mining, Mozambique. Mr. Devidal is an engineer specialist of ICP-MS-LA at the Laboratoire Magmas et Volcans, Clermont Ferrand, France.

ACKNOWLEDGMENTS

We are grateful to Vincent Pardieu, senior manager of field gemology at GIA's Bangkok laboratory, for his valuable aid during the preparation and progress of the expeditions. We thank Vincent's contacts for acquiring blue spinel samples. We are grateful to Mr. Chuãn, our guide, for his knowledge of the field and his logistical support. We also thank Pham Van Long, director of the Center for Gem and Gold Research and Identification in Hanoi, for his logistical support and for exporting the samples collected. GIA's laboratory in Bangkok and its director, Kenneth Scarratt, provided technical and logistical support. Jean-Pierre Lorand (LPGN-CNRS) generously shared his knowledge about sulfides. We thank Alexandre Droux from the Laboratoire Français de Gemmologie for EDXRF measurements. We also thank Tobias Häger of Johannes Gutenberg University in Mainz, Germany, for his help with interpreting UV-Vis spectra. We also thank reviewers that participated to improve this study.

REFERENCES

Abritta T., Blak F.H. (1991) Luminescence study of $ZnGa_2O_4$:Co. *Journal of Luminescence*, Vol. 48–49, pp. 558–560.

Anczkiewicz R., Viola, G., Müntener O., Thirlwall M.F., Villa I.M., Qong N.Q. (2007) Structure and shearing conditions in the Day Nui Con Voi massif: Implications for the evolution of the Red River shear zone in northern Vietnam. *Tectonics*, Vol. 26, pp. 1–21.

Bosi F., Hålenius U., D'Ippolito V., Andreozzi G.B. (2012) Blue spinel crystals in the $MgAl_2O_4$-$CoAl_2O_4$ series: Part II. Cation ordering over short-range and long-range scales. *American Mineralogist*, Vol. 97, No. 11–12, pp. 1834–1840, http://dx.doi.org/10.2138/am.2012.4139.

Bucher K, Frey M. (1994) *Petrogenesis of Metamorphic Rocks*, 6th ed. Springer-Verlag, 308 pp.

Burns G., Geiss E. A., Jenkins B.A., Nathan M. I. (1965) Cr^{3+} fluorescence in garnet and other crystals. *Physical Review A*, Vol. 139, No. 5A, pp. A1687–A1693, http://dx.doi.org/10.1103/PhysRev.139.A1687.

Delaunay A. (2008) Les spinelles bleus. http://www.geminterest.com/.

Dickson B.L., Smith G. (1976) Low-temperature optical absorption and Mössbauer spectra of staurolite and spinel. *Canadian Mineralogist*, Vol. 14, pp. 206–215.

D'IppolitoV., Andreozzi G. B., Hålenius U., Skogby H., Hametner K., Günther D. (2015) Color mechanisms in spinels: cobalt and iron interplay for the blue color. *Physics and Chemistry of Materials*, http://dx.doi.org/10.1007/s00269-015-0734-0.

Duan X., Wang X., Yu F., Liu X. (2012) Effects of Co content and annealing temperature on the structure and optical properties of $Co_xMg_{1-x}Al_2O_4$ nanoparticles. *Materials Chemistry and Physics*, Vol. 137, No. 2, pp. 652–659, http://dx.doi.org/10.1016/j.matchemphys.2012.10.016.

Ferry J.M., Ushikubo T., Valley J.W. (2011) Formation of forsterite by silicification of dolomite during contact metamorphism. *Journal of Petrology*, Vol. 52, No. 9, pp. 1619–1640, http://dx.doi.org/10.1093/petrology/egr021.

Fraas L.M., Moore J.E., Salzberg J.B. (1973) Raman characterization studies of synthetic and natural $MgAl_2O_4$ crystals. *The Journal of Chemical Physics*, Vol. 58. No. 9. pp 3585–3592, http://dx.doi.org/10.1063/1.1679704.

Gaffney E.S. (1973) Spectra of tetrahedral Fe^{2+} in $MgA1_2O_4$. *Physical Review B*, Vol. 8, No. 7, pp. 3484–3486.

Garnier V., Giuliani G., Maluski H., Ohnenstetter D., Phan Trong T., Hoàng Quang V., Pham Van L., Vu Van T., Schwarz D. (2002) Ar-Ar ages in phlogopites from marble-hosted ruby deposits in northern Vietnam: evidence for Cenozoic ruby formation. *Chemical Geology*, Vol. 188, pp. 33–49, http://dx.doi.org/10.1016/S0009-2541(02)00063-3.

Garnier V., Ohnenstetter D., Giuliani G., Maluski H., Deloule E., Phan Trong, T., Pham Van L., Hoàng Quang V. (2005) Age and significance of ruby-bearing marble from the Red River Shear Zone, northern Vietnam. *The Canadian Mineralogist*, Vol. 43, pp. 1315–1329.

Garnier V., Giuliani G., Ohnenstetter D., Fallick A.E., Dubessy J., Banks D., Vinh H.Q., Lhomme T., Maluski H., Pêcher A., Bakhsh K.A., Long P.V., Trinh P.T., Schwarz D. (2008) Marble-hosted ruby deposits from Central and South-East Asia: Toward a new genetic model. *Ore Geology Reviews*, Vol. 34, pp. 169–191, http://dx.doi.org/10.1016/j.oregeorev.2008.03.003.

Giuliani G., Hoàng Quang V., Phan Trong T., France-Lanord C., Coget P. (1999) Carbon isotopes study on graphite and coexisting calcite-graphite pairs in marbles from the Luc Yen and Yen Bai district, North of Vietnam. *Bulletin de Liaison S.F.M.C.*, Vol. 11, pp. 80–82.

Giuliani G., Dubessy J., Banks D., Hoàng Quang V., Lhomme T., Pironon J., Garnier V., Phan Trong T., Pham Van L., Ohnenstetter D., Schwarz D. (2003) CO_2-H_2S-COS-S_8-AlO(OH)-bearing fluid inclusions in ruby from marble-hosted deposits in Luc Yen area, North Vietnam. *Chemical Geology*, Vol. 194, pp. 167–165, http://dx.doi.org/10.1016/S0009-2541(02)00276-0.

Hauzenberger C.A., Häger T., Hofmeister W, Quang V.X., Rohan Fernando G.W.A. (2003) Origin and formation of gem quality corundum from Vietnam. *Geo- and Materials-Science on Gem-Minerals of Vietnam, Proceedings of the International Workshop*, Hanoi, October 1–8.

Huong L.T.-T., Häger T., Hofmeister W., Hauzenberger C., Schwarz D., Long P.V., Wehmeister U., Khoi N.N., Nhung N.T. (2012) Gemstones from Vietnam: An update. *G&G*, Vol. 48, No. 3, pp. 158–176, http://dx.doi.org/10.5741/GEMS.48.3.158.

Janardhan A.S., Sriramguru K., Basava S., Shankara M.A. (2001) Geikielite-Mg.Al.Spinel-titanoclinohumite association from a marble quarry near Rajapalaiyam area, part of the 550 Ma of southern granulite terrain, southern India. *Gondwana Research*, Vol. 4, No. 3, pp. 359–366, http://dx.doi.org/10.1016/S1342-937X(05)70335-X.

Jolivet L., Beyssac O., Goffé B., Avigad D., Lepvrier C., Maluski H., Than T.T. (2001) Oligo-miocène midcrustal subhorizontal shear zone in Indochina. *Tectonics*, Vol. 20, No. 1, pp. 46–57.

Krzemnicki M.S. (2008) Trade Alert: Flux grown synthetic spinels again on the market. *SSEF Newsletter*, October.

Kuleshov N.V., Mikhailov V.P., Sherbitsky V.G., Prokoshin P.V., Yumashev K.V. (1993) Absorption and luminescence of tetrahedral Co^{2+} ion in $MgAl_2O_4$. *Journal of Luminescence*, Vol. 55, pp. 265–269, http://dx.doi.org/10.1016/0022-2313(93)90021-E.

Kušnír I. (2000) Mineral resources of Vietnam. *Acta Montanistica Slovaca*, Vol. 5, No. 2, pp. 165–172.

Leloup P.H., Lacassin R., Tapponnier P., Schärer U., Dalai Z., Xiaohan L., Liangshang Z., Shaocheng J, Phan Trong T. (1995) The Ailao Shan-Red River shear zone (Yunnan, China), Tertiary transform boundary of Indochina. *Tectonophysics*, Vol. 251, pp. 3–84, http://dx.doi.org/10.1016/0040-1951(95)00070-4.

Leloup P.H., Arnaud N., Lacassin R., Kienast J.R., Harrison T.M., Phan Trong T.T., Replumaz A., Taponnier P. (2001) New constraints on the structure, thermochronology, and timing of the Ailo Shan-Red River shear zone, SE Asia. *Journal of Geophysical Research*, Vol. 106, No. B4, pp. 6683–6732.

Lepvrier C., Vuong N.V., Maluski H., Thi P.T., Vu T.V. (2008) Indosinian tectonics in Vietnam. *Comptes Rendus Geoscience*, Vol. 340, No. 2–3, pp. 94–111, http://dx.doi.org/10.1016/j.crte.2007.10.005.

Long P.V., Giuliani G., Garnier V., Ohnenstetter D. (2004) Gemstones in Vietnam. *The Australian Mineralogist*, Vol. 22, No. 4. pp. 162–168.

Manson D.V., Stockton C.M. (1984) Pyrope-spessartine garnets with unusual color behavior. *G&G*, Vol. 20, No. 4, pp. 200–207, http://dx.doi.org/10.5741/GEMS.20.4.200.

Muhlmeister S., Koivula J.I., Kammerling R.C., Smith C.P., Fritsch E., Shigley J.E. (1993) Flux-grown synthetic red and blue spinels from Russia. *G&G*, Vol. 29, No. 2, pp. 81–98, http://dx.doi.org/10.5741/GEMS.29.2.81.

Nassau K. (1980) *Gems Made by Man*. Chilton Book Co., Radnor, PA, 364 pp.

Overton T.W., Shen A.H. (2011) Gem News International: Cobalt blue-colored spinel from Khuoi Ngan, Vietnam. *G&G*, Vol. 47, No. 4, pp. 328–329.

Pappalardo R., Wood D.L., Linares R.C. (1961) Optical absorption study of Co-doped oxide systems. II. *The Journal of Chemical Physics*, Vol. 35, No. 6, pp. 2041–2059, http://dx.doi.org/10.1063/1.1732208.

Pardieu V. (2012) FE34 Vietnam blue spinels. http://www.fieldgemology.org

Pardieu V., Hughes R.W. (2008) Spinel: The resurrection of a classic. *InColor*, Summer, pp. 10–12 (also on www.ruby-sapphire.com and www.fieldgemology.org).

Proyer A., Mposkos E., Baziotis I., Hoinkes G. (2008) Tracing high-pressure metamorphism in marbles: Phase relations in high-grade aluminous calcite-dolomite marbles from the Greek Rhodope massif in the system CaO-MgO-Al_2O_3-SiO_2-CO_2 and indications of prior aragonite. *Lithos*, Vol. 104, No. 1–4, pp. 119–130, http://dx.doi.org/10.1016/j.lithos.2007.12.002.

Rice J.M. (1980) Phase equilibria involving humite minerals in impure dolomitic limestones: part I. Calculated stability of clinohumite. *Contributions to Mineralogy and Petrology*, Vol. 71, No. 3, pp. 219–235, http://dx.doi.org/10.1007/BF00371664.

Saeseaw S., Wang W., Scarratt K., Emmett J.L., Douthit T.R. (2009) Distinguishing heated spinels from unheated natural spinels and from synthetic spinels. http://www.gia.edu/gia-news-research-NR32209A.

Satish-Kumar M. (1999) An overview of petrology of calc-silicate granulites from the Trivandrum block, southern India. *Journal of Geosciences*, Vol. 42. Osaka City University, pp. 127–159.

Senoble J.B. (2010) Beauty and rarity – A quest for Vietnamese blue spinels. *InColor*, Summer, pp. 2–7.

Shigley J.E., Stockton C.M. (1984) "Cobalt-blue" gem spinels. *G&G*, Vol. 20, No. 1, pp. 34–41, http://dx.doi.org/10.5741/GEMS.20.1.34.

Skvortsova V., Mironova-Ulmane N., Riekstina D. (2011) Structure and phase changes in natural and synthetic magnesium aluminum spinel. *Proceedings of the 8th International Scientific and Practical Conference*, Vol. II, pp. 100–106.

Tapponnier P., Peltzer G., Le Dain A.Y., Armijo R., Cobbold P. (1982) Propagating extrusion tectonics in Asia: New insights from simple experiments with plasticine. *Geology*, Vol. 10, No. 12, pp. 611–616, http://dx.doi.org/10.1130/0091-7613(1982)10<611:PETIAN>2.0.CO;2.

Tapponnier P., Lacassin R., Leloup P.H., Shärer U., Dalai Z., Haiwei W., Xiaohan Liu, Shaocheng J., Lianshang Z., Jiayou Z. (1990) The Ailao Shan/Red River metamorphic belt: Tertiary left-lateral shear between Indochina and South China. *Nature*, Vol. 343, No. 6257, pp. 431–437, http://dx.doi.org/10.1038/343431a0.

Ulmer P., Luth R.W. (1991) The graphite-COH fluid equilibrium in P, T, fO2 space. *Contributions to Mineralogy and Petrology*, Vol. 106, pp. 265–272.

Webster R. (1994) *Gems: Their Sources, Descriptions and Identification*, 5th ed. Butterworth-Heinemann, Oxford, edited by P.G. Read, 1026 pp.

Wherry E.T. (1929) Mineral determination by absorption spectra II. *The American Mineralogist*, Vol. 14, No. 9, pp. 323–328.

Wood D.L., Imbusch G.F., Macfarlane R.M., Kisliuk P., Larkin D.M. (1968) Optical spectrum of Cr^{3+} ions in spinels. *The Journal of Chemical Physics*, Vol. 48, No. 11, pp. 5255–5263, http://dx.doi.org/10.1063/1.1668202.

Yu J., Mao J., Chen F., Wang Y., Che L., Wang T., Liang J. (2014) Metallogeny of the Shilu Fe-Co-Cu deposit, Hainan Island, South China: Constraints from fluid inclusions and stable isotopes. *Ore Geology Reviews*, Vol. 57, pp. 351–362, http://dx.doi.org/10.1016/j.oregeorev.2013.08.018.

The Chinese Soul in Contemporary Jewelry Design

Andrew Lucas, Merilee Chapin, Moqing Lin, and Xiaodan Jia

When the same gems and precious metals are used in jewelry, design is the element that ultimately distinguishes one piece from another. Real success is measured not only by the value of its materials but also by the character and quality of the design and craftsmanship. Once considered a weak point of China's gem and jewelry industry, design has seen tremendous progress over the last decade. Benefiting from the availability of more gem materials and the power of a rapidly growing consumer market, Chinese designers now have the freedom to develop their design concepts and craftsmanship skills. Designers from mainland China, Hong Kong, and Taiwan share the bond of cultural identity and have found ways to create jewelry that expresses the Chinese soul.

From dangling hair ornaments to exquisite jade pendants and splendid crowns, jewelry has always served as personal adornment for the Chinese people, from ordinary citizens to royal families (figure 1). Throughout the civilization's 5,000-year history, masters of jewelry design and manufacturing have emerged continually, applying innovations while developing their skills.

China's Cultural Revolution (1966–1976) followed more than a century of social and economic upheaval that hindered almost every aspect of national growth. During this period, jewelry came to represent capitalism, and wearing it was considered offensive. Designers and craftsmen avoided persecution by simply stopping their work.

In the last decades of the 20th century, the Chinese gem and jewelry industry experienced a dramatic upswing. By the end of the 1990s, there were about 20,000 jewelry businesses and some three million people involved in the trade (Hsu et al., 2014). The country's jewelry markets became saturated with similar products, many of low quality (J. Bai, pers. comm., 2013).

This lack of innovation caused a sense of stagnation, which led some industry pioneers to find a new approach. Professional training and degree programs

Figure 1. In this replica of a Qing dynasty hairpin, outlines of flowers, leaves, and other patterns were created with very thin gold threads using the filigree technique. Kingfisher feathers mounted in the frame provide the bright blue color. Unlike dyes, the feathers show natural color and shading as well as biological texture. Ruby cabochons are mounted as the center stones. Photo by Eric Welch, courtesy of Zhaoyi Xintiandi (Beijing) Jewelry Co., Ltd.

See end of article for About the Authors and Acknowledgments.
GEMS & GEMOLOGY, Vol. 51, No. 1, pp. 18–30,
http://dx.doi.org/10.5741/GEMS.51.1.18.

Figure 2. This ring is from the "Jade That She Wants" collection, designed by Hong Kong–based Grace Lee, chief designer of Zhaoyi Jade House. The 18K white gold ring features a transparent jadeite cabochon center stone and fancy sapphire accent stones. Photo courtesy of Zhaoyi Xintiandi (Beijing) Jewelry Co., Ltd.

in jewelry design have been offered since the early 1990s. Over the last 10 years, many leading universities and art academies have formed their own jewelry design and manufacturing departments to serve an expanding market. Foremost among these are Tsinghua University, China University of Geosciences, and China Central Academy of Fine Art. Jewelry competitions have been created to foster the development of young talent. Many companies have invited designers from Hong Kong and overseas to bring their skills to China and to train locals (figure 2). At the same time, Chinese artists have begun going overseas to the UK, the United States, Italy, and Germany to study Western jewelry manufacturing.

It is widely believed by domestic consumers that Chinese jewelry designs should capture the "Chinese soul." This concept is a reflection of the native culture, "a collective programming of the mind" that distinguishes a group of people (Hofstede and Bond, 1988). Rather than being genetically transferred, cultural inheritances can only be acquired by native experience. For thousands of years, the core values of Chinese culture have not fundamentally changed. The process begins at birth and continues throughout a person's life, as one gains a deeply rooted understanding of Chinese culture, including its distinct traditions, philosophy, religions, and preferred materials. This understanding allows the native-born designer to easily and naturally incorporate traditional elements into jewelry for domestic audiences and accurately interpret their meanings (see figure 3, for example). The spiritual message carried by a piece of jewelry can be reflected by combining some Chinese design elements, but this is not always the case. Simply using Chinese elements is not enough: The designers must think in the Chinese way.

In 2010 China overtook Japan to become the world's second-largest economy, after the United States. China is now also the second-largest jewelry market and is projected to become the largest by 2020 ("Chinese jewelry firms…," 2014). To cater to the rapidly expanding market for luxury goods, the Chinese began developing their own innovative jewelry designs.

CHINESE DESIGN ELEMENTS

One recent jewelry trend is to incorporate Chinese elements such as dragons, the phoenix, bamboo, and Chinese characters into their products. Many award-winning pieces from international design and gem-

Figure 3. This fragrance locket ring was designed by Dickson Yewn. Ancient Chinese scholars and social elites often carried small lockets filled with fragrance to freshen the air or even act as an insecticide. The ring symbolizes the wearer's virtue, which in turn can influence their peers. Although flowers and lockets are not considered traditional symbols of Chinese culture, this ring is a reminder of the important virtues one should bear. Photo courtesy of Yewn.

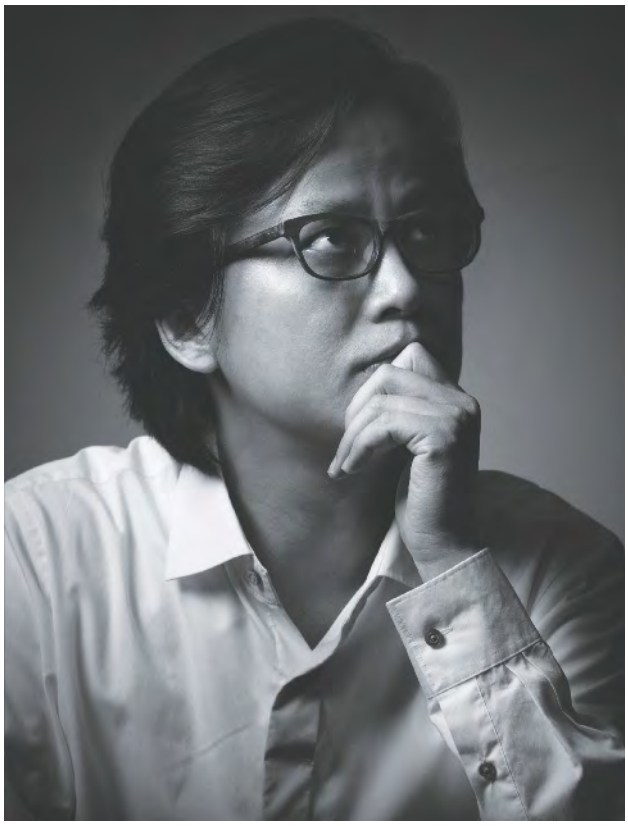

Figure 4. Hong Kong designer Dickson Yewn is devoted to creating jewelry inspired by Chinese traditions. Photo courtesy of Yewn.

cutting competitions feature these elements (Chen, 2014). While several Western designers have embraced traditional Chinese symbols, they sometimes do not apply or combine them properly, making them less meaningful. According to Hong Kong jewelry designer Dickson Yewn, "Jewelry is a new way to interpret a culture that has been suppressed for decades." He believes China is a fundamental resource for jewelry design and that after prolonged social upheaval, it is time to recapture its glory.

Trained as a painter, Yewn has always been interested in Chinese culture and history (figure 4). Having spent years in the West, he has a deep appreciation for its culture but prefers to create jewelry that is distinctly Chinese rather than mixing cultural designs (World Gold Council, 2014). He is also engaged in reviving traditional Chinese jewelry craftsmanship.

While many designers focus on generating new concepts, Yewn digs deeply into native traditions and fuses them with contemporary luxury. His common themes include lattice patterns, paper cutting, Manchurian motifs, and peonies—the Chinese national flower. One of his collections, "Lock of Good Wishes," is based on such traditions (figure 5). The earliest known lock in China was uncovered from a tomb dated 3000 BC. While the basic function of the lock has not changed, the style, materials, and craftsmanship have continued to evolve, and its meaning as a decorative motif has broadened. As a symbol of security, a lock also represents good health and longevity in Chinese culture. Newborns are given precious metal lock pendants to "lock" health and happiness into their lives forever. This type of pendant is still one of the most popular jewelry gifts for babies in China.

Yewn's jadeite and diamond "Wish Fulfilling" ring features a traditional lattice window shank. Lattice windows were a common sight in ancient Chinese gardens, their delicate patterns inviting the viewer to look through and enjoy the beautiful scenery within. They originated in southern China, home of the Classical Gardens of Suzhou. These private gardens, a UNESCO World Heritage Site, date from the 11th through 19th centuries. Their lattice windows are among the most important elements, framing the view with a mysterious veil (figure 6). Yewn borrowed this concept from the garden masters, intending the ring to create a connection between the wearer's mind and the outside world.

Figure 5. This diamond and emerald bracelet is from Dickson Yewn's "Lock of Good Wishes" collection. The four corners of the lock panel are decorated with simplified bat patterns, which symbolize good luck and happiness in Chinese culture. The clasp is a realistic recreation of an ordinary gate lock from ancient China. The concept is typically used in baby jewelry to make the wearer feel blessed throughout life, and Yewn has successfully applied it to adult pieces. Photo courtesy of Yewn.

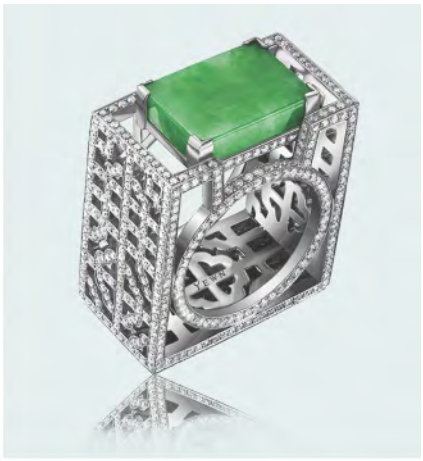

Figure 6. Left and top right: The inspiration for the "Wish Fulfilling" ring worn by First Lady Michelle Obama came from the exquisite lattice windows used in ancient Chinese gardens. The lattice patterns add variety to the inner and outer parts of the ring. Photo courtesy of Yewn. Bottom right: A representative lattice window in the Humble Administrator's Garden in the Classical Gardens of Suzhou. The exquisite design and craftsmanship of this window lend elegance to the view behind it. Photo by Wenrong Cao.

This ring was a favorite of First Lady Michelle Obama, who wore it in 2011 when President Obama hosted a banquet for Queen Elizabeth II and Prince Philip. The ring caught the attention of many notable guests that evening (Adducci, 2011).

TRADITIONAL CRAFTSMANSHIP

China has a long history of using gold and silver in jewelry design, and gold still dominates the domestic jewelry market. Imperial artisans were once able to spend considerable time on a piece of jewelry commissioned by the emperor. Today very few can afford to practice time-consuming traditional craftsmanship. Yet the rise of mainland China's luxury market is changing this by encouraging the adoption of classic techniques.

One of these is filigree inlay art (figure 7). This combines two crafting skills: The first is filigree, the use of gold or silver threads of different weights. The second is inlay work, which involves setting stones and carving or filing precious metals around them. The artist responsible for the revival of this technique is Master Jingyi Bai (figure 8).

Master Bai's interest in both painting and pattern serves as the basis for her design life. As an art school student of precious metals, she gained some knowledge and skills, but she felt they were not enough to make her a successful master goldsmith and designer. Over the next 40 years, she perfected her technique in a filigree inlay art factory, where she was trained by older-generation master goldsmiths. In 2008, filigree inlay art was designated the Intangible Cultural Heritage of China, and Master Bai was named the official Representative Inheritor. Master Bai's participation in promoting filigree inlay art accelerated in 2009, after she began designing for well-known Chinese jade jewelry brand, Zhaoyi. These two events took her career to new heights.

In Brief

- After years of stagnation, Chinese jewelry design has undergone a renaissance, combining innovative techniques with culturally relevant motifs.
- Individual designers are able to develop unique pieces based on exposure to both Western methods and traditional Chinese craftsmanship.
- The growth of the Chinese jewelry market has led to a greater presence in the international industry, particularly in the luxury market.

Figure 7. This is a replica of a Qing dynasty hairpin recovered from a tomb in Beijing. The two main pearl-mounted patterns, composed of two layers of gold threads, are called ruyi *in Chinese and symbolize the fulfillment of one's wishes. Photo by Eric Welch, courtesy of Zhaoyi Xintiandi (Beijing) Jewelry Co., Ltd.*

Master Bai has created many replicas of historic filigree inlay art pieces. Today, she works full-time in her studio as Zhaoyi's chief designer of filigree inlay products (figure 9). Her jewelry is thoroughly Chinese, from the materials to the themes and craftsmanship. Her filigree inlay jewelry set "Royal Classic: Ripping Cloud" won Best Craft Inheritance Award at the second National Jewelry Processing Craft Competition in 2011.

Figure 8. Master Jingyi Bai is China's official Representative Inheritor of filigree inlay art. She works in her studio to create haute couture jewelry for high-end consumers. Photo courtesy of Zhaoyi Xintiandi (Beijing) Jewelry Co., Ltd.

Figure 9. This pair of earrings is from an award-winning filigree inlay jewelry suite by Master Bai. Thin gold threads were bent to form springs, which were rolled to form the individual cones. Craftsmen then joined the cones to shape each earring before mounting the faceted jadeite. This filigree technique, known as piling, gives the pieces a light, airy feel. Photo by Eric Welch, courtesy of Zhaoyi Xintiandi (Beijing) Jewelry Co., Ltd.

Master Bai's design philosophy is that a piece must succeed on its own in the market. To reach this goal, she considers both the quality of the craftsmanship and the contemporary composition. She says the first filigree inlay jewelry suite she designed and made for Zhaoyi was purchased—unexpectedly—by a young couple. For years, China's younger generation, especially in large cities, considered high-purity gold jewelry somewhat out of fashion. This was largely due to the lack of creative design. Today, young consumers prefer innovative gold jewelry.

DEPICTIONS OF CHINESE PHILOSOPHIES

Chinese jewelry designers benefit from many sources of inspiration. Poems, fairy tales, and paintings, for instance, are full of generations-old Chinese philosophies. Yue-Yo Wang (figure 10), a jewelry designer from Taiwan, has devoted herself to traditional Chinese jewelry design using such themes. She combines Chinese knotting art with modern design and manufacturing techniques to create her own pieces, giving each of them its own story.

Figure 10. Taiwanese designer Yue-Yo Wang, pictured here, creates jewelry that expresses Chinese philosophy and traditions. Photo courtesy of Wang Yue-Yo Creative Jewelry Design.

In China, knotting art can be traced back to around 1600 BC. Today the younger generation is embracing this ancient art with renewed interest. Wang began with knotted teapot covers and then developed her product lines to include clothing and decorations. She eventually realized that knotting art could be combined with modern jewelry manufacturing methods (figure 11), and established Wang Yue-Yo Creative Jewelry Design in Taipei about 20 years ago. The flagship store opened in 2007 in Beijing. Since then her company has greatly expanded its number of retail outlets. In 2012 Wang formed the Taiwan Creative Jewelry Design Association, hoping to attract designers focused on artistry and a desire to spread Chinese culture to the rest of the world (figure 12).

Wang's designs feature traditional Chinese symbols with elements of Chinese knotting art, such as long tassels and thread patterns. Gem materials often seen in her designs include opal, coral, jadeite, tourmaline, and chalcedony (figure 13). These gems are time-honored favorites of the Chinese people. Wang believes that every gem has its own spirit, and she is inspired to find it and express it through her jewelry.

Wang's designs, with their balanced and harmonious color and materials (figure 14), reflect the philosophy laid out circa 500 BC in *Zhong Yong*, translated as *The Doctrine of the Mean*. *Zhong* symbolizes impartiality, while *Yong* represents permanence. This classic text was one of the first books composed by the disciples of Confucius and has been a central tenet of the philosophy ever since. Intellectuals practiced this philosophy in their daily lives, while the ruling class applied it to management strategy. After generations, Confucian philosophy became the barcode of Chinese culture and remains so to this day. This is reflected in art, symmetry patterns, and motifs. The aesthetic standard the Chinese people hold is also based on this philosophy. Chinese painting, calligraphy, and carving all reflect this standard, which is exemplified by Wang's jewelry.

Figure 11. This necklace by Yue-Yo Wang features a knotted neckpiece and a rose quartz pendant mounted in 18K gold. Photo courtesy of Wang Yue-Yo Creative Jewelry Design.

Figure 12. Yue-Yo Wang's design and marketing style has taken her jewelry into the world of high fashion. Photo courtesy of Wang Yue-Yo Creative Jewelry Design.

INNOVATIVE DESIGN TECHNIQUES

Shirley Zhang, one of China's leading designers (figure 15), has been in the industry since the 1990s. She has created her own patented jewelry-making methods while importing Western techniques. Zhang's small factory, Meiher Jewelry Styling Research Center, performs every manufacturing step from design to finished product. This allows Zhang to test and develop new manufacturing processes.

Figure 13. Jadeite is one of China's most treasured gemstones. This ring by Yue-Yo Wang uses jadeite to portray the dragon and 18K gold for the phoenix. In Chinese culture, the dragon and phoenix symbolize man and woman, respectively. The dragon and phoenix are seen rejoicing together in the sky, a scene that represents the prosperity of a nation or a family. Photo courtesy of Wang Yue-Yo Creative Jewelry Design.

Figure 14. Yue-Yo Wang used a combination of green jadeite and red coral in this necklace. The goldfish symbolizes good fortune in Chinese culture, while a pair of goldfish symbolizes everlasting marriage. The Chinese character between the two fish is a traditional wedding symbol, while the boy and the lotus beneath them represent wishes for the family's prosperity. The immediate sense of perfect symmetry characterizes many of Wang's designs. Photo courtesy of Wang Yue-Yo Creative Jewelry Design.

These efforts proved worthwhile when Zhang's masterpiece, "Dancing on the Flowers" (figure 16), won a special award at the 2012 National Gems & Jewelry Technology Administrative Centre jewelry design and manufacturing skills competition. The suite, accented with bee and flower designs, includes a shoulder drape, a cuff bracelet, and a pair of earrings. In Chinese culture, bees symbolize the essential character trait of diligence. This design competition was a salute to the accomplishments of the Chinese gem and jewelry industry over the previous 20 years, and Zhang used the bees to represent the industry's diligent work. A variety of

Figure 15. Independent jewelry designer Shirley Zhang's creative philosophy rests on the belief that the piece must integrate craftsmanship and inspiration. Photo courtesy of Shenzhen Meiher Jewelry, Ltd.

gemstones and setting techniques were applied. Of these items, the shoulder drape is the most breathtaking. It features patented "dumbbell" buckle links between the honeycomb cells, allowing the piece to move freely and drape perfectly on the wearer's shoulder, giving the feeling of silk fabric rather than gold. The wearer can also reshape the piece by disconnecting and reattaching the links in various combinations for versatility.

Another patented technique applied to this shoulder drape is the "honeycomb" setting of the colored stones in the flowers, allowing more light to pass through the stones. The color and setting are equally attractive on both sides of the petals, resolving an age-old design and setting challenge.

Zhang's experience working overseas opened her eyes to the Western jewelry industry and inspired her to apply some of its methods. One example is her use of plique-à-jour (figure 17). Developed in France and Italy in the early 14th century, this technique differs from standard enameling in that the precious metal frames that contain the glass material have no backing, allowing light to pass through. This creates the stunning effect of a miniature stained glass window within a piece of jewelry. Plique-à-jour is commonly applied to jewelry and pocket watches by Western jewelers, including internationally known brands such as Van Cleef & Arpels, Cartier, and Tiffany. Zhang and her team spent years researching and test-

Figure 16. Shirley Zhang's award-winning jewelry suite "Dancing on the Flowers" features a total of 1,002 colored stones and 4,986 diamonds. Zhang applied several of her patented jewelry manufacturing techniques in its creation. Photo courtesy of Shenzhen Meiher Jewelry, Ltd.

Figure 17. This plique-à-jour pocket watch cover was created by Shirley Zhang. Courtesy of Shenzhen Meiher Jewelry, Ltd.

ing this technique. Her company is now the only one in mainland China that applies it to jewelry.

Zhang's jewelry emphasizes the fine colors of the gemstones, aiming for harmony. She also likes to coordinate colors with different shapes or cultural themes and to express her love of nature through her designs. Her styles blend innovative craftsmanship with oriental aesthetics, making use of unique combinations of materials and colors.

REAL JEWELRY AND REAL JOY

In his 2011 book *Luxurious Design: My Way of Designing Jewelry*, Jin Ren (figure 18) shares the words he lives by: "If you want a nicely designed ring, come visit me." If the whole luxury market is an ivory tower, he believes that natural gemstone jewelry is the top of that tower and design is its structure and soul. The ring is one of the most common jewelry items but also the hardest to design, according to Ren. He considers his work in ring design the major accomplishment of his career. One of the most famous jewelry designers in China, he is also a founder of the School of Gemology at China University of Geosciences in Beijing and author of the first Chinese jewelry design textbook.

With a PhD in geology, Ren never expected that one day he would co-host an haute couture show in Paris with world-class fashion designer Laurence Xu. When asked about his design education, Ren confesses that he barely had any. His career as a designer began purely by chance, starting just as the Chinese gem and jewelry industry boomed in the 1990s. At

Figure 18. Jin Ren is also a jewelry design professor at China University of Geosciences in Beijing. Photo courtesy of RJ Jewelry Co.

the time, he was a professor in the country's only gemological program. The turning point came in 1993, when a magazine invited him to write about jewelry fashion trends. His reputation grew from there, eventually providing a foundation for his own brand, RJ (Ren, 2011).

Along with his name, the RJ brand stands for "Real Jewelry and Real Joy." He considers jewelry design a matter of controlling shape, size, color, and dynamics, combined with a strong emphasis on culture (Ren, 2011). His designs combine traditional and contemporary concepts, encompassing mechanical design techniques and often reflecting a storyline that connects one piece to another (figure 19).

Ren and his friend Laurence Xu often get together to discuss fashion trends and design ideas. Because they share common interests, Xu invited Ren to be the jewelry designer for his collection at Paris Haute

Figure 19. This suite with colorless, yellow, and black diamonds was inspired by snakeskin and its ability to be shed. The earrings (left) depict the beginning of the shedding process, when the removal of old skin starts to expose the new skin beneath it. The ring (center and right) represents the culmination, when the beautiful new skin is fully revealed. Jin Ren considers this a metaphor for human beings, who must experience periodic transformations. Photos courtesy of RJ Jewelry Co.

Couture in 2013. Xu's majestic garments and Ren's matched jewelry suites reflect their shared identity and heritage (figure 20).

Ren says his themes come from outings with family and friends, where he is inspired by people, architecture, movies, and ancient fairy tales (Ren, 2011). His jewelry suite "Journey to the West" is based fairy tale that is considered one of the four great masterpieces of Chinese literature. Baroque pearls represent the four main characters on their expedition to the West, including the famous Monkey King (figure 21). Their adventures are treasured childhood memories for almost every Chinese person.

REVIVAL OF GOLD-JADE CULTURE

Jade-mounted gold jewelry has a long history in Chinese culture, where gold represents splendor and jade symbolizes elegance. Chinese people use the relationship between gold and jade to symbolize a happy marriage. For political and economic reasons, the market for this type of jewelry was very limited for many years ("Revival of gold-jade culture…," 2014). After the jade-mounted 2008 Olympic medals were announced, the market sensed an opportunity to revive what is known as the gold-jade culture.

Shanghai jewelry designer Kaka Zhang's interests and talents encompass art, science, and business (fig-

Figure 20. This suite includes earrings and a bangle inspired by the peacock, which is also the theme of the gown. Carefully chosen tourmaline, sapphire, topaz, tsavorite, and diamonds set in 18K white gold represent the peacock's feathers. Jin Ren designed the pieces so that each feather moves freely. A 3 ct diamond hidden under the bangle's feathers can be disconnected and worn separately. Photos courtesy of RJ Jewelry Co.

Figure 21. Left: Jin Ren's 2014 collection "Journey to the West" is based on the Chinese fairy tale of the same name, as illustrated here. Right: Baroque pearls portray the master and his three disciples, capturing their essential qualities (clockwise from top left): Master Tang Sanzang's mercy, the Monkey King's boldness, Sha Wujing's honesty, and Zhu Bajie's greed. Courtesy of microfoto (left) and RJ Jewelry Co. (right).

ure 22). She designs for the high-end, mid-range, and commercial markets, using designs and jadeite qualities to suit each market level. When she was three, her father taught her painting. Her high school and university studies included science and technology as well as gemology, leading her to a career in jewelry design and e-commerce.

Ninety percent of Zhang's business is on the Internet, where she has a loyal and enthusiastic following. She operates her design studio and website from her home. Her jewelry is manufactured in Shenzhen, where skilled master jewelers turn her designs into finished pieces.

When Kaka Zhang purchased her first piece of jadeite jewelry as an adolescent, she never expected to become a designer in her own right. Along with the highly desirable imperial jadeite, Zhang uses colorless transparent jadeite, which has gained popularity among young female consumers in the past several years.

Most of Kaka Zhang's design inspirations come from nature, also a major theme of traditional Chinese paintings (figure 23). She takes advantage of various colors and patterns and is often inspired by the jadeite carving itself. If its shape reminds her of something she has seen or heard—an old saying, a poem, a scene, or a painting—she bases her design on that theme (figures 24 and 25).

Jadeite is most often available as a carving whose beauty has been interpreted and revealed by the carver. The designer must consider the carving and envision the form or theme it will take. Although the gem cannot be altered, the composition may be enhanced by precious metal craftsmanship and other elements to express the theme in the designer's inimitable style.

Zhang believes that to achieve success, she must educate her customers about jewelry design, materials, and manufacturing. Her dream is to establish a private jewelry club where she can create a relaxed environment and connect with each customer.

THE FUTURE

Over the past decade, Chinese jewelry designers have made great strides in matching the rapid growth of

Figure 22. Shanghai jewelry designer Kaka Zhang is devoted to reviving the gold-jade culture. Photo courtesy of Kaka's Gem Eyes.

the domestic gem and jewelry market. Many are now well-known internationally. As Chinese designers continue to gain recognition, many more jewelry professionals will consider a future in design.

Native designers have come to understand that they must take advantage of their common cultural background, drawing from the heritage of time-honored craftsmanship and respect for the Chinese philosophical system. In the luxury market of the future, uniqueness will surpass high value (Yang, 2014).

Figure 23. The hairpin was one of the most important personal decorations for women of ancient China, and the butterfly is the traditional symbol of the loyalty of love. The dangling butterfly can be easily detached and worn as a pendant. Photo courtesy of Kaka's Gem Eyes.

Haute couture has a long history in China, though it was once limited to the royal family and the highest social classes. The high-end design market has seen more progress than other market sectors in the past decade. Now all top brands—and even some independent designers and small-scale stores—offer high-end custom design services. Designers now focus more on catering to the main-

Figure 24. This small jadeite carving reminded Kaka Zhang of a fish. She designed a fishing pole and breaking wave around that theme and called the piece "Fishing Fun." One Chinese adage describes a famous intellectual fishing with no bait and the hook above the water. Rather than forcing things to happen, the true intellectual "goes with the flow." Many Chinese consider this the highest spiritual state. Photo courtesy of Kaka's Gem Eyes.

Figure 25. Named "Beautiful Opera Singer," this ring displays intricate metalwork resembling a style of hat once worn by female Peking Opera singers. The jadeite cabochon symbolizes the beauty of their faces and the purity of their hearts. Photo courtesy of Kaka's Gem Eyes.

stream commercial jewelry market by learning from the Western world while maintaining many of their valued traditions. Leading jewelry enterprises are improving commercial jewelry design, hopefully resulting in more innovation in the near future. In 2013 and 2014, Rio Tinto launched a series of commercial lines of its Argyle diamond jewelry in China. Instead of marketing the diamonds themselves, Rio Tinto featured their commercial line designers in promotions through multiple media channels. The majority of them were young Chinese designers.

Chinese designers, especially large brands, are also making a global impact in the high-end jewelry market. Two recent examples are Chow Tai Fook Jewellery Group's purchase of the U.S. diamond company Hearts on Fire and French luxury retailer Kering's acquisition of Chinese jewelry house Qeelin. While Western brands have typically dominated the market, Chinese brands have gained an international foothold through their distinctive design, cultural connotations, and fine craftsmanship. The influence of the "Chinese soul" goes both ways.

ABOUT THE AUTHORS

Mr. Lucas is manager of field gemology and Ms. Chapin is managing editor for content strategy at GIA in Carlsbad, California. Moqing Lin and Xiaodan Jia are gemologists at GIA's Hong Kong laboratory.

ACKNOWLEDGMENTS

The authors thank GIA for funding the trip to China. They are grateful for the assistance of Dickson Yewn, Shirley Zhang, Jingyi Bai, Jin Ren, Yue-Yo Wang, and Kaka Zhang, who agreed to be interviewed and provided their own photos as well as jewelry pieces to photograph. Special thanks also go to the designers' assistants for facilitating this project.

REFERENCES

Adducci S. (2011) Contemporary Chinese jewelry. *Departures*, http://www.departures.com/articles/contemporary-chinese-jewelry.

Chen W.H. (2014) Jewelry design contests. *China Gems*, Vol. 94, pp. 24–29 [in Chinese].

Chinese jewelry firms design brighter future (2014) *China Daily*, October 3, http://europe.chinadaily.com.cn/epaper/2014-09/12/content_18587486.htm.

Hofstede G., Bond M.H. (1988) The Confucius connection: From cultural roots to economic growth. *Organizational Dynamics*, Vol. 16, No. 4, pp. 5–21.

Hsu T., Lucas A., Qiu Zh. L., Li M., Yu Q.Y. (2014) Exploring the Chinese gem and jewelry industry. *G&G*, Vol. 50, No. 1, pp. 2–29, http://dx.doi.org/10.5741/GEMS/50.1.2.

Ren J. (2011) *Luxurious Design: My Way of Designing Jewelry*. Zhejiang University Press [in Chinese].

Revival of gold-jade culture in the modern gem and jewelry industry (2014) *China Jeweler*, http://biz.ifeng.com/zhubaowang/zhubaohangye/tebiezhuanti/wdhjwzzhjzbzgf/detail_2014_06/09/2400792_0.shtml [in Chinese].

World Gold Council (2014) LoveGold meets Dickson Yewn. *LoveGold*, http://www.lovegold.com/lovegold-meets/dickson-yewn.

Yang F. (2014) Haute couture of jewelry (in Chinese). *China Gems*, Vol. 95, pp. 158–161.

The Dr. Edward J. Gübelin Most Valuable Article AWARD

First Place

Sri Lanka: Expedition to the Island of Jewels

Summer 2014

Andrew Lucas, Armil Sammoon, A.P. Jayarajah, Tao Hsu, and Pedro Padua


Andrew Lucas


Armil Sammoon


A.P. Jayarajah


Pedro Padua

Andrew Lucas is a field gemologist in GIA's content strategy department. He researches and documents the entire mine-to-market gem and jewelry industry for GIA education; he also presents seminars on colored stones and diamonds. **Armil Sammoon** is the founder of the Sapphire Capital Group and a member of the board of directors of the National Gem and Jewellery Authority. **A.P. Jayarajah** is CEO of Wellawatta Nithyakalyani Jewellery and chairman of the Sri Lanka Gem and Jewellery Association. **Tao Hsu** is the technical editor of *Gems & Gemology* and a contributor to the Research and News section of GIA's website. She received her doctorate in geology from the University of Southern California. **Pedro Padua** is the senior video producer at GIA. He also contributes to GIA website articles and educational course material. He received his master's degree in communications from Loyola Marymount University.

Second Place

Exploring the Chinese Gem and Jewelry Industry

Spring 2014

Tao Hsu, Andrew Lucas, Zhili Qiu, Mu Li, and Qingyuan Yu


Tao Hsu


Zhili Qiu


Mu Li


Qingyuan Yu

Tao Hsu and **Andrew Lucas** were profiled in the first-place entry. **Zhili Qiu** is a professor in the earth science department of Sun Yat-sen University. Dr. Qiu received his doctorate in geology from Zhejiang University and has been devoted to gemological research and education since the early 1990s. **Mu Li** is the vice chairman of the Diamond Administration of China (DAC). **Qingyuan Yu** is the colored stone director of a global mineral company in Guangdong, China.

Third Place

Three-Phase Inclusions in Emerald and Their Impact on Origin Determination

Summer 2014

Sudarat Saeseaw, Vincent Pardieu, and Supharart Sangsawong


Sudarat Saeseaw


Vincent Pardieu


Supharart Sangsawong

Sudarat Saeseaw is a senior manager of colored stones at GIA's Bangkok lab. She obtained a master's degree in analytical chemistry from Mahidol University in Thailand. **Vincent Pardieu** is senior manager of field gemology at GIA in Bangkok. He has led 64 successful field expeditions to gemstone mining areas in order to collect samples for the GIA reference collection. **Supharart Sangsawong** is a research scientist at GIA in Bangkok. He earned his doctorate in analytical chemistry from Mahidol University.

Thank you to all the readers who voted. In additon to our winning authors, we congratulate **Richard Xu** of Bakersfield, California, whose name was randomly drawn from the entries to win a one-year subscription to *G&G*.

Most Valuable Article

AMETHYST FROM BOUDI, MOROCCO

Fabrizio Troilo, Abdelghani El Harfi, Salahaddine Mouaddib, Erica Bittarello, and Emanuele Costa

Amethysts from Boudi, Morocco, are characterized by double terminations and hourglass-shaped color zoning. This study provides information about the geology of the deposit, the mining of the material, and its internal and external features. Photos show the amethyst's strong color zoning. Analysis of the needle-shaped mineral inclusions identified them as hematite, oriented along the crystal's growth direction.

For 25 years, the Moroccan locality of Boudi in the Tata province (part of the Guelmim-Es-Semara region) has yielded amethyst crystals that show double termination and hourglass-shaped color zoning (figure 1). The deposit was discovered in 1990, and for years the amethyst was extracted on a small scale by local villagers using handheld tools. Only small quantities were sold to tourists, and the low market value limited production. The first foreign mineral dealer to visit the location was Zee Haag in 2007. These specimens debuted internationally at the 2009 Mineral & Gem show at Sainte-Marie-aux-Mines, Europe's second-largest mineral event. Since then, dealers and collectors have visited the site, and the deposit was featured in an *extraLapis* monograph on amethyst (Praszkier and Rakovan, 2012).

In early 2012, the Geostone Group in Casablanca obtained exclusive rights to the mine (an open quarry, in accordance with Moroccan law). The company began production in early 2013, after building an off-road track to comply with environmental regulations. This article focuses on the geological setting of the deposit and the gemological features of the amethysts obtained from it.

LOCATION AND ACCESS

The village of Boudi (figure 2) is located in the arid Central Anti-Atlas mountain range, about 30 km

Figure 1. The color zoning of amethyst from Boudi often displays a characteristic hourglass shape. Photo by Abdelghani El Harfi and Salahaddine Mouaddib.

See end of article for About the Authors and Acknowledgments.
GEMS & GEMOLOGY, Vol. 51, No. 1, pp. 32–40,
http://dx.doi.org/10.5741/GEMS.51.1.32.

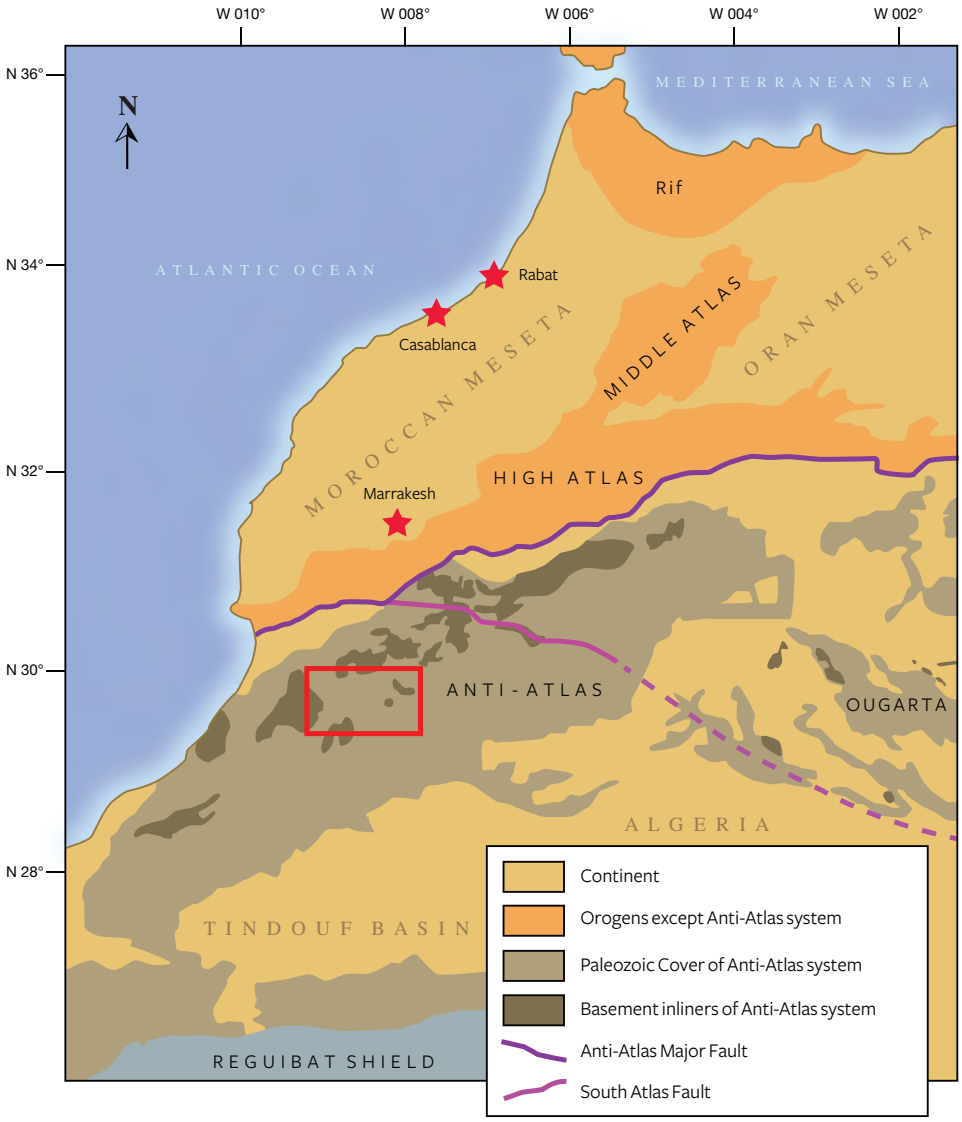

Figure 2. This map shows the location of the Boudi quarry (outlined in red), in the Anti-Atlas mountain range of Morocco. From Faik (2005).

northeast of the town of Tata. Boudi is accessed by taking National Road 12 for 40 km, followed by a sinuous 14 km road and a newly built off-road track for the final 4 km. The region is mountainous, with an altitude ranging from 1,400 to 1,800 m, and set in a very arid and forbidding environment (figure 3). The mine is located 6 km east of the Tagragra Tata Precambrian basement, a kind of erosive depression on the crest of an anticline, similar to a tectonic window. Figure 4 shows a simplified geological map of the region; amethysts are found in the Lower Cambrian Issafen Formation (Faik et al., 2001; Faik, 2005).

GEOLOGY AND MINERALOGY

The deposit is exposed along an eroded area on the south side of an anticline formed by rock of Cambrian age. It covers hundreds of square meters in a fractured area crossed by hydrothermal veins. The host rock is siltstone-sandstone belonging to the Issafen Formation of the Lower Cambrian, a schist formation composed of mudstone with marl and sandstone intercalations in the upper zone, dolomitic limestones (with stromatolites) in the middle, and purplish red mudstones in the lower part, again with intercalations of stromatolitic limestones and dolostones, all of these in stratigraphic contact. In the simplified geological map, the Issafen Formation is below the Schist-Limestone and Limestone series of Lower Cambrian age, and thus is not visible (again, see figure 4).

At Boudi, quartz is found either scattered in a silt-sandstone matrix or within cavities of a complex fault and fractures system. Small openings are completely filled with interlocking quartz crystals. In the

Figure 3. The area near Boudi is arid and rich in geological features. Photo by Abdelghani El Harfi and Salahaddine Mouaddib.

reddish mudstones, floating quartz specimens are always found as single crystals without matrix, usually singly terminated but sometimes doubly. The amethyst clearly formed by hydrothermal deposition, but the condition of the crystals suggests they were removed from the original site of crystallization and subsequently encapsulated in the mudstones. The deposit could be regarded, then, as both primary and secondary. The authors hypothesize that the well-shaped quartz crystals originated in the faults and veins in the surrounding limestone, and then eroded and redeposited in the residual mudstones.

In Brief

- Amethyst mined from Boudi, Morocco, features distinctive hourglass-shaped color zoning, double termination, and red needle-shaped hematite inclusions.
- These inclusions help to differentiate the formation and the origin of the Boudi specimens.
- Recent mechanized mining efforts have led to greater availability of gem-quality Boudi material, which rivals "Siberian" amethyst in coloration.

MINING

Conditions are challenging due to the location's remoteness, the hot summer temperatures, and the lack of water and electrical power at the mine. Since the beginning of 2013, the open pit has been worked by an excavator and a loader that easily remove the fractured limestone and mudstone containing scattered quartz crystals and fragments (figure 5). The miners come from Boudi, Targuant, and other surrounding villages, so the mine is an economic resource for the area. Figure 6 shows a selection of the production from the mine.

The quarried amethyst crystals vary in size, color, and quality. Four-wheel-drive vehicles carry the production to storage facilities. About 90% of the crystals are well formed and detach from the matrix as individual crystals. High-pressure washing with a

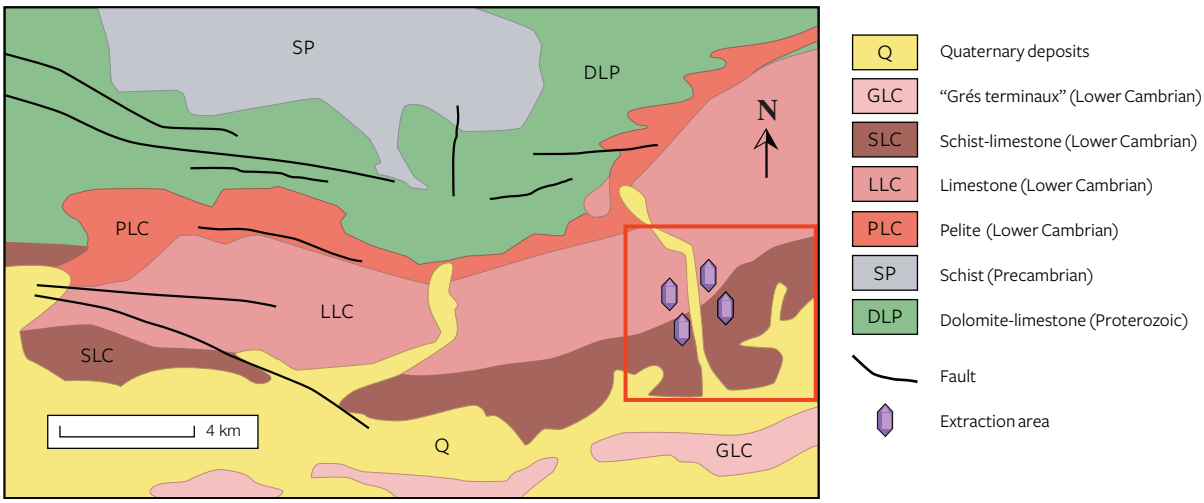

Figure 4. A simplified geologic map of the area hosting the amethyst quarry. The Issafen Formation lies below the Limestone series of Lower Cambrian age and is not visible in the map. The red square indicates the mining area. From Faik (2005).

brush and water gun removes the clays that cover the crystals. Encrusted crystals are soaked for a short time in a mixture of diluted hydrochloric acid to dissolve the residual limestone.

DESCRIPTION OF THE AMETHYST

Amethyst from Boudi displays a fairly typical morphology. The crystals have well-developed prism faces, and in some cases they present the double termination that characterizes the locality. Rhombohedral faces are well developed (figure 7). Euhedral crystals are common, ranging from 1 to 10 cm in length and rarely up to 15 cm. The highest-quality material is in the 1–5 cm range. The crystal faces are normally clean or coated by carbonates and clay minerals.

The color quality and distribution varies widely, from light purple to very deep purplish red, often showing sharp color concentration along the rhom-

Figure 5. The front of the open quarry in Boudi. Photo by Abdelghani El Harfi and Salahaddine Mouaddib.

Figure 6. The amethysts extracted from the piles are still covered with matrix and carbonates. The well-shaped crystals range from 2 to 5 cm in diameter. Photo by Abdelghani El Harfi and Salahaddine Mouaddib.

bohedral direction. The color concentration usually resembles a core, beyond which the quartz becomes colorless toward the surface. Abundant oriented, needle-like reddish inclusions are often found, mainly in the deeply colored stones. Color banding may also be evident in the deeply colored core, mostly oriented parallel to the rhombohedral crystal faces.

Figure 7. This crystal from Boudi displays the classic morphology of amethyst. Clearly visible is the habit of the hexagonal prism and the two different rhombohedra (positive and negative). The hematite inclusions, mainly oriented perpendicular to the surface of the prism, are clearly visible in the outer colorless portion. Photo by Abdelghani El Harfi and Salahaddine Mouaddib.

Figure 8. This suite of amethyst from Boudi, titled "Purple Champagne," received first place in the 2014 AGTA Spectrum Awards, Pairs & Suites. Courtesy of Ai Van Pham Gem & Gold Creations, Scottsdale, Arizona.

The purple coloration of amethyst is caused by the presence of an interstitial Fe^{4+} color center in the quartz (Rossman, 1994), combined with irradiation from natural gamma-ray sources. Irradiation creates color centers that absorb some light wavelengths and produce the very attractive tone seen in this material. The hourglass zoning distinctive of the Boudi mine is created when the iron is incorporated preferentially along the rhombohedral faces. During the growth of the crystal, with the development of the face, the purple sector assumes its typical form.

While most of the material produced is cabochon-grade, a consistent percentage—maybe 20%—is suitable for faceting. Most of the rough shows color zoning, which is often regarded as an unwanted feature but can be very attractive in the hands of skilled and creative gem cutters. This was the case with an award-winning suite recently cut from Boudi amethyst (figure 8). Both cabochon- and facet-grade

Figure 9. This 22.5 ct faceted trilliant is from the Boudi quarries. Photo by Abdelghani El Harfi and Salahaddine Mouaddib.

material can display strong colors, and significant amounts of rough show a deep reddish purple color. The best crystals exhibit purple flashes with a red tinge. Faceting this deeply colored material can reveal strong red overtones; these stones are known in the trade as "Siberian" amethyst (Wise, 2005). Fine stones larger than 20 carats are regularly faceted, but most of the faceting material is in the 5–10 ct range. Cabochon-grade material up to 100 ct is common. To date, we have not seen heat treatment applied to amethyst from Boudi, which is rarely dark enough to warrant it (Götze and Möckel, 2012; figure 9).

MATERIALS AND METHODS

Gemological properties of 20 faceted amethysts supplied by the Geostone Group were analyzed using standard gem testing instruments. The samples were representative of the material produced from this locality in both their color (light pinkish purple to dark reddish purple) and size range (6.06–17.92 ct).

Refractive indices and birefringence values were obtained with a standard refractometer and a near-monochromatic light source. Specific gravity was determined using a Mettler-Toledo hydrostatic meter. Reactions to ultraviolet radiation were observed using standard long-wave (365 nm) and short-wave (254 nm) lamps. Visible absorption spectra were obtained with a Krüss prism spectroscope. Visual features were observed using an SZM-2 zoom microscope from Gemmarum Lapidator with darkfield illumination at 20×–80× magnification. Inclusions were photographed with an Olympus BX41 microscope using immersion techniques.

Chemical composition data were obtained with semi-quantitative, non-destructive EDS microanalysis for determination of major and minor elements. Micro-Raman spectroscopy was used for mineral inclusion identification purposes.

EDS data were acquired at Turin University's Department of Earth Science using a Cambridge Stereoscan 360 scanning electron microscope, equipped with an Oxford Inca Energy 200 EDS for microanalysis and a Pentafet detector and an ultrathin window for the determination of elements with atomic number down to boron. All spectra were obtained at 15 kV accelerating voltage, 25 mm working distance, and 1 µA probe current for 60 to 300 seconds. Primary standardization was performed on SPI Supplies and Polaron Equipment analytical standards. Daily standardization was performed on a high-purity metallic cobalt standard.

Unoriented micro-Raman spectra were obtained at Turin University with a HoribaJobin Yvon LabRam HRVIS apparatus, equipped with a motorized x-y stage and an Olympus microscope. The backscattered Raman signal was collected with a 50× objective, and the Raman spectrum was obtained for a non-oriented position. The 632.8 nm line of a He-Ne laser was used as the excitation wavelength; laser power was controlled by a series of density filters. The minimum lateral and depth resolution was set to a few µm. The system was calibrated using the 520.6 cm^{-1} Raman band of silicon before each experimental session. The spectra were collected in 8 to 10 acquisitions with single counting times ranging between 40 and 120 seconds. Spectral manipulation such as baseline adjustment, smoothing, and normalization were performed using the LabSpec 5 software package (HoribaJobin Yvon, 2004 and 2005). For band component analysis, we used the Fityk software package (Wojdyr, 2010), which enabled us to select the type of fitting function and fix or vary specific parameters accordingly. The spectra were recorded for the 100–1300 cm^{-1} range using the LabSpec 5 program.

RESULTS AND DISCUSSION

The refractive indices of the 20 amethyst samples from Boudi varied from 1.540 to 1.542 (o-ray) and 1.549 to 1.552 (e-ray), with birefringence from 0.009 to 0.010. Pleochroism, observed with a calcite dichro-

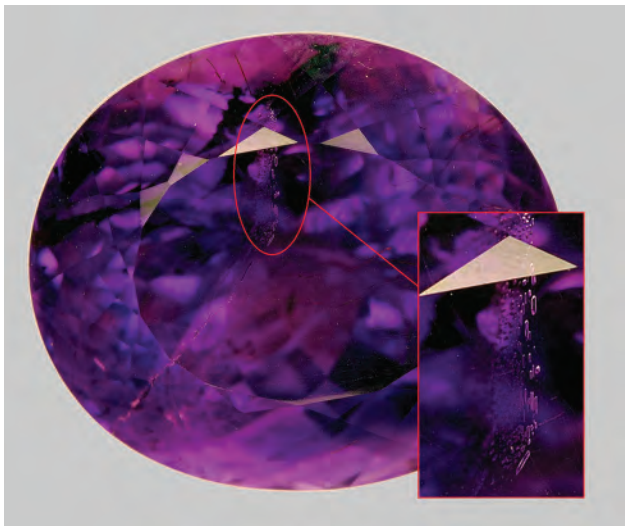

Figure 10. This amethyst sample weighs 17.94 ct. Clearly visible in the magnified inset is a veil consisting of one- and two-phase inclusions. Photo by Emanuele Costa and Fabrizio Troilo.

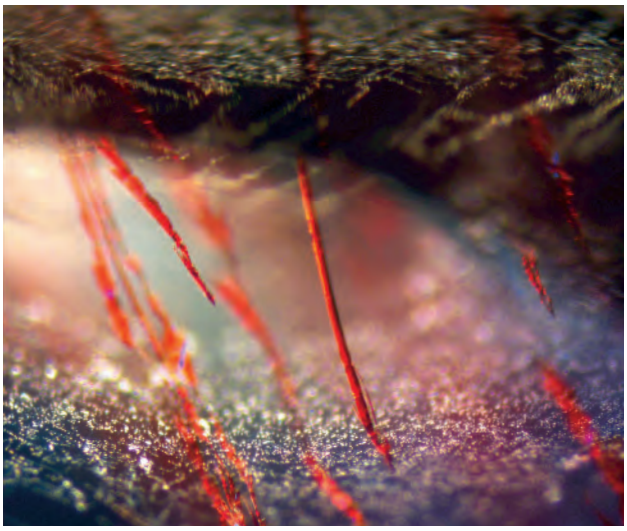

Figure 11. Microscopic observation reveals the red hematite inclusions. Photo by Emanuele Costa and Fabrizio Troilo, field of view 210 mm.

scope, varied from weak to medium bluish purple to reddish purple. None of the samples showed any reaction to either short- or long-wave UV radiation. No absorption spectra were observed using the Krüss spectroscope.

Fluid inclusions with a veil-like pattern (figure 10) were common in the amethyst samples from Boudi. Individual fluid inclusions sometimes showed a moderate negative crystal form. Some of these inclusions had a two-phase character, with liquid and gas components.

The red, elongated solid inclusions were also the most interesting internal features and could be observed in almost every specimen analyzed (figure 11). The crystals' near-colorless zones were permeated by a series of fibrous red inclusions, approximately oriented from the different crystal faces toward the colored core, in which they gradually disappeared. The orientation of the tiny fibers was not crystallographic, but the general distribution of the fibers followed the crystal growth direction (figures 12 and 13). The needles had different lengths, but their diameters were quite consistent. Their microscopic appearance showed a morphology that seemed less angular and fragmented and more straight and continuous than the hematite "beetle leg" inclusions (once believed to be lepidocrocite) reported in the literature (Hyršl and Niedermayr, 2003; Leon-Reina et al., 2011).

These inclusions distinguish the material from synthetic amethyst, and their distribution and orientation within the stone could help to identify their origin as the Boudi deposit. To the best of our knowledge, such inclusions have not been described in detail until now.

Figure 12. A 9.14 ct faceted amethyst from Boudi displaying red hematite needle inclusions. Photo by Emanuele Costa and Fabrizio Troilo.

Figure 13. This 14.30 ct sample, viewed in immersion, clearly shows the distribution of the hematite inclusions, together with the uneven but distinct zoning of the purple color. Photo by Emanuele Costa and Fabrizio Troilo.

The nature of the inclusions was confirmed by EDS and Raman analysis. The EDS spectra showed only the presence of silicon and oxygen (from the host quartz crystal) as well as iron, but it was impossible to discriminate between various iron oxides and hydroxides. Raman analysis (figure 14) showed a close match between the obtained spectrum and those of quartz (R040031) and hematite (R050333) in the RRUFF database (Downs, 2006). Visible in detail were the typical intense band of quartz around 467 cm^{-1} and weak broad bands at 132, 209, 359, and 811 cm^{-1}. Additionally, the distinctive bands of hematite inclusions were observed. The Raman spectrum showed an intense band at around 299 cm^{-1}, with a weak shoulder at 302 cm^{-1}; multiple bands at 231, 251, and 267 cm^{-1}; medium-intensity bands at 413 and 619 cm^{-1}; and weak peaks at 490 (a shoulder of the most intense band of quartz), 664, 703, and 1160 cm^{-1}.

CONCLUSIONS

The Boudi quarry in the Anti-Atlas mountain range of Morocco was worked for more than 20 years in a largely artisanal and sporadic manner. Since 2014, mechanized mining has produced commercial quantities of amethyst for the jewelry industry. The deposit also yields amethyst with deep red tones that rival the highly sought "Siberian" material (Wise,

Figure 14. This Raman spectrum clearly indicates the peaks of hematite in the quartz matrix.

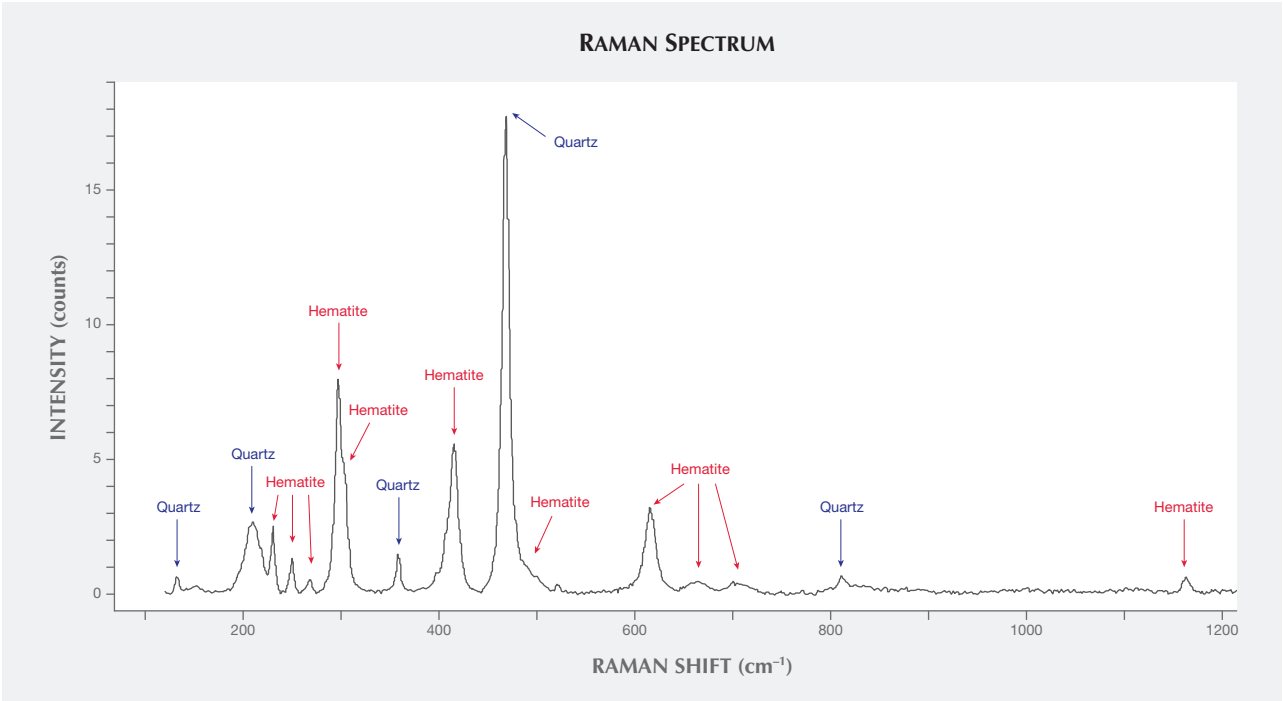

2005). The color of the stones varies, but a considerable quantity exhibits a deep purplish red color. Moreover, singular internal features distinguish the material's natural origin (about 50% of the stones have distinctive red needle hematite inclusions, typically observed in stones with deep color). Production is likely to expand, which means the gem market could see more of this amethyst.

ABOUT THE AUTHORS

Mr. Troilo is a geologist and graduate gemologist from the Istituto Gemmologico Italiano. He has published works about gemstone mining abroad as well as gemstone deposits in the Alps. Dr. El Harfi is professor of geodynamics in the geology department of Ibn Zohr University in Agadir, Morocco. Mr. Mouaddib is CEO at Geostone Group in Casablanca, Morocco (www.moroccanfire.com). Dr. Bittarello is a PhD geologist graduate at Turin University in Italy and an expert in mineralogical analysis. Dr. Costa (emanuele.costa@unito.it) is researcher and professor in biomineralogy and environmental geochemistry in the earth sciences department at Turin University.

ACKNOWLEDGMENTS

The authors would like to thank the reviewers for their helpful and constructive observations and suggestions, and the Geostone Group for providing the samples used in this study.

REFERENCES

Anderson B.W., Jobbins E.A. (1990) *Gem Testing*. Butterworths, 360 pp.

Downs R.T. (2006) The RRUFF Project: an integrated study of the chemistry, crystallography, Raman and infrared spectroscopy of minerals. *Program and Abstracts of the 19th General Meeting of the International Mineralogical Association in Kobe*, Japan. O03-13.

Faik F. (2005) Lithostratigraphie et structure de l'Anti-Atlas centre-occidental : du rifting fini-protérozoïque a l'orogenèse hercynienne. Master's thesis, Ibn Zohr University, Agadir, Morocco, 176 pp.

Faik F., Belfoul M.A., Bouabdelli M., Hassenforder B. (2001) Les structures de la couverture Néoprotérozoïque terminal et Paléozoïque de la région de Tata, Anti-Atlas centre-occidental, Maroc: Déformation polyphasée, ou interactions socle/couverture pendant l'orogenèse hercynienne? *Journal of African Earth Sciences*, Vol. 32, No. 4, pp. 765–776, http://dx.doi.org/10.1016/S0899-5362(02)00053-2.

Gotze J., Mockel R (2012) *Quartz: Deposits, Mineralogy and Analytics.* Springer, Berlin, 377 pp.

Horiba Jobin Yvon GmbH (2004, 2005) LabSpec [Software for Raman spectroscopic data analysis, acquisition and manipulation]. Version 5.64.15.

Hyršl J., Niedermayr G. (2003) *Magic World: Inclusions in Quartz.* Bode Verlag, Haltern, Germany 240 pp.

Leon-Reina L., Compana J.M., De la Torre A.G., Moreno R., Ochando L.E., Aranda M.A.G. (2011) Powder diffraction analysis of gemstone inclusions. *Powder Diffraction*, Vol. 26, No. 1 pp. 48–52, http://dx.doi.org/10.1154/1.3552672.

Praszkier T., Rakovan J. (2012) Hourglass figures – Bou Oudi amethyst. In H.A. Gilg, S. Liebetrau, G.A. Staebler, and T. Wilson, Eds., *Amethyst: Uncommon Vintage,* No. 16, Lithographie, Ltd., Denver, Colorado, pp. 102–105.

Rossman G.R. (1994) Colored varieties of the silica minerals. In P.J. Heaney, C.T. Prewitt, and G.V. Gibbs, Eds., *Silica: Physical Behavior, Geochemistry, and Materials Applications.* Reviews in Mineralogy, Vol. 29. Mineralogical Society of America. pp. 433–468.

Wise R.W. (2005) *Secrets of the Gem Trade: The Connoisseur's Guide to Precious Gemstones*. Brunswick House Press, Lenox, MA.

Wojdyr M. (2010) Fityk: a general-purpose peak fitting program. *Journal of Applied Crystallography,* Vol. 43, No. 5, pp. 1126–1128, http://dx.doi.org/10.1107/S0021889810030499.

VISIBLE ABSORPTION SPECTRA OF COLORED DIAMONDS

James E. Shigley and Christopher M. Breeding

Diamond color is usually the result of selective absorption of incident white light. The unabsorbed portion of this light is transmitted through the diamond and is interpreted by the human vision system as the perceived color. The spectroscope allows a gemologist to observe some of the more intense and narrower absorptions in the visible spectrum of diamond as dark bands at specific wavelengths. Yet the broader regions of absorption, which can be difficult to observe with the spectroscope, often have a greater influence on a diamond's color. A chart has been prepared to illustrate the visible spectra of various colored diamonds as recorded at low (liquid-nitrogen) temperatures with a spectrophotometer. The chart shows how similar diamond colors can result from different light absorption patterns.

In 2013, the authors published a simple chart listing the major optical defects that can occur at the atomic lattice level in diamond (Shigley and Breeding, 2013). The chart presented some basic information on those defects, including the ones responsible for the colors and ultraviolet fluorescence reactions of most diamonds. The brief article that accompanied the chart discussed the ongoing challenge presented by the identification of natural, treated, and synthetic diamonds. It also discussed how spectroscopy techniques, used to detect absorption and/or emission bands caused by those optical defects, play a leading role in making this important determination. GIA's laboratory staff, which has the opportunity to examine a large number of colored diamonds, faces this identification challenge on a daily basis.

A theoretically pure and defect-free diamond would be completely colorless, and a unique attribute would be its transparency (or lack of light absorption) across a wide portion of the electromagnetic spectrum from the ultraviolet through the visible and into the infrared regions. There are, however, intrinsic absorption features in the spectra of all actual diamonds. As discussed in our 2013 article, most diamonds also contain lattice defects which, in sufficient concentrations, can produce selective absorption of incident light. (In these instances, the lattice defects are often referred to as optical defects.) When white light strikes a polished diamond, some of the light is reflected, while the rest enters the diamond where it is refracted and dispersed based on wavelength. Some of the light energies (i.e., wavelengths) are absorbed by the defects, while the unabsorbed wavelengths are transmitted. When they exit the diamond, these transmitted wavelengths in combination can create the sensation of color in the human vision system (figure 1). Visible absorption spectroscopy is the analytical tool for understanding most causes of diamond coloration.

At GIA's laboratory, visible spectra of diamonds are recorded with a spectrophotometer. Since diamond is optically isotropic, the same spectrum can be recorded in any direction through the sample. The faceted stone can be positioned in any orientation as long as the light transmitted through it is sufficient to reach the instrument's detector. The gem's shape and facet arrangement can make this a challenge, though. The best positions are those where the light travels directly from the table facet to the culet, or across the diamond through the opposing girdle facets. The diamond is held in a cryogenic unit and cooled to low temperatures with liquid nitrogen. Removing heat from the sample produces a less noisy spectrum. Under these conditions, absorption features that result from certain optical defects are stronger and sharper. Data collection conditions are selected to produce a spectrum that extends from about 350 to 800 nanometers (nm).

Because of a polished diamond's high refractive index, light can be internally refracted a number of times within it, so the total distance traveled cannot be directly measured or calculated. This uncertainty makes it difficult to relate the strength of the light absorption (as recorded by the spectrophotometer) to the

See end of article for About the Authors and Acknowledgments.
GEMS & GEMOLOGY, Vol. 51, No. 1, pp. 41–43,
http://dx.doi.org/10.5741/GEMS.51.1.41.

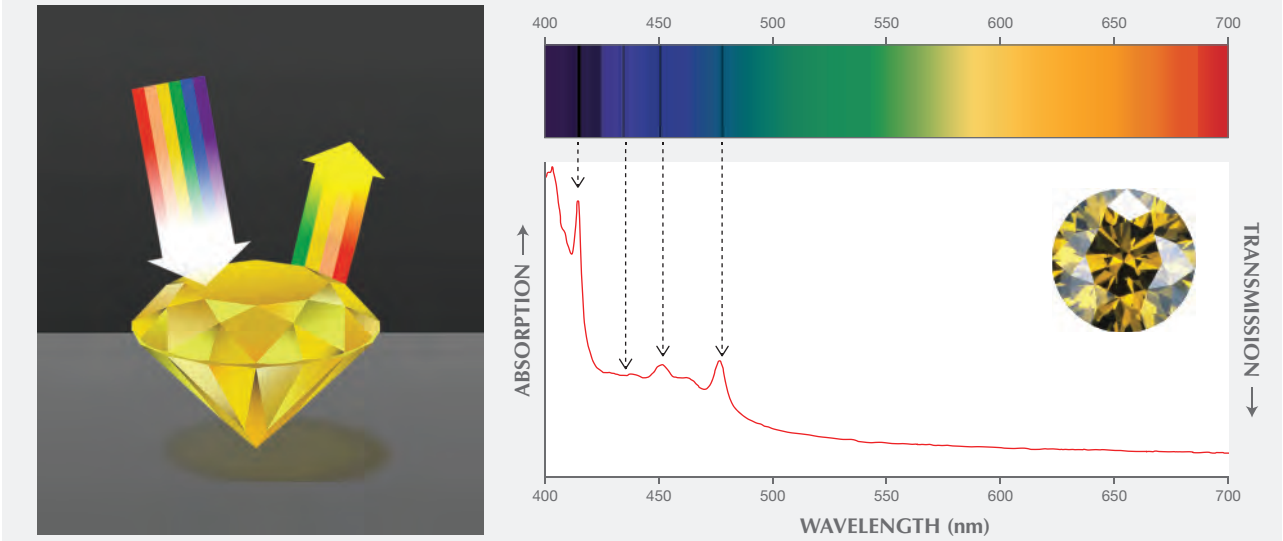

Figure 1. In most cases, transparent gemstones owe their color to selective absorption of light. In the case of a yellow diamond, the blue portions of the incident white light are absorbed by the diamond, while the remaining portions in combination are transmitted to the eye and interpreted by our vision system as a yellow color. In the spectroscope, this selective absorption is seen as a darkening toward the blue end of the spectrum (below 425 nm). Recording the spectrum with a spectrophotometer produces a graph of wavelength (horizontal scale) versus absorption (vertical scale). Greater absorption is represented by the higher portions of the spectrum trace, and greater transmission by the lower portions. Below 425 nm, the height of the spectrum trace increases. In the case of this yellow diamond, superimposed on this increasing absorption are several sharp absorption bands or peaks on the spectrum trace between 415 and 478 nm due to the N3 optical center. Gemologists often refer to this set of dark bands as the "Cape" absorption lines characteristic of type Ia yellow diamonds.

path length of light traveled within the gemstone. Yet this relationship can be estimated by comparing absorption peak height to the heights of some intrinsic absorption features. This relationship also provides an indirect way of comparing the visible spectra of diamonds of different sizes and faceting styles. Because of internal reflection and longer path lengths within the polished diamond, the face-up saturation of the color may appear stronger than the intensity of the absorption features (i.e., height of the absorption bands) in the visible spectrum would suggest.

Natural diamonds occur in all colors of the spectrum. A few colors, such as yellow and brown, are very common, but most are very rare. Nitrogen is the most widespread and abundant impurity element in diamond. It can be present in several optical defects, all of which produce absorption toward the blue end of the spectrum. These factors help explain the prevalence of yellow diamonds in nature. While the face-up appearance of colored diamonds is also influenced by their size and the choice of faceting style, visible absorption spectra provide a tool to understand most causes of diamond coloration.

The accompanying chart contains representative visible spectra and photos of the major color categories of diamond. The spectra are shown over the 400–750 nm wavelength range. Relative absorption is shown on the vertical scale of each graph, with light absorption increasing higher on the scale (and,

In Brief

- While lattice defects and physical causes such as mineral inclusions may contribute to diamond coloration, most color perception is due to the selective absorption of white light.
- The accompanying reference chart details the effect of light absorption patterns, recorded with a spectrophotometer, on diamond color.

conversely, light transmission increasing lower on the scale). Thus, the lower portion of each graph represents the transmitted portion of the spectrum that creates the material's color sensation. The chart summarizes the major categories of colored diamonds; it is not intended as a detailed discussion of diamond coloration. The graphs are grouped in columns and ranked in descending order of frequency. The colored diamonds included in the chart were selected because their spectra (and color) are principally the result of one main lattice defect. As discussed in our 2013 article, the cause of some defects is well understood, while others are not. We occasionally encounter unusual colors in diamonds whose visible spectra do not correspond to any of the categories shown on the chart.

The information presented on the chart suggests several observations:

1. In most cases, diamond colors result from different absorption spectrum patterns, with each pattern originating from one or more optical defects. This can be seen for the different yellow diamonds shown in the first column.
2. Broad and intense spectral absorption features are more important in producing various colors than sharp or weak bands. Conversely, sharp absorption bands (such as the N3 observed at 415 nm, H4 at 496 nm, and H3 at 503 nm) that can be seen using the spectroscope are helpful in gem identification. We used a spectrophotometer to record the visible spectra, as it can better capture broad absorption bands that are difficult or impossible to see with the eye through a spectroscope.
3. Similar diamond colors can result from different absorption spectra patterns. In other words, since perceived color is a combination of the wavelengths transmitted to the eye, different absorption patterns can produce similar colors. For example, type Ia and type Ib diamonds, which have different visible spectra patterns, can both exhibit a yellow color (although the color is usually more intense for the latter).
4. Some diamond colors are the result of just one optical defect, while others result from more than one defect. For example, the chart indicates that the GR1 defect can create a blue or a green color. The defect alone produces a blue color, but when there is also absorption toward the blue end of the spectrum due to nitrogen impurities, the resulting color is green.
5. Some diamond colors are simply the result of selective light absorption, while others stem from a combination of light absorption and light emission (or luminescence). For example, certain greenish yellow diamonds are yellow due to absorption, while the green component is due to luminescence.
6. Variations in the types of optical defects, and in their relative concentrations, produce slight color variations among similar diamonds.
7. Where a diamond photo is shown without an accompanying visible spectrum, the color is due to physical causes other than light absorption—most often the presence of mineral inclusions (e.g., numerous graphite inclusions causing black color in natural diamonds).

This chart is intended as a simple reference for those interested in understanding diamond coloration. While the visible spectra of diamonds are often presented in the gemological literature, compilations of spectra are rarely encountered.

REFERENCE

Shigley J.E., Breeding C.M. (2013) Optical defects in diamonds: A quick reference chart. *G&G*, Vol. 49, No. 2, pp. 107–111, http://dx.doi.org/10.5741/GEMS.49.2.107.

ABOUT THE AUTHORS

Dr. Shigley is distinguished research fellow, and Dr. Breeding is a research scientist, at the GIA Laboratory in Carlsbad, California.

Causes of Diamond Coloration

Yellow

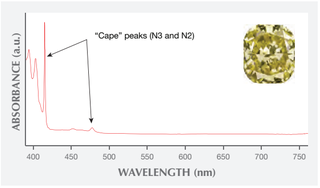

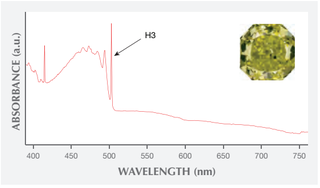

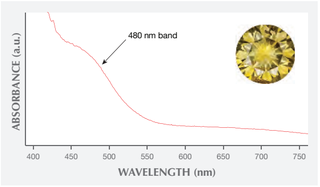

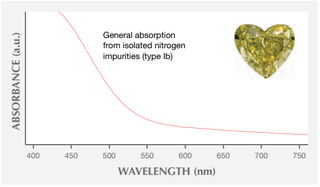

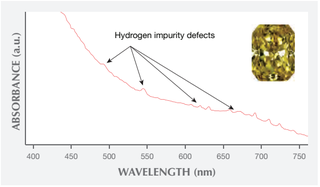

Green

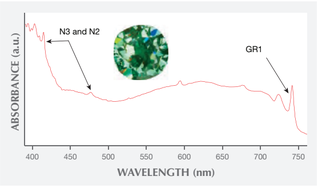

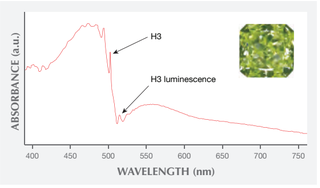

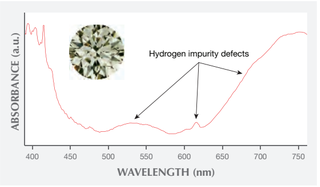

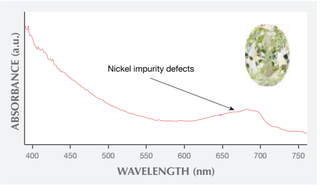

Blue/Gray/Violet

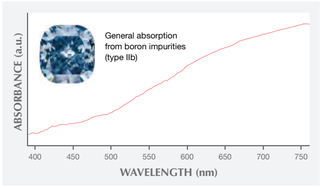

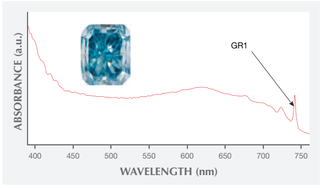

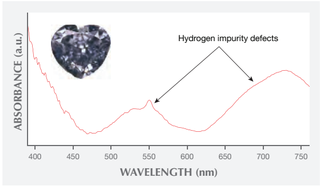

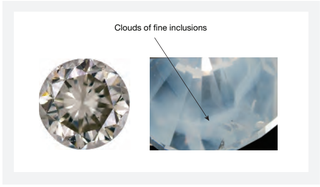

Orange/Brown

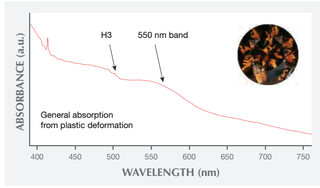

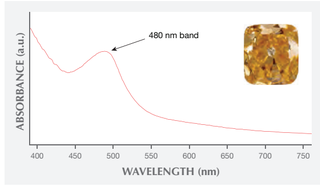

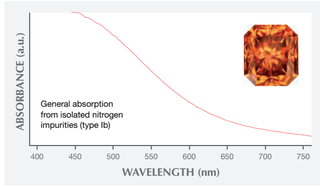

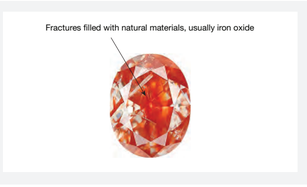

In most cases, transparent gemstones such as diamond owe their coloration to selective absorption of light. With a yellow diamond, the blue portions of the incident white light are absorbed by the diamond, while the remaining portions are transmitted in combination to the eye and interpreted by our vision system as a yellow color. A gemologist uses a spectroscope to detect this selective absorption—the instrument separates light into its component colors, and the portions of the spectrum that are absorbed as they pass through the gemstone appear as dark lines or bands at particular wavelength locations. An alternative method involves recording the absorption with a spectrophotometer, and then depicting the spectrum as a line on a graph. The peaks on the graph correspond to the dark lines or bands seen with the spectroscope.

This chart illustrates representative visible spectra and photos of the major color categories of diamond. The graphs are grouped in six columns and ranked in descending order of occurrence. These colored diamonds were selected because their spectra (and colors) are principally the result of one main lattice defect (a disruption of the atomic structure that causes selective light absorption by the diamond).

Red/Pink/Purple

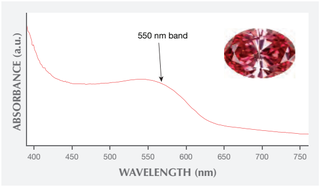

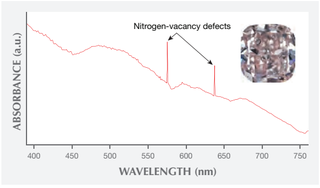

Other Colors

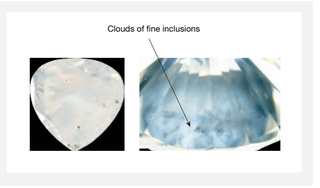

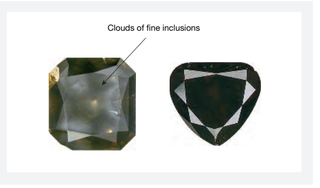

Example Visible Absorption Spectrum

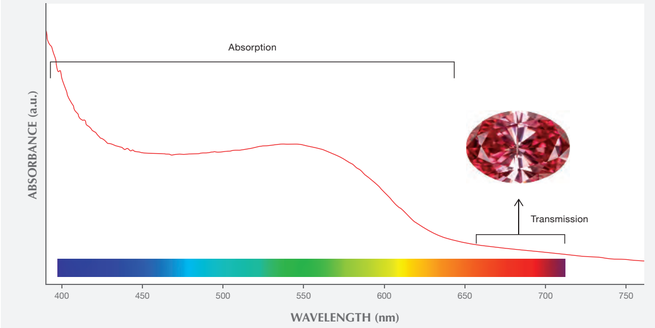

This chart was published in conjunction with J.E. Shigley and C.M. Breeding, "Visible Absorption Spectra of Colored Diamonds," *Gems & Gemology*, Vol. 51, No. 1, pp. 41-43.

MOZAMBIQUE: A RUBY DISCOVERY FOR THE 21ST CENTURY

Merilee Chapin, Vincent Pardieu, and Andrew Lucas

The Republic of Mozambique is located in southeastern Africa along the Indian Ocean. Separated from Madagascar by the Mozambique Channel, it is bordered by Tanzania to the north, South Africa to the south, and Zimbabwe, Malawi, and Zambia to the east (figure 1).

The country boasts rich resources of natural gas, coal, titanium, and hydroelectric power. Agriculture is also important to the economy and includes extensive production of cotton, cashew nuts, sugarcane, tea, manioc root, tapioca, fruits, potatoes, beef, and poultry. Ruby mining is one of the newer economic sectors, with major developments in the northeastern part of the country in the mid to late 2000s.

The Montepuez ruby deposit was discovered in May 2009 (Pardieu et al., 2009). Shortly thereafter, thousands of miners, supported by foreign traders, began to illegally work the area. This continued until June 2011, with the formation of the Montepuez Ruby Mining company (MRM), a partnership between Mozambique's own Mwiriti Ltd. and the multinational British gemstone mining company Gemfields. MRM acquired a 25-year concession in March 2012 and has expended considerable effort and capital to improve the mine's infrastructure, machinery, staffing, security, and public relations.

While the public is generally unaware of Mozambique as a ruby source, the deposit near Montepuez is considered by the trade to be the world's largest supplier. Gemfields' first Mozambique ruby auction took place in Singapore in June 2014, marking a milestone for the global trade (figure 2). The US$33.5 million revenue generated by the auction put the spotlight on the MRM ruby deposit, as the entire inventory was the direct result of the ongoing bulk sampling at Montepuez. This bulk sampling will guide further development of large-scale mine operations.

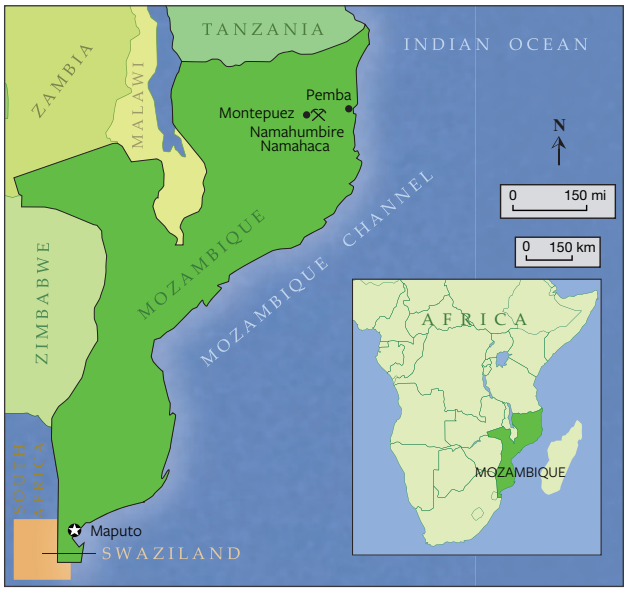

Figure 1. Mozambique, located in southeastern Africa, is the world's newest major ruby source. Its ruby mines are concentrated in the country's northeastern corner. Adapted from Hughes (2014).

The company employs about 400 people at the mine, plus another 300 contractors. Along with experienced personnel imported from other countries, the company also trains Mozambican locals, who make up the vast majority of the workforce, to attain high skill levels.

In September 2014, GIA researchers Tao Hsu, Vincent Pardieu, and Andrew Lucas visited the Montepuez ruby deposit (figure 3). Hosted by MRM, the expedition's purpose was to witness the evolution and operation of this major deposit and to gather research samples for study by GIA's laboratory.

See end of article for About the Authors and Acknowledgments.
Note: The full version of this article was originally published as Hsu et al. (2014).
GEMS & GEMOLOGY, Vol. 51, No. 1, pp. 44–54,
http://dx.doi.org/10.5741/GEMS.51.1.44.

Figure 2. The large amount of ruby produced by MRM allowed Gemfields to offer goods in a wide variety of qualities at their 2014 Singapore auction. Photo by Andrew Lucas/GIA.

AREA GEOLOGY

Northeastern Mozambique is located at a geologically critical junction between the north-south trending Mozambique Belt and the east-west trending Zambezi Belt (figure 4). Both are "treasure-bearing" Neoproterozoic (approximately 500–800 million years old) orogenic belts within the global Pan-African tectonic framework. Several major geologic complexes are separated by major thrusts and shear zones. Complex thermal and deformational events provided ideal temperature and pressure for the formation of ruby, garnet, and other minerals of economic importance.

The Montepuez ruby mine lies about 150 km west of the beautiful coastal city of Pemba (again, see figure 1). It is located within the wedge-shaped Montepuez Complex (Boyd et al., 2010). Its mineral assemblages indicate that the whole complex underwent amphibolite-grade metamorphism, generally at a pressure of 0.4–1.1 GPa and a temperature of 550–750°C.

Ruby forms only within a very limited range of pressure and temperature conditions, and only in the presence of a sufficient supply of aluminum, chromium, and oxygen. Around Montepuez, ruby formation seems to have resulted mainly from a metasomatic process, when fluid derived from the

Figure 3. The GIA team that visited the Montepuez ruby deposit in September 2014 consisted of (left to right) Tao Hsu, Vincent Pardieu, and Andrew Lucas. Photo by Stanislas Detroyat.

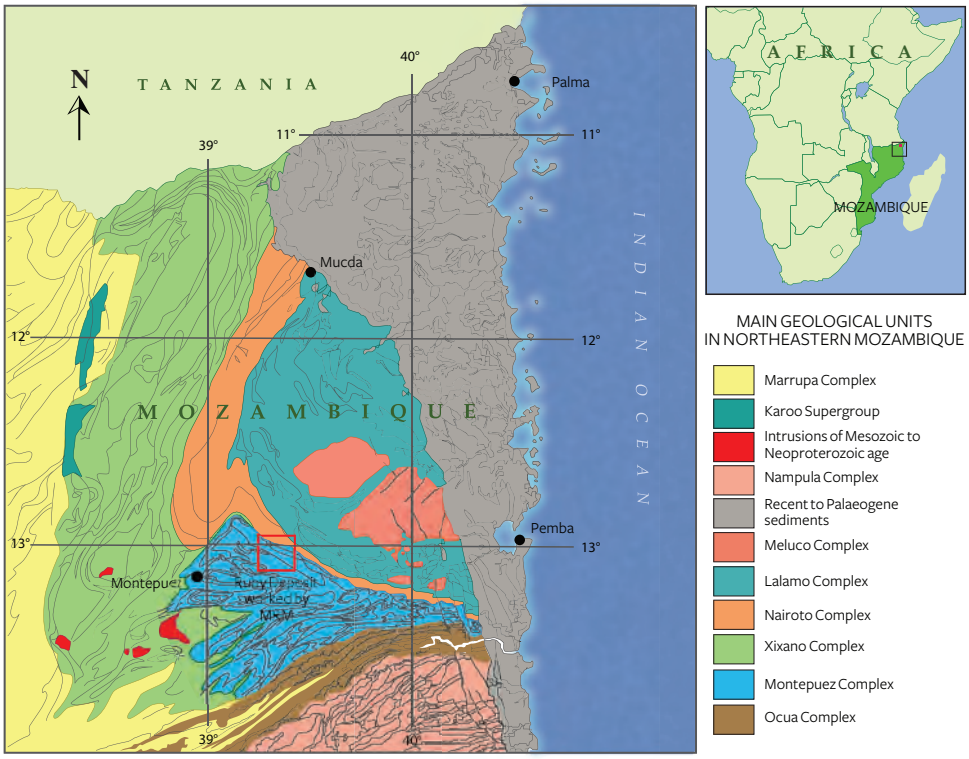

Figure 4. The Montepuez ruby deposit is at the geologically critical location between two large tectonic structures along two directions at right angles to each other. Adapted from Boyd et al. (2010).

parental magma interacted with the host rocks in a low-silica environment.

The Montepuez operation consists of mostly secondary deposits, with only one primary deposit exposed so far. The composition of the rocks in the Montepuez complex ranges from granitic to amphibolitic, while quartzite and marble can be found inside and outside the concession property. The rocks are also strongly folded into tight isoclinal folds on all scales, later cut by a number of shear zones trending northeast to southwest.

The MRM concession is located on one limb of a fold with a subvertical axial plane striking east-west. At least four different deformation phases occurred in this area. The strong deformation history complicated the rock units on all scales, making the exploration and prediction of the primary ore very complex.

The pit walls in Maninge Nice, where the only

Figure 5. Left: A clear contact between the topsoil and the ruby-containing amphibolite can be found on the walls of the primary deposit pit. Photo by Andrew Lucas/GIA. Right: The top of the ruby-containing layer has been extensively weathered, and the rock is very fragile. Photo by Vincent Pardieu/GIA.

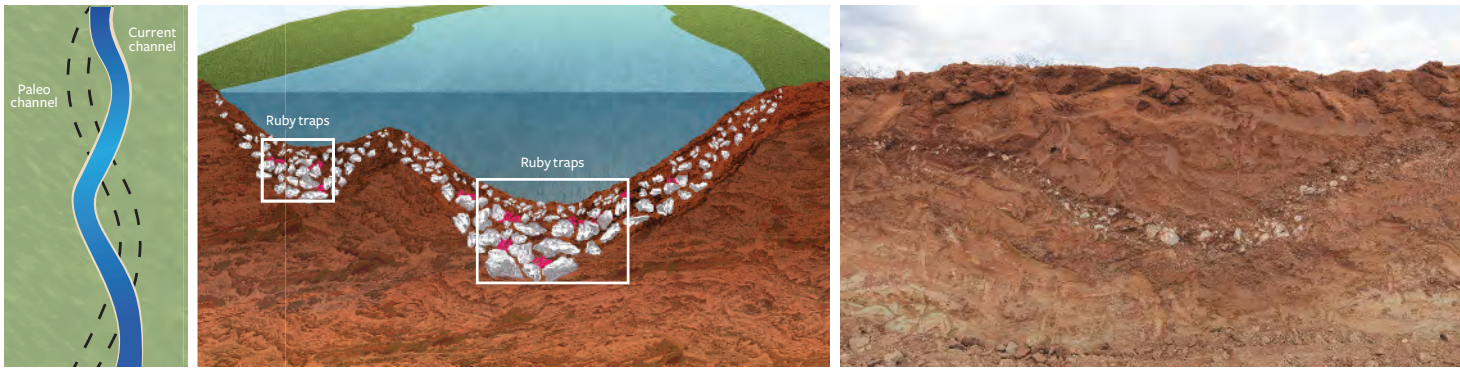

Figure 6. Left: River channel morphology changes constantly over time. Center: Rubies are trapped and concentrated in certain areas along those channels. Right: Cross-sections of former river channels can be seen in the wall of pit 3. Photo by Andrew Lucas/GIA.

primary deposit discovered so far is located, show an obvious contact zone between the topsoil and the weathered ruby-containing amphibolite, which is very fragile and easily crumbled by hand (figure 5). Ruby is found in close association with white feldspar, mica, and dark green amphibole. Core drilling data indicate that the amphibolite extends about 30 meters below the surface and lies on top of the basement gneiss. The whole amphibolite unit strikes roughly east-west.

Hundreds of millions of years of erosion have made the secondary ruby deposits in Montepuez far easier to uncover and work than the primary deposits. Rubies liberated from the host rock were transported and concentrated by water and eventually settled in the alluvial, colluvial, and eluvial deposits being worked today.

PALEOCHANNELS AND RUBY TRAPS

Cycles of weathering and erosion are constantly shaping the surface of the earth. Once the ruby-bearing rock is weakened and broken down by physical and chemical weathering, it is ready for erosion. In Montepuez, rubies and other minerals liberated from the parent rocks were picked up and carried by water and, due to their high specific gravity and hardness, trapped and concentrated in certain locations along current or former river beds, above the weathered basement rocks.

River channel morphology has also changed constantly over time. Hundreds of millions of years ago, the stream channels were at different positions; traces of their original flows are known by geologists as "paleochannels" (figure 6).

The concession has a well-developed drainage system. The local topography causes the water to flow generally from north to south. Present-day stream channels are quite recognizable and easy to work. MRM targets these as well as the richest paleochannels, where large reserves of fine rubies are buried.

Pit 3, the largest being worked by MRM, is located along one of the main paleochannels. On the wall of this pit, observers can see some superb cross-sections of former river channels (figure 6, right). Gravel size increases visibly from the edge to the bottom of these "traps," where gravity caused heavier gravels to settle and concentrate at the bottom of a depression.

Larger gravels are better at slowing the water speed. Since the specific gravity of ruby is relatively high, it tends to settle along the bottom of a depression with other heavy minerals.

Heavy mineral traps occur at different places along the river channel, wherever the water current slows. The traps themselves work as natural jigs, usually leaving a higher concentration of ruby at the bottom of the trap. These ruby "traffic jams" are ideal locations for gem hunters.

Since there are numerous granitic rocks in the area, the gravels are mainly quartz crystals and aggregates of different sizes. Their shape and sharp corners indicate that they were not transported very far from their source rocks. The focus of secondary deposit exploration is to find old stream channels and better define the distribution of this ruby-bearing gravel layer.

THE MINE

The MRM concession encompasses roughly 400 square kilometers, with both primary and secondary deposits. Most of the bulk sampling takes place at the secondary deposits, but sampling is planned for both types within the current fiscal year. The only area with a primary deposit as well as secondary gravels is Maninge Nice, a local name given because of the

Figure 7. This photo shows the bulk sampling pit in Maninge Nice. The greenish layer is the weathered ruby-bearing amphibolite, and the contact between the topsoil and the amphibolite is visible. Photo by Vincent Pardieu/GIA.

"nice" stones that have come from there (figure 7).

Another major bulk sampling area is Mugloto. Pit 3 is in an area of Mugloto called Mashamba, a local name for the maize once farmed on the site (figure 8). Pit 5 is in an area called Mercado, which means "market" in Portuguese, as it was once an illegal miners' market.

BULK SAMPLING METHODOLOGY

Secondary deposits host a concentration of fine stones. They are fairly easy to sample because most of the fractured and included stones were ground into sand by weathering. In the secondary deposits, everything above the gem-bearing gravel is overburden. MRM samples the gravel down to bedrock, often using two excavators—one to strip the overburden down to the gravel and the other to load the gravel into trucks that take it to the processing plant (figure 9).

The long-term bulk sampling strategy at the secondary pits is dictated mostly by the geology. MRM opened several bulk sampling locations based on exploratory auger drilling and on small 50 × 50 meter pits that all follow a single paleochannel. In one area, the company plans to merge several pits at some point, forming a massive operation along the paleochannel. The paleochannel in this area is approximately 4.5 kilometers in length, and the width of the pits varies from 50 to 150 meters. The large pit connecting them is about 2.5 kilometers long, and is expected to become longer. The end result will be a massive colored gemstone pit-mining operation.

MRM conservatively predicts the removal of 1.7 million tons of potentially gem-bearing gravel from the pit along this paleochannel. This will involve the handling of 15 million tons of rock. At the time of our visit, MRM was using four excavators, and another two were scheduled to arrive shortly. This will allow more pits to be sampled simultaneously, the doubling up of excavators in pits identified as crucial, and the starting of new pits.

As primary deposits go, the one at Maninge Nice is relatively easy to sample. The host rock is soft, weathered amphibolite, so removing it is not difficult

Figure 8. The main bulk sampling pit in the Mugloto area is the most productive pit by value. Photo by Stanislas Detroyat.

Figure 9. In the secondary deposit at pit 3, excavators and trucks work together to strip the overburden, load the ruby-bearing gravel, and transport it to the washing plant. Photo by Vincent Pardieu/GIA.

or destructive to the crystals. This type of weathered rock offers a tremendous advantage in keeping costs down and production high. Still, future sampling at the MRM concession will likely involve the extraction of more primary rock at greater depths, increasing the challenge.

FURTHER EXPLORATION

The current bulk sampling and resource analysis stage is scheduled to be completed in 2016, which should give a clearer picture of the potential production figures and life of the mine.

Primary and secondary deposits require different drilling methods and strategies. The goal of secondary deposit exploration is to better define the distribution of the ruby-bearing gravel layer in the concession. Contours of the gravel layer will be constructed from this, as well as data on the concentration of rubies.

Auger drilling, a method not typically seen by GIA researchers, is used to explore the secondary deposits. The auger consists of a rotating helical screw driven into the ground. The screw blade is shaped to lift earth up from the borehole. As earth is pulled out of the hole, workers remove the loose gravel from between the drill blades (figure 10). This is different from core drilling, which removes solid or fragmented cores from hard rock. Auger drilling is considered an efficient way to explore soft unconsolidated material or weak weathered rocks.

Gemfields' geologists have divided the target area into blocks and plan to drill boreholes in 100-meter grids. The drill bits and other equipment are hauled by truck to drilling sites. Every exploration team is composed of a geologist, a technician, and four or five workers. From setting up the machine to refilling the borehole, it takes about an hour to finish one spot. The goal is to finish eight to nine drill holes each day. The sites are cleaned and prepared before the drilling starts.

Figure 10. Workers remove the soil and gravel that come up with the auger and then dump the material into a container for further processing. Photo by Andrew Lucas/GIA.

Figure 11. The soil and the gravel are sampled at every meter until the drill strikes bedrock. The machine will continue another meter or two to finish the sampling. Photo by Andrew Lucas/GIA.

From ground level, the drill removes one meter of earth with every sampling until it hits the basement rock, where it will continue removing two to three meters of rock before it stops (figure 11). The average depth of the drill holes is about eight meters, and the team's goal is to finish about 70–80 meters of drilling each day. MRM runs two shifts per day.

Drilling results will indicate the depth and thickness of the ruby-bearing gravel layer at each location. After thousands of drillings are done, a contour map will be constructed to show the depth and thickness of the area's gravel bed. Prior to our visit, auger drilling had already helped delineate the aforementioned 2.5 km paleochannel, as well as many other sites with strong potential. Sampling the topsoil also gives the geologists a good idea how much waste they will need to remove before reaching the ore-containing gravel layer.

Figure 12. These bags of gravel layers will be transported to the washing plant and then to the sorting house. This will give a reasonable estimation of ruby concentration. Photo by Andrew Lucas/GIA.

To obtain a representative sample, each meter of earth removed from the drill bit above the ruby-bearing gravel layer is thoroughly mixed, and then 50–100 grams of sample are taken for geochemical analysis to quantify certain elements. The results will guide further exploration and evaluation.

At the gravel layer, the drill removes 10–20 kilograms of ruby-bearing gravel, which is bagged and transported back to the washing plant and the sorting house for processing to get a rough estimate of ruby concentration (figure 12). The top one to two meters of basement rock are also washed to minimize the risk of losing rubies. The leftovers from all samples are carefully stored for future reference. The process is completed by refilling the drill hole in an environmentally responsible manner.

Ultimately, understanding the geology of the primary deposit is the key to sustaining a profitable mine. Geologists use geophysical tools to locate the host rock, targeting related amphibolite and magmatic intrusions.

Different mineral assemblages in rocks give off distinct magnetic signatures that can be displayed by a detailed magnetic scan. The results are used to model the distribution of certain rock types. Amphibolite usually gives a high magnetic anomaly that is easily distinguished from other rocks in the area. A high-resolution magnetic survey helps geologists form a map pinpointing the location of the amphibolite. Next, a radiometric survey on uranium, thorium, and potassium is performed to detect the alkaline magmatic intrusions in the area. Further exploration plans are based on these results.

The current exploration of the primary deposit involves extensive core drilling around the exposed Maninge Nice area (figure 13). The goal is to better define the distribution of ruby-bearing amphibolite below the surface. Each drilling extends about 50 meters deep and takes one week to finish, at an average rate of 10 meters per day. Drill bits coated with synthetic diamond are used to sample the rock at every meter. Drill sites are positioned every 100 meters unless more lithological variation is observed, in which case the distance is shortened to 50 meters.

Through extensive core drilling, the geologists have made some important underground discoveries. Each core starts with the loose topsoil, which is bagged. The ruby-bearing amphibolite is usually

Figure 13. The setup of the core-drilling instrument. Water from a tank next to the working platform is run the whole time to cool the drill bit. Photo by Andrew Lucas/GIA.

found at a depth of 10–30 meters, gradually becoming granitic gneiss, the basement rock in the area (figure 14). The exploration team drills down into the basement rock as well to see if the amphibolite repeats. Sometimes they discover a secondary ruby-bearing gravel bed above the primary deposit.

In addition to the amphibolite, which contains various concentrations of rubies, two marble bodies north of Maninge Nice have been defined. No rubies were found in the marbles, however. A detailed report on the primary deposit will be submitted to MRM in 2016.

PRODUCTION

As part of its bulk sampling operation, MRM has handled around 1.8 million tons of rock at Montepuez, recovering approximately 8 million carats of ruby and sapphire of various colors. The company hopes to double its capacity to 3.6 million tons of rock in 2015 and eventually increase that figure to 10 million tons of rock a year.

Figure 14. Ruby is contained in the amphibolite, which is not weathered and very hard to break. Photo by Andrew Lucas/GIA.

The actual recovery of ruby in the secondary deposits is more difficult to predict. The amount of ruby per ton can vary dramatically, and so can the quality of the rubies recovered. For example, the recovery rate in Mugloto pit 3 is relatively low: 0.60–1 gram per ton of ore processed. Yet the pit yields high-quality ruby, making it economically advantageous to sample, even with the low recovery rate. This pit also produces some large rough crystals of 6–8 grams. For comparison, Maninge Nice has a higher recovery rate of 20–35 grams per ton, but generally produces much lower-value material.

Overall, the recovery rate for the primary deposit is around 162 carats per ton, while the secondary deposits produce 31 carats per ton. The figure for the secondary deposits includes only processed gravels and not the amount of overburden topsoil moved.

WASHING AND SORTING

The Montepuez processing plant (figure 15) is organized into four major areas: (1) dry screening; (2) disintegration with a log washer, where the removal of waste particles begins; (3) wet screening; and (4) sizing and concentration. In an auxiliary section, water is held in a reservoir and cleaned for use in washing.

The washing process uses two screening systems and two jig systems, both of which separate the material by size (figure 16). The jigs have a batch system where any overflow from the first upper-level jig is retrieved by the lower-level jig. The 150 tons washed per hour deliver concentrated gravel containing various amounts of corundum rough.

Suction hoses pull the gravels from the jigs into canisters. Then the gravels are poured into bags and taken to the sorting house. The concentrated gem gravels are loaded into the back portion of a sorting

Figure 15. After the gravel passes through a grating, conveyor belts carry it through the washing stages until the ruby is finally trapped by the sluices. Photo by Vincent Pardieu/GIA.

Figure 17. The first step of sorting is to separate ruby and garnet from the washed gravel. Sorters do not touch the gravels with their hands. Instead, they wear rubber gloves attached to cloth sleeves. Photo by Andrew Lucas/GIA.

box, a rectangular case with an angled glass window for viewing. This is the beginning of the process of separating ruby from the gravels and garnets.

To reduce the possibility of theft, the sorters never actually touch the rubies. They wear sleeves with rubber gloves attached (figure 17). They drop the retrieved stones into two holes, one for garnets and the other for corundum. The sorters base the identification on visual appearance, especially crystal morphology.

Next, a senior staff member and a member of the security team unlock the box holding the gemstones, and the corundum crystals are cleaned and sorted. The rough is divided into dark and light tones, representing ruby and pink sapphire, respectively. The rubies are then classified into four further categories: premium, facet-grade, translucent to opaque, and basic corundum.

The grading of the premium ruby rough is done in an adjacent room, first by color and then clarity. White tables provide the background, while windows just in front of the graders provide ample daylight for color grading. The Gemfields ruby grading system is based on the rough's size, color, shape, and clarity (figure 18).

Figure 16. Two sluices, or jigs, are used for different-sized gravel. The heavier material is trapped in the grooves of the jig, while other material goes into the piles in front. Photo by Vincent Pardieu/GIA.

PRELIMINARY GEMOLOGY

Rubies from Montepuez are very important to the trade because of the large quantities and the wide range of qualities and sizes produced. Their colors bridge the gap between those from the classic sources of Burma (highly fluorescent, with low iron content) and Thailand/Cambodia (weakly fluorescent, with high iron content).

Rubies owe their red color to chromium, but their color is modified by the presence of iron, which reduces the chromium-caused fluorescence. An interesting aspect of rubies from the amphibole-related deposit near Montepuez is their iron content, which ranges from nearly as low as Burmese marble-type rubies to as high as rubies found in basalt-related deposits along the Thai-Cambodian border. This means they have the potential to suit a range of different markets.

A small but significant percentage of the material has a combination of color and clarity that requires no

Figure 18. Top-grade ruby rough from Montepuez. Photo by Vincent Pardieu/GIA.

heat treatment. Others lack transparency due to fissures or the presence of inclusions. Heat treatment transforms this lower-quality material so it can find a market within the jewelry industry. Lead-glass filling is used for heavily fractured stones, while more traditional heat treatment (with or without borax-like additives) is performed on less-fractured stones with a milky or silk-like appearance (Pardieu et al., 2010). Overall, treated products are much more readily available than unheated material (Scarratt, 2012).

Each of Montepuez's bulk sampling areas yields rubies with slightly different appearances. The material from Maninge Nice looks purplish red to red. Rough rubies from other areas tend to be darker and more brownish or orange. They generally have higher iron content—similar to Thai/Cambodia rubies—than the samples from Maninge Nice.

Rough rubies from Montepuez are mostly tabular. Specimens from the primary deposit are usually more euhedral, but also more fractured, and contain amphibole and mica inclusions (figure 19, left). Rough from the secondary deposit is generally more tumbled, more transparent, and less included (figure 19, right).

While there are some exceptionally large stones over 100 ct, most of the unheated faceted rubies from Montepuez are under 3 ct. Faceted stones over 10 ct were seen at the Bangkok and Hong Kong shows in September 2013. With their even coloration, high transparency, and good luster, unheated rubies from Montepuez are very suitable for calibrated cuts.

COLLECTING REFERENCE SAMPLES

GIA's Bangkok lab has been collecting reference samples and mining information from sources since 2008. A study of the gemological characteristics of 131 ruby samples from Mozambique was completed by the laboratory and published by Pardieu et al. (2013). Studies of inclusions and chemical composition are in progress, and the results will be presented in future articles. The team's current main focus is to collect and study ruby, sapphire, and emerald reference samples following GIA protocols.

At Maninge Nice, the team was allowed to search

Figure 19. Left: Rough rubies from the primary deposit at Maninge Nice have sharp edges and corners. Their color is brighter because they contain less iron than other deposits in this area. Right: Classic secondary-deposit rubies from the Mugloto area. Most are tumbled and clean from millions of years of weathering and erosion by the rivers. The darker color is caused by their higher iron content. Photos by Vincent Pardieu/GIA.

Figure 20. Expedition guest Stanislas Detroyat and Vincent Pardieu collect samples on the ground at Maninge Nice under the supervision of Gemfields security guards. Photo by Andrew Lucas/GIA.

the ground under the supervision of company security guards (figure 20). The host amphibolite was highly weathered, making it very easy to extract the rubies from the host rock. Using rock hammers, the team collected a fair number of high-quality samples that met the requirements for lab preparation and analysis.

The specimens collected are especially valuable because they are "type A" samples. This means they were obtained directly from the rock by the gemologists themselves. Samples that are collected by the miners but not under the direct supervision of GIA researchers are classified as "type C" samples. These valuable reference samples will be important additions to the GIA reference sample database.

REFERENCES

Boyd R., Nordgulen Ø., Thomas R.J., Bingen B., Bjerkgård T., Grenne T., Henderson I., Melezhik V.A., Often M., Sandstad J.S., Solli A., Tveten E., Viola G., Key R.M., Smith R.A., Gonzalez E., Hollick L.J., Jacobs J., Jamal D., Motuza G., Bauer W., Daudi E., Feitio P., Manhica V., Moniz A., Rosse D. (2010) The geology and geochemistry of the East African Orogen in northeastern Mozambique. *South African Journal of Geology*, Vol. 113, No. 1, pp. 87–129, http://dx.doi.org/10.2113/gssajg.113.1.87.

Hsu T., Lucas A., Pardieu V. (2014) Mozambique: A ruby discovery for the 21st century. *GIA Research & News*, www.gia.edu/gia-news-research-mozambique-expedition-ruby-discovery-new-millennium.

Hughes R. (2014) *Ruby & Sapphire: A Collector's Guide*. Gem and Jewelry Institute of Thailand, Bangkok.

Pardieu V., Jacquat S., Senoble J., Bryl L.-P., Hughes R., Smith M. (2009) Expedition report to the ruby mining sites in northern Mozambique (Niassa and Cabo Delgado provinces). http://www.gia.edu/gia-news-research-NR121709

Pardieu V., Sturman N., Saeseaw S., Du Toit G., Thirangoon K. (2010) FAPFH/GFF treated ruby from Mozambique: A preliminary report. http://www.giathai.net/pdf/Flux_heated_and_glass_filled_rubies_from_Mozambique.pdf

Pardieu V., Sangsawong S., Muyal J., Chauviré B., Massi L., Sturman N. (2013) Rubies from the Montepuez area. *GIA News from Research*, http://www.gia.edu/gia-rubies-from-montepuez-area.

Scarratt K. (2012) A discussion on ruby-glass composites & their potential impact on the nomenclature in use for fracture-filled or clarity enhanced stones in general. http://www.giathai.net/pdf/Ruby-Glass_Composites.pdf.

ABOUT THE AUTHORS

Merilee Chapin is managing editor of content strategy at GIA in Carlsbad. Vincent Pardieu is senior manager of field gemology at GIA in Bangkok, and Andrew Lucas is manager of field gemology for content strategy at GIA in Carlsbad.

ACKNOWLEDGMENTS

The authors gratefully acknowledge the assistance provided by Gemfields and MRM personnel, including Ian Harebottle, CEO; Adrian Banks, product director; Ashim Roy, head of geology and exploration; Raime Raimundo Pachinuapa, executive director; Sanjay Kumar, project manager; Philippe Ressigeac, assistant product manager; Mohun Raman, head of security; and Angus Barthram, logistics manager.

Visit *G&G* online to explore free multimedia content. Scan the QR codes with your smartphone or tablet, or enter the links below.

Brazil: Explore Brazil's emerald and tourmaline mines and follow the production of the gems step by step. Exclusive videos and slideshows highlight the fascinating discoveries.
www.gia.edu/gia-news-research-an-overview-of-2014-gia-brazil-expedition

Zambian Emeralds: Documents the mining and gemological characteristics of emeralds from Kagem, the world's largest emerald mine.
www.gia.edu/gia-news-research-kagem-emerald-mine-zambia

LA Museum of Natural History: A rare behind-the-scenes look at the outstanding gem and mineral specimens in LA's Natural History Museum, featuring insight from the museum's curators.
www.gia.edu/gia-news-research-natural-history-museum-los-angeles-county

Botswana's Scintillating Moment: Discover more about Botswana's strategies and challenges as it develops a thriving diamond and jewelry industry.
www.gia.edu/gems-gemology/summer-2014-weldon-botswana-scintillating-moment

Gemological Field Expeditions: GIA's Andy Lucas and Vincent Pardieu discuss the challenges and rewards of gemology fieldwork. Contains slideshows from local mines and markets.
www.gia.edu/gia-news-research-behind-scenes-gemological-field-expedition

Chinese Gem and Jewelry Industry: The authors explore the development, impact, and future of China's domestic and international gemstone and jewelry market. Includes artisan video interviews, on-site slideshows, and a Chinese language PDF.
www.gia.edu/gems-gemology/spring-2014-lucas-chinese-gem-industry

TAKE THE 2015 GEMS & GEMOLOGY CHALLENGE

The following 25 questions are from the Spring, Summer, Fall, and Winter 2014 issues of *Gems & Gemology*. Refer to the articles in those issues to find the single best answer for each question.

Mark your choice on the response card provided in this issue or visit gia.edu/gems-gemology to take the Challenge online. Entries must be received no later than **Monday, August 3, 2015**. All entries will be acknowledged with an e-mail, so please remember to include your name and e-mail address (and write clearly).

Score 75% or better, and you will receive a certificate of completion (PDF file). Earn a perfect score, and your name also will be listed in the Fall 2015 issue of *Gems & Gemology*.

1. Which city is the world's largest center for diamond sorting, valuing, and selling?
   A. Shanghai, China
   B. Mumbai, India
   C. Antwerp, Belgium
   D. Gaborone, Botswana

2. What happens if the c-axis is parallel to the table facet of a strongly pleochroic stone?
   A. No pleochroism can be observed through the table.
   B. A "bow tie" may be observed.
   C. For a biaxial stone, all three colors can be observed through the table, whereas only two colors can be observed for a uniaxial stone.
   D. Only the ordinary ray is observed.

3. Why do natural blue sapphire and Verneuil synthetic blue sapphire often display differences in pleochroism?
   A. The table facets are often oriented differently.
   B. The blue color is caused by different trace impurities.
   C. Verneuil material does not display pleochroism.
   D. Weight retention is more of a concern with natural material.

4. Which of the following is a valid GIA diamond color grade?
   A. Fancy Intense red.
   B. Fancy Vivid purplish pink.
   C. Fancy Vivid purplish red.
   D. Fancy Deep Vivid purplish pink.

5. In 2013, China was the world's largest consumer of _____.
   A. jadeite and platinum
   B. gold and diamonds
   C. diamonds and jadeite
   D. jadeite, platinum, diamonds, and gold

6. What determines the final color of treated amber?
   A. Presence of bubbles.
   B. Pressure during treatment.
   C. Presence of liquid inclusions.
   D. Atmosphere during heating.

7. What can be said about an emerald that contains a significant amount of alkali metal impurities?
   A. It may contain an extra FTIR absorption band around 1140 cm^{-1}.
   B. Its composition (stoichiometry) is ideal.
   C. It does not contain water.
   D. It is most likely a synthetic.

8. All of the following statements are true of "Jedi" spinels except _____.
   A. there are other sources besides the Namya deposit in Myanmar
   B. they have no dark tone
   C. they are sometimes found in matrix
   D. they have lower iron content on average than Mogok spinel

9. The top three diamond producers are:
   A. Rio Tinto, Alrosa, BHP
   B. De Beers, Alrosa, Rio Tinto
   C. Rio Tinto, Alrosa, De Beers
   D. Dominion Resources, Rio Tinto, De Beers

10. The green and orange-red phosphorescence displayed by natural and untreated type IIb blue diamonds when exposed to

short-wave UV can potentially be attributed to _____.
A. the recombination of donor-acceptor pairs and possibly plastic deformation
B. their origin in the Cullinan mine
C. high levels of nitrogen
D. the presence of boron

11. Which diamond mine is the world's richest as of 2014?
A. Argyle
B. Jwaneng
C. Orapa
D. Diavik

12. With the emergence of rough diamond tender sales, small manufacturers _____.
A. now face rough shortages
B. have seen stability in the supply of rough
C. have experienced overall industry profits
D. have seen increased selection and availability of rough

13. Most gemstones from Sri Lanka are found in _____.
A. pegmatites
B. skarns
C. alluvial deposits
D. eluvial deposits

14. Which type of treated amber can be produced by two different methods?
A. Beeswax amber
B. Golden flower amber
C. Red flower amber
D. Sun spark amber

15. Which of these statements about beaded pearls is true?
A. Nacre deposition requires a solid surface.
B. The bead determines the size and shape of the pearl.
C. Their density is consistent from specimen to specimen.
D. The bead is not always in direct contact with the nacre.

16. All the following statements are true of "pen pearls" except _____.
A. they are commonly non-nacreous
B. they tend to craze
C. they are used as nuclei in cultured pearls
D. they are mainly found in the Arabian (Persian) Gulf

17. Pink to red diamonds are cut to _____.
A. maximize color and clarity
B. retain as much weight as possible
C. maximize color grade and weight
D. ensure a better clarity grade than I

18. What is true about nephrite from Hechi, China?
A. Colors include white, green, black, purple, and gray.
B. Only secondary material displays dendrites.
C. Band- and dendrite-free material is the most prized.
D. The specific gravity of this material is unusually low.

19. When comparing high karatage gold jewelry from Sri Lanka and India, which is true of Sri Lankan jewelry?
A. It contains more copper.
B. It is more yellow.
C. It is manufactured exclusively with traditional methods.
D. Weddings are a more significant source of business.

20. In China, which metal do brides generally prefer for wedding rings?
A. 22–24K gold
B. Platinum
C. 18K gold
D. Silver

21. The actual boron content in a blue diamond is _____ its calculated value from FTIR absorption spectroscopy.
A. equal to or greater than
B. equal to or less than
C. generally equal to
D. None of the above.

22. All of the following statements are true of high-pressure high-temperature (HPHT) synthetic diamonds except _____.
A. near-colorless type IIa material is grown by using higher-purity solvents, catalysts, and carbon sources
B. they are produced via belt, BARS, cubic, or toroid presses
C. most colorless material to date has been grown for non-jewelry purposes
D. yellow is the most common color for jewelry use

23. What is required of the observation lighting to see the greenish blue color of blue amber?
A. Only sunlight allows the observation of this phenomenon.
B. Any light source will reveal the blue color.
C. It must have an ultraviolet component.
D. It must cover the full visible range.

24. What inclusion feature is reportedly unique about Zambian emeralds from the Kafubu area?
A. Some multiphase inclusions contain crystals visible only with cross-polarized light.
B. Kafubu is the only source of emeralds containing solid inclusions with no associated liquid or gas inclusions.
C. Of all Zambian emeralds, they had inclusions most similar to those of Colombian emeralds.
D. The most common inclusions were three-phase, containing two or more colorless crystals.

25. Which is not a regular characteristic of HPHT synthetic diamonds?
A. Patterned color zoning.
B. Inclusions that are attracted to a strong magnet.
C. Strong fluorescence to short-wave UV illumination.
D. Presence of trace levels of Si.

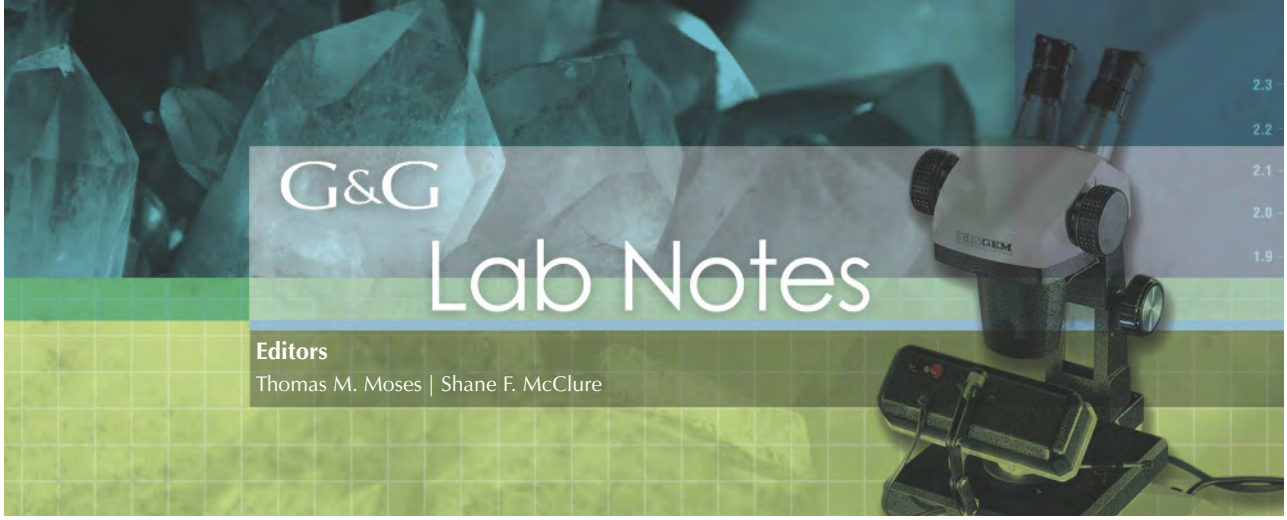

Pink and Reddish Purple COBALTOCALCITE

Cobaltocalcite is a pink to purple variety of calcite. The mineral is popular as a collector's item because of its striking purplish pink color, which is caused, as the name suggests, by the presence of cobalt. Cobalt occurs in calcite in octahedral coordination as Co^{2+} (E. Fritsch and G.R. Rossman, "An update on color in gems. Part 1: Introduction and colors caused by dispersed metal ions," Fall 1987 *G&G*, pp.126–139).

Recently, GIA's laboratory in Bangkok examined the botryoidal purplish pink and rough reddish purple cobaltocalcite specimens shown in figure 1. Gemological properties were obtained from both, and we also prepared several polished wafers for advanced testing.

Standard gemological testing of these translucent stones revealed strong double refraction with an RI of 1.49–1.66 (as expected for a carbonate material) and an SG of approximately 2.70. The reddish purple cobaltocalcite exhibited a very weak purplish pink reaction to long-wave UV radiation and an inert reaction to short-wave UV. The purplish pink stone had a moderate orangy pink reaction to long-wave UV and weak pink to short-wave. Magnification revealed white particulate flakes of a fibrous nature forming bands in the reddish purple specimen, while the purplish pink one contained pronounced irregular fibrous inclusions forming a mosaic pattern in areas (figure 2).

Figure 1. The pink and reddish purple cobaltocalcite specimens (246.3 and 361.0 g, respectively) are shown with some of the wafers cut from them.

Figure 2. Left: The reddish purple cobaltocalcite showed a banded structure formed by white particles with a fibrous appearance. Field of view 4.1 mm. Right: Irregular bands of fibrous inclusions in the pink stone formed a mosaic pattern. Fiber-optic illumination, field of view 4.1 mm.

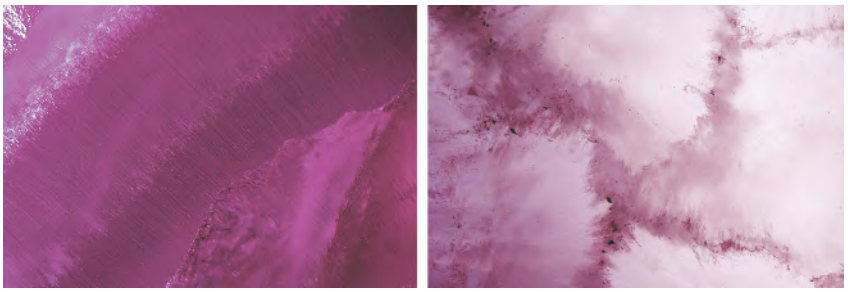

Editors' note: All items were written by staff members of GIA laboratories.

Gems & Gemology, Vol. 51, No. 1, pp. 58–67.

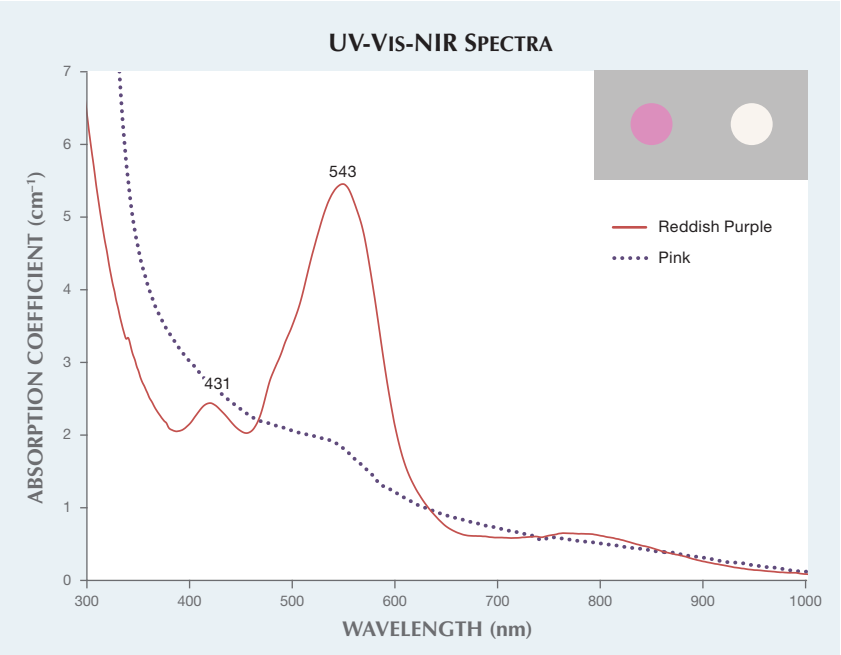

*Figure 3. UV-Vis-NIR spectra in the 300–1000 nm region showed broad absorption bands at approximately 431 and 543 nm in the reddish purple cobaltocalcite, and a weak broad band at 543 nm in the pink stone. Inset: The reddish purple and pink stones' CIE L*a*b* color coordinates (71, 47, 24 and 96, 3, 4, respectively) are reproduced from their UV-visible spectra.*

The UV-Vis-NIR spectrum of the reddish purple cobaltocalcite wafer (figure 3) showed a dominant absorption band at 543 nm and a small peak at 431 nm. The pink wafer only showed a weak absorption feature at 543 nm. Color calculations (see box A in R. Lu, "Color origin of lavender jadeite: An alternative approach," Winter 2012 *G&G*, pp. 273–283) were consistent with the respective reddish purple and purplish pink color of the two specimens (figure 3, inset).

Elemental analysis was performed using laser ablation–inductively coupled plasma–mass spectrometry (LA-ICP-MS). Besides the main constituent calcium, both the reddish purple and the purplish pink cobaltocalcites showed significant amounts of Co at 5673 and 730 ppmw, respectively. The reddish purple sample's higher concentration is consistent with a higher Co level produces a more saturated color. The concentration of Co is consistent with the intensity of the 543 nm absorption bands in the visible region of both samples. The purplish pink cobaltocalcite also showed 8719 ppmw of Mn. Manganese can cause pink to purple color in appropriate concentrations, so its contribution to the purplish pink color in this material may require further analysis.

Piradee Siritheerakul and Supharart Sangsawong

DIAMOND

Analysis of Melee Diamonds Using FTIR Spectroscopy

The jewelry industry has expressed increasing concern over the possibility of treated or synthetic diamonds being mixed in with natural melee goods (those weighing less than 0.20 ct). Recently, GIA's laboratory has seen a surge in notably small faceted melee diamonds submitted for identification. In melee sizes less than 0.01 ct, a standard Fourier-transform infrared (FTIR) spectrometer provides a less stable environment for analysis and produces an indistinct spectrum. Diamonds smaller than 0.01 ct prove challenging for other screening devices as well. Meanwhile, there is heightened pressure to identify both loose and mounted melee diamonds in the laboratory quickly and reliably so that each stone can be analyzed. In late 2014, GIA developed a new protocol to use an FTIR microscope to focus on melee diamonds as small as 0.00054 ct (figure 4) to produce high-quality spectra suitable for diamond typing.

Operating the FTIR microscope in reflection mode allows for fine-tuned aligning of the beam within a sample, improving the detail of the infrared spectra. Once a faceted round brilliant melee is stationed on a slide, the microscope beam can be focused either through the pavilion (if the melee is table-down) or through the table at an angle to reflect off an inner pavilion facet (if the melee is resting on the pavilion). Many of the samples were so small that the position of the stone remained unknown until the microscope was focused. Nevertheless, spectral quality was independent of stone position.

All 70 melee examined were natural round brilliants, the smallest a

Figure 4. This 0.00054 ct colorless round brilliant was submitted for identification as a natural or synthetic diamond. Despite the specimen's small size, an FTIR microscope can focus a beam through the facets to capture a high-quality infrared spectrum.

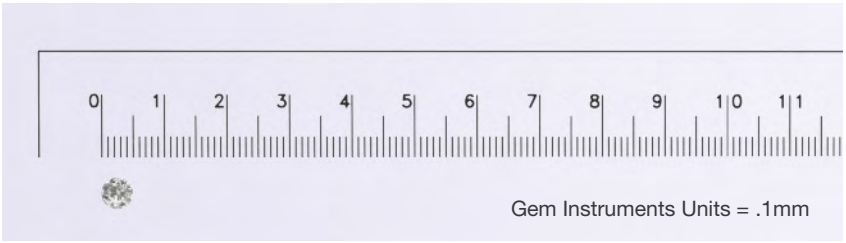

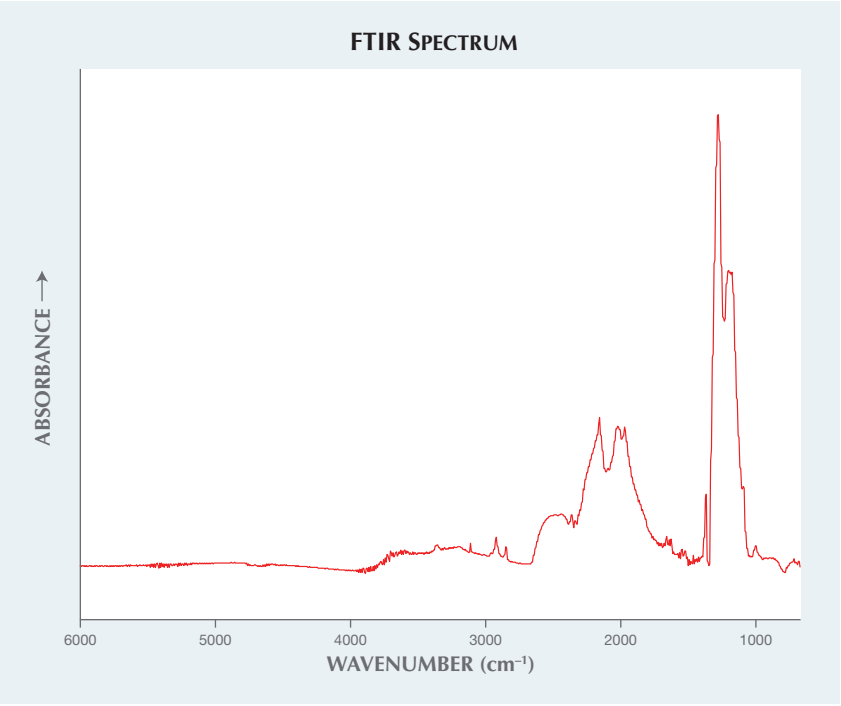

Figure 5. This infrared spectrum of the 0.00054 ct diamond in figure 4, obtained using an FTIR microscope, shows the detail that can be captured from very small melee sizes.

0.00054 ct colorless sample identified as a type Ia diamond (figure 5). A few screening devices for treatment and synthetics have been introduced for diamonds over 0.01 ct. The FTIR microscope has proved very effective in analyzing melee smaller than this size, either loose or mounted.

The knowledge that GIA can type such small stones and determine their origin, either loose or mounted, apart from being an impressive test of FTIR microscopy, will increase consumer confidence in these remarkable melee diamonds.

Rachel Sheppard, Tom Moses, and Wuyi Wang

Artificially Irradiated Color-Change Diamonds

Diamonds that exhibit a temporary color change, commonly referred to as "chameleon" diamonds, are rare in nature. Their color changes with gentle heating, or when they are left in darkness for a period of time. The change from a dark greenish to a lighter yellow hue upon gentle heating is due to the thermochromic properties of these diamonds (D.J. Content, Ed., *A Green Diamond: A Study of Chameleonism*, W.S. Maney & Son, Leeds, England, 1995, 42 pp.).

Recently the New York laboratory examined two chameleon diamonds, a 0.35 ct Fancy Deep yellow-green marquise and a 0.27 ct Fancy Deep grayish yellowish green marquise (figure 6). Spectroscopic analysis and gemological observations confirmed that these were typical chameleon diamonds. After excitation with short-wave UV light, both exhibited a strong blue to yellow phosphorescence often seen in natural chameleon diamonds. Their UV-Vis absorption spectra showed a broad band at about 480 nm, as expected for this type of diamond. But the spectra also displayed a peak at 741 nm (figure 7), known as GR1 (general radiation damage), that can contribute to a green color in diamonds. Because this radiation-related feature is not found in untreated natural chameleon diamonds, we concluded that both stones had been artificially irradiated.

A chameleon diamond is an unlikely candidate for artificial irradiation treatment to enhance the stone's green or blue bodycolor. It is likely that this property was not known or understood before the irradiation process. A permanent color change may occur if these treated chameleon stones are heated for a prolonged period, so it is important to exercise caution during testing. Because the diamonds' original colors are unknown, they were issued reports stating that they had been artificially irradiated to enhance their color.

Sally Chan, Jessie Yixin Zhou, and Paul Johnson

Diamond in Diamond

The New York laboratory recently examined a 1.69 ct Fancy black round brilliant diamond (figure 8). The type Ia diamond contained an abundance of tiny cloud inclusions and strong hydrogen-related absorptions, both common features for this type of diamond. We observed numerous etch channels with brown radiation staining, also normal features for diamonds of this type and color. But we also observed a sizable octahedral crystal inclusion that broke the surface of a pavilion facet (figure 9, left). The surface-breaking area was approximately 150 × 250 microns according to the Raman microscopic

Figure 6. These two chameleon diamonds (0.35 and 0.27 ct) were color-treated with artificial irradiation.

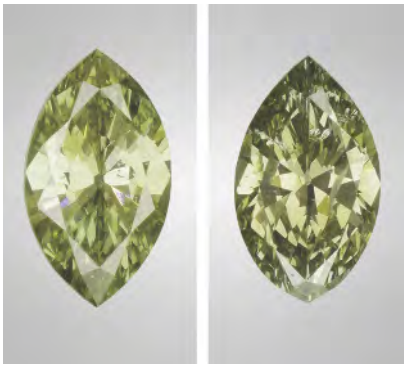

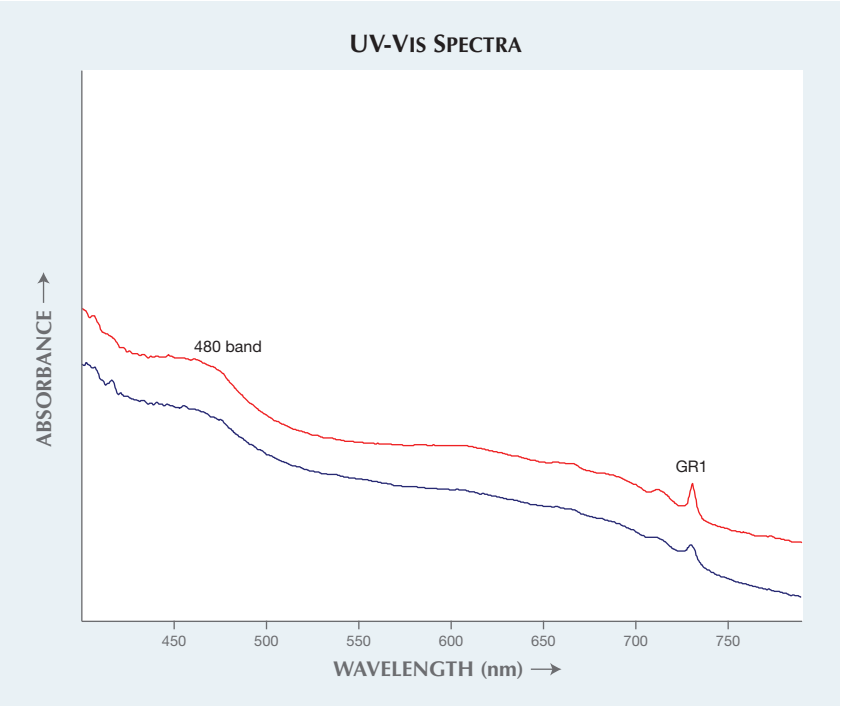

Figure 7. The UV-Vis spectra for the two chameleon diamonds show a broad absorption peak around 480 nm and an atypical GR1 feature at 741 nm.

image. The actual dimensions of the entire included crystal could not be determined.

The exposed crystal inclusion had the morphology of a natural diamond crystal, and Raman analysis easily identified it as diamond. Both the host diamond and inclusion show sharp 1332 cm^{-1} Raman bands, indicating high crystallinity. The graphite peak at approximately 1580 cm^{-1} was not observed in either. Raman mapping showed that the full width at half-maximum (FWHM) of the inclusion's 1332 cm^{-1} peak was different from that of the host diamond (figure 9, center). In the map, each colored pixel represents the FWHM value of the 1332 cm^{-1} Raman peak. The colored pixels of the inclusion were decidedly different from those of the host dia-

Figure 8. This 1.69 ct Fancy black round brilliant diamond contained an octahedral diamond crystal.

Figure 9. Left: This photomicrograph reveals natural etch channels with brown radiation staining, as well as an octahedral crystal inclusion (the inset shows the surface-breaking outline). Center: The Raman map of the 1332 cm^{-1} FWHM clearly outlines the surface break of the octahedral diamond inclusion. The inset in the left-side image represents the Raman mapping area. The image was taken in a grid pattern measuring FWHM of the diamond Raman peak at 1332 cm^{-1}. More than 300 Raman spectra collected at multiple points on the grid were translated into this map by the software. Each colored pixel represents the FWHM value, and similar FWHM values will be shown in similar colors. Noticeably different colors outlining the inclusion indicate that it is not part of the host diamond and that it formed in a different geological environment. Right: DiamondView imaging shows that the diamond inclusion was captured during the second phase of growth.

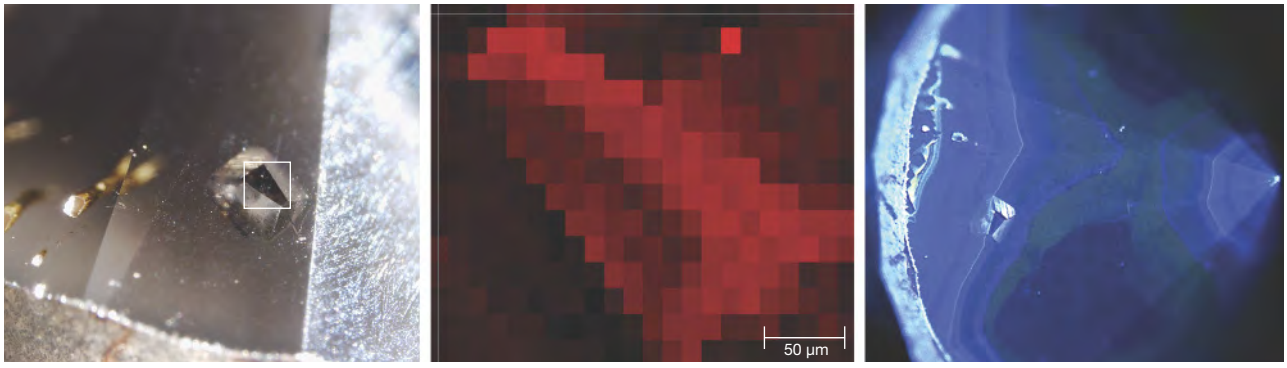

mond, confirming that it formed in a different geological environment. We also observed differences between the photoluminescence (PL) spectra of the inclusion and the host diamond, evidence that the diamond inclusion formed in a different environment and was later incorporated as a protogenetic inclusion. This also suggests that this diamond may have traveled from its original formation environment to another geological environment after crystallization.

A DiamondView image shows the diamond crystal to have been captured in a second growth phase of the host diamond crystal (figure 9, right). This is the first documented case of a diamond crystal inclusion with a different origin than that of the host diamond.

Paul Johnson and Kyaw Soe Moe

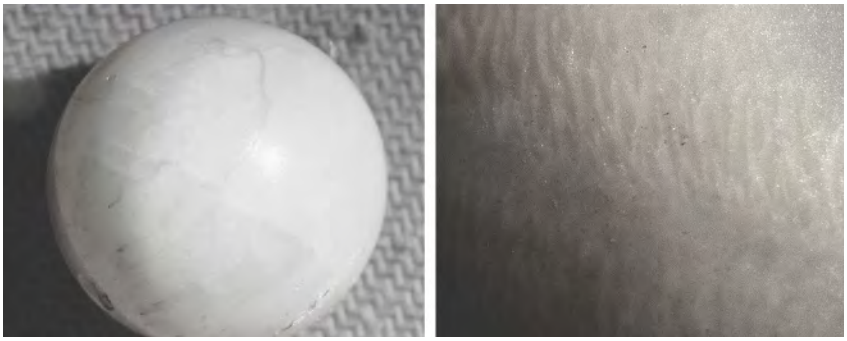

Figure 10. Left: This white shell bead (10.08 mm) was visible after the coating was removed from one of the imitation pearls. Right: A subtle flame structure was observed on the surface of the shell bead; magnified 40×.

PEARLS

Conservation Concerns over Use of *Tridacna* Shell in Imitation Pearls

Last year the New York laboratory reported on the use of shell as a pearl imitation (Summer 2014 Lab Notes, pp. 153–154) and the improper nomenclature applied by those marketing it. We decided to delve deeper and investigate the nature of the shell beads used in such imitation pearls following correspondence with Dr. Henry A. Hänni, who previously reported on this issue (see Summer 2004 Gem News International, p. 178, and references within).

After removing the outer coating on one of the imitation pearls by immersing it in acetone, we observed a banded white bead (figure 10, left). Magnification revealed fine and subtle flame structures (figure 10, right), indicating the bead was most likely fashioned from the shell of a *Tridacna* (giant clam) species.

All species of the Tridacnidae family are currently listed in Appendix II of the Convention on International Trade in Endangered Species of Wild Fauna and Flora (CITES). Some species, such as *Tridacna gigas*, are more vulnerable than others, such as *Tridacna squamosa* or *Tridacna maxima*. These large saltwater clams can have heavy shells fluted with multiple folds (figure 11) and colorful mantles. Their natural habitats lie in the warm marine waters of the Indo-Pacific, a fragile region that has been heavily impacted by human activities.

These beautiful marine animals are commonly harvested from their natural habitats or aquaculture farms for food (*Center for Tropical and Subtropical Aquaculture Publication No. 114*, University of Hawaii), and their shells are fashioned into beads or ornaments that are prized by some cultures. Despite their protection under CITES, these shell products are readily available on the Internet and often very inexpensive (figure 12). Imitation

Figure 11. These three shells of Tridacna *species are part of the collection at GIA's Bangkok laboratory. The two largest measure approximately 33 × 20 cm each. The two larger shells were found empty by Thai divers, while the smaller shell was donated to the Bangkok lab several years ago and comes from an unknown source.*

Figure 12. Tridacna *shell beads of various sizes (4.5 to 10.5 mm) are readily available from various commercial sites. The carved beads shown on the left are marketed as "Tibetan prayer beads."*

Figure 13. This northern quahog pearl exhibited a fine color and shape.

shell "pearls" fashioned from these endangered and protected mollusks do not offer any obvious advantages over common freshwater mussel shells, and it is extremely difficult to identify the exact *Tridacna* species or whether the mollusks were farmed or harvested from the wild. We urge manufacturers to stop using *Tridacna* shell beads when producing imitation pearls.

Jessie Yixin Zhou and Chunhui Zhou

Large Natural Quahog Pearl

A notable purple non-nacreous pearl (figure 13) recently submitted to GIA's New York laboratory measured 13.69 × 11.80 mm and weighed 16.64 ct. It was immediately recognizable as an outstanding specimen due to its clean surface, which possessed an attractive sheen reminiscent of fine porcelain. It had good symmetry, featuring a near-round button shape with a perfect dome top and a rounded base, and a richly saturated and well-distributed mid-purple color.

Real-time microradiography revealed a tight internal structure, a common characteristic of certain natural non-nacreous/porcelaneous pearls. Raman spectroscopy using 514 nm laser excitation (figure 14) showed characteristic aragonite peaks at 702, 706, and 1086 cm^{-1}, as well as 1130 and 1520 cm^{-1} peaks related to a mixture of polyenic (polyacetylenic) compounds, the natural pigments responsible for its purple color, as previously observed in similar pearls (Winter 2008 GNI, pp. 374–375). The characteristic natural purple color and non-nacreous porce-

Figure 14. The quahog pearl's Raman spectrum showed the typical aragonite peaks seen in most pearls, together with 1130 and 1520 cm^{-1} peaks related to a natural coloring compound.

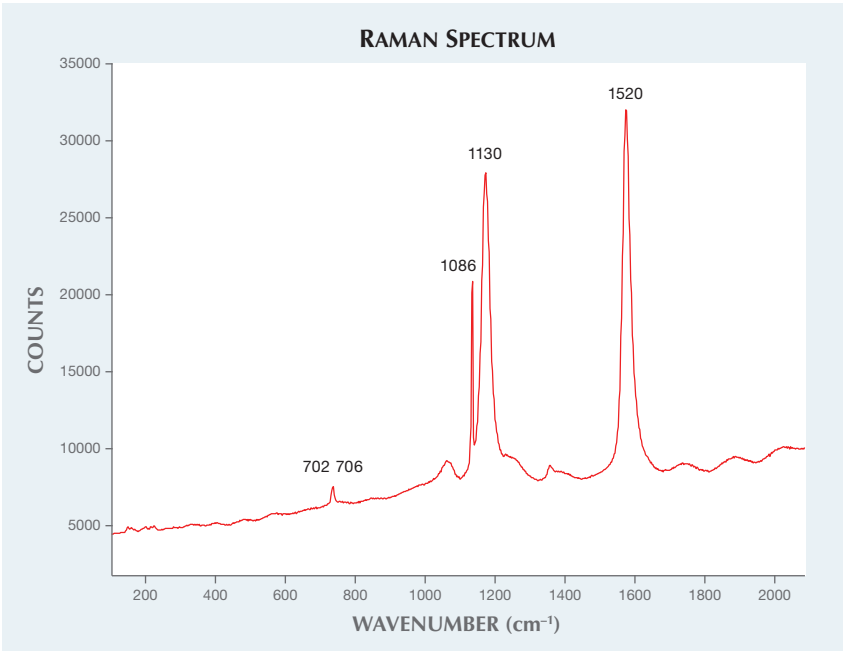

Figure 15. This quahog shell from the eastern coast of the United States has a naturally attached pearl.

laneous appearance indicated a pearl from the bivalve mollusk *Mercenaria mercenaria* (belonging to the Veneridae family), also referred to as the "northern quahog."

Quahogs are native to the Atlantic shores of North America from Canada to Georgia, especially on the coast of the New England states, and can also be found along California's Pacific coast. They can produce nonnacreous porcelain-like pearls, and their shells typically exhibit an uneven white and purple interior color (figure 15). Quahog pearls may occur in a variety of colors ranging from white to brown and from faint pinkish purple to dark purple. Like other natural pearls, quahog pearls are rarely spherical. Button shapes with flat bases are most often encountered.

Natural northern quahog pearls are often submitted to GIA labs. Most are below 10 carats with a flat-based button shape, usually with a dark or light purple color, and tales of their accidental discovery while eating clams are not uncommon. This quahog pearl's large size, clean surface, fabulous luster, near-round shape, and evenly distributed rich color combine to make it an exceptionally fine and rare example of its type.

Joyce Wing Yan Ho

SYNTHETIC DIAMOND

HPHT Synthetic Diamond Melee in High-Quality Jewelry Piece

Advances in the laboratory growth of diamonds have led to an increase in the number of synthetic diamonds seen at GIA. The existence of high-quality synthetic diamonds in melee sizes is of particular concern. This is due in part to the expense of examining melee relative to their value. While GIA can reliably identify synthetic melee, this requires individual analysis of each stone, preferably before mounting. In a complicated piece with hundreds of melee, this can be prohibitively expensive or time-consuming. The same is true for melee parcels. A synthetic diamond mixed into a packet may not be identified until later, deceiving dealers, jewelers, and consumers and potentially causing damage to the trade.

Recently, a pendant with 118 mounted stones was submitted to GIA's New York laboratory for color origin analysis of each individual melee (figure 16). The pendant consisted of a central pear-shaped stone surrounded by three consecutive rows of round brilliant melee. Of the 118 stones, 58 were fancy yellow, including the center stone, and 60 were colorless. Using a Fourier-transform infrared (FTIR) microscope in reflection mode allowed detailed focusing of the infrared beam on the mounted stones, including those that were partially obscured. Analysis was carried

Figure 16. A photo and a detailed illustration of the melee-set pendant show the location of all 118 samples. The single HPHT synthetic melee is highlighted in both images.

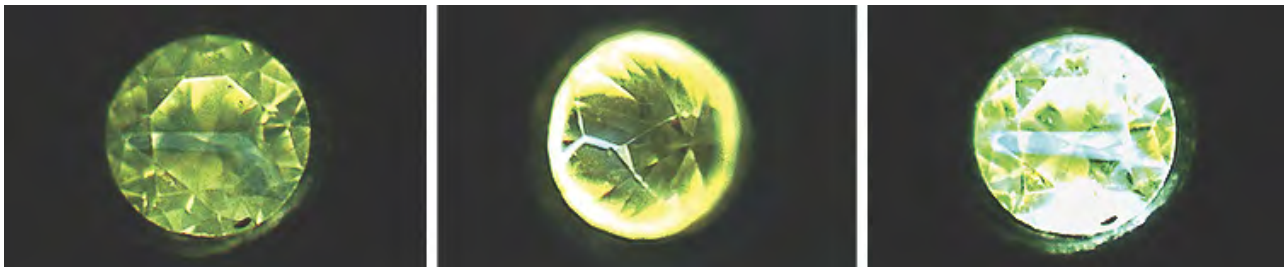

Figure 17. Left and center: DiamondView fluorescence images of the 0.00431 carat type Ib diamond show clear cuboctahedral HPHT synthetic growth sectors. Right: The sample's strong phosphorescence is atypical for a diamond of this type and color.

out on a Thermo Nicolet iN10 FTIR microscope, which determined the diamond type classification of each melee stone from its mid-IR absorption spectra (C.M. Breeding and J. E. Shigley, "The 'type' classification system of diamonds and its importance in gemology," Summer 2009 *G&G*, pp. 96–111). One melee was identified as an HPHT-grown (high-pressure, high-temperature) synthetic diamond, based on its infrared spectrum as well as its color, fluorescence pattern, and phosphorescence behavior. This 0.00431 ct melee was removed from the setting to confirm its origin as HPHT-synthetic. The rest were confirmed as natural diamonds.

Of the 118 melee, 114 were classified as type IaA or type IaAB. These were characterized by absorption from aggregated nitrogen centers, where A-centers (nitrogen pairs) and B-centers (four nitrogen atoms symmetrically surrounding a vacant lattice site) absorb infrared light at 1282 and 1174 cm^{-1}, respectively. These spectra revealed sufficient A-center concentrations, eliminating the possibility of HPHT treatment, which would have deaggregated the centers into isolated nitrogen atoms (A.T. Collins, "The colour of diamond and how it may be changed," *Journal of Gemmology*, Vol. 27, No. 6, 2001, pp. 341–359). Since A- and B-center absorptions occur solely in the infrared range, their presence does not produce color. Instead, the yellow color observed in 57 of these type IaA/IaAB stones resulted from absorption from the N3 defect at 415 nm (a complex of three nitrogen atoms surrounding a vacancy) and associated peaks at 453, 452, 465, and 478 nm. This spectrum is known as the "Cape series," and such goods are commonly referred to as "Cape yellow."

Two colorless stones were classified as type IaB, showing only pure B-aggregate absorption; the remaining colorless stone was type IIa, meaning it did not show IR absorption from any nitrogen-related impurities. Finally, a partially obscured yellow stone near the bottom of the piece was type Ib, showing absorption due to isolated nitrogen impurities, and characterized by features at 1130 and 1344 cm^{-1}. Isolated nitrogen centers also produce a broad absorption feature in the UV-visible range (approximately 270 nm), resulting in a coloration often described as "Canary yellow." Type Ib diamonds are very rare, representing only 0.1% of all natural diamonds (R. Tappert and M.C. Tappert, *Diamonds in Nature*, Springer, Berlin, 2011). Conversely, this diamond type is common in yellow synthetic diamonds. Due to the absence of A-centers, these four samples required further testing.

Photoluminescence spectroscopy confirmed that the type IaB and IIa stones were natural in origin. However, the type Ib stone (marked in figure 16) was further examined with DiamondView imaging, which showed that it exhibited strong yellow-green fluorescence under deep ultraviolet illumination (wavelength <230 nm) and indicated growth sector patterns typical of HPHT synthetic diamonds, as well as strong blue phosphorescence inconsistent with natural yellow type Ib diamonds (J.E. Shigley et al., "A chart for the separation of natural and synthetic diamonds," Winter 1995 *G&G*, pp. 256–264; J.E. Shigley et al., "Gemological properties of near-colorless synthetic diamonds," Spring 1997 *G&G*, pp. 42–53). The 0.00431 ct yellow stone was removed from its mounting for more comprehensive examination with the DiamondView (figure 17). Its cuboctahedral synthetic growth sectors were clearly seen from both the table and pavilion, confirming its HPHT synthetic origin.

Although this could have been an isolated event, it underscores the need for caution when buying melee parcels or mounted pieces from unfamiliar sources. Nevertheless, it is important to note that such stones can be unequivocally identified as lab-grown. Colorless and near-colorless (D–N) unmounted diamonds larger than 0.01 ct can be tested using commercially available testing equipment such as the GIA DiamondCheck. Meanwhile, colored diamonds, smaller stones, and mounted jewelry need to be tested by a reputable gemological laboratory. Increased industry awareness, combined with diamond testing, may deter the spread of undisclosed synthetics, ultimately benefiting both sellers and buyers of polished diamond goods.

Rachel Sheppard, Ulrika D'Haenens-Johansson, Kyaw Soe Moe, Tom Moses, and Wuyi Wang

Large HPHT-Grown Synthetic Diamonds Examined in GIA's Hong Kong Laboratory

Over the last decade, the jewelry industry has seen rapid improvement in the quality of synthetic diamond

Figure 18. These two large synthetic diamonds were produced using HPHT growth methods by the Russian firm New Diamond Technology. The 4.30 ct specimen on the left has D color and SI_1 clarity. On the right is a 5.11 ct sample with K color and I_1 clarity.

grown by the CVD (chemical vapor deposition) method. Colorless and near-colorless CVD synthetics with sizes up to 3.04 ct, with I color and SI_1 clarity, have been reported. GIA's Hong Kong laboratory recently examined two large synthetic diamonds created using the HPHT (high-pressure, high-temperature) method that demonstrated parallel progress in the two growth technologies. These samples, shown in figure 18, were produced in Russia by New Diamond Technology.

The first was a 4.30 ct cushion shape with D color and a clarity grade of SI_1, based on three small clusters of metallic inclusions. The other was a 5.11 ct cut-cornered rectangular modified brilliant. It had K color and a clarity grade of I_1, the result of a few metallic inclusions and two small fractures in the girdle area. Neither one showed reaction to long-wave UV radiation. When they were exposed to short-wave UV, a medium to strong green-yellow fluorescence was observed. Both showed strong yellow-green phosphorescence lasting more than 20 seconds. One noteworthy feature was the absence of pinpoint inclusions, which are common in HPHT synthetic diamonds and often distributed throughout the crystal.

Absorption spectra in the infrared region demonstrated these were type II diamonds, with no absorption band detected in the one-phonon region (approximately 1350–1000 cm^{-1}) where nitrogen impurities occur. A very weak 2800 cm^{-1} band was attributed to trace substitutional boron. A higher boron concentration was recorded in the D-color synthetic diamond (7 ± 1 ppb, compared to 1.2 ± 0.2 ppb). Photoluminescence spectra collected at liquid-nitrogen temperature with varying laser excitations revealed an emission doublet at 736.6/736.9 nm from the silicon-vacancy defect, and an 882.7/884.4 nm doublet from the well-known Ni-related defect. Very weak emissions from nitrogen-vacancy centers at 575.0 and 637.0 nm were detected only in the K-color sample. Besides metallic inclusions, another important identification feature of HPHT synthetics is fluorescence. Typical fluorescence patterns showing multiple-sector growth were observed in both samples.

These two diamonds were disclosed as HPHT synthetic when submitted for examination. Tested using the GIA DiamondCheck device, both were referred for further testing. Gemological observations and spectroscopic features confirmed they were HPHT synthetics.

Examination of these improved HPHT synthetic diamonds, the largest synthetic diamonds produced by any method that GIA has examined so far, demonstrated significant progress in this growth technology. In addition to their use as gem materials, crystals of this size have many potential industrial applications.

Ping Yu Poon, Shun Yan Wong, and Carmen Lo

SYNTHETIC MOISSANITE Melee in a Colored Diamond Bracelet

A colored diamond bracelet submitted to the New York laboratory for identification (figure 19) contained 162 round brilliants ranging from 0.05 to 0.20 ct, with a color range from near-colorless to fancy yellow and brownish yellow. Melee-size dia-

Figure 19. This fancy-color melee diamond bracelet contained two synthetic moissanites.

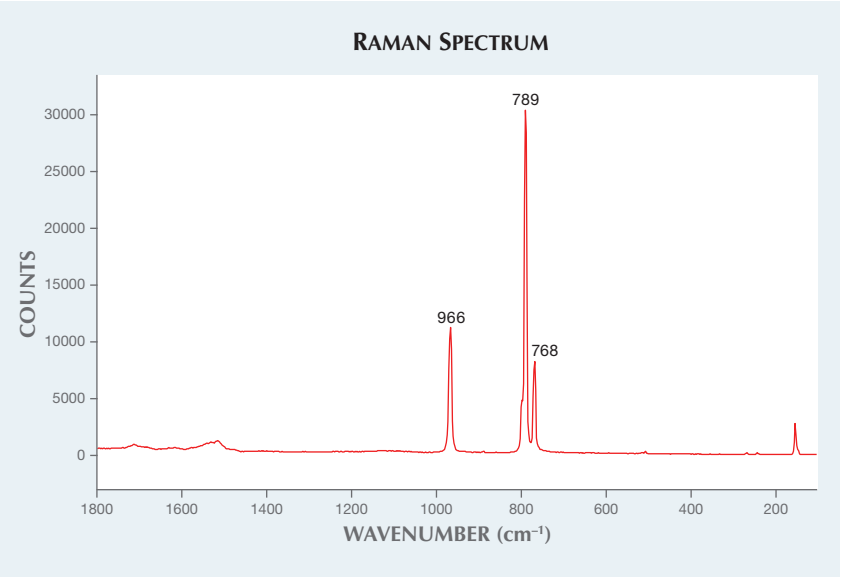

Figure 20. Raman spectroscopy confirmed the identification of two colorless round brilliants as synthetic moissanite with peaks at 768, 789, and 966 cm^{-1}.

monds below 0.20 ct are usually not screened for synthetics and imitations, and melee set into fine jewelry are very seldom tested due to limitations from the mounting. But because of recent concerns over fine diamond jewelry set with melee-size synthetics and imitations (see H. Kitawaki et al., "Identification of melee-size synthetic yellow diamonds in jewelry," Fall 2008 *G&G*, pp. 202–213; Winter 2014 Lab Notes, pp. 293–294), we decided to conduct a full analysis on the mounted round brilliants in this bracelet.

Testing was first performed on the 60 near-colorless round brilliants with the DTC DiamondSure. Several samples were referred and sent for further testing using Raman spectroscopy. Of these, two round brilliants were suspected as imitation. Close examination under the optical microscope revealed obvious doubling on the facet junctions, a key identification feature for synthetic moissanites (K. Nassau et al., "Synthetic moissanite: A new diamond substitute," Winter 1997 *G&G*, pp. 260–275). Further testing with Raman spectroscopy confirmed this identification with three peaks at 768, 789, and 966 cm^{-1} (figure 20).

FTIR spectroscopy performed on the other referred near-colorless and colored melee identified them as natural. One melee was found to be type IaB, while the others were type IaA.

This analysis showed that melee-sized diamond imitations are being mixed with natural diamond parcels and set into fine jewelry without proper disclosure. Therefore, proper identification by a gemological laboratory is an essential tool to maintaining the integrity of the industry.

Jessie Yixin Zhou

PHOTO CREDITS:
Nuttapol Kitdee—1, 11; Jonathan Muyal—2; Jian Xin (Jae) Liao—4, 6, 8, 13, 16 (left); Paul Johnson—9 (left and right); Kyaw Soe Moe—9 (center); Jessie Yixin Zhou—10, 19; Sood Oil (Judy) Chia—12, 19; Robert Weldon—15; Martha Altobelli—17; Ming Yin Poon—18.

G&G

Gem News International

Contributing Editors
Emmanuel Fritsch, *CNRS, Team 6502, Institut des Matériaux Jean Rouxel (IMN), University of Nantes, France* (fritsch@cnrs-imn.fr)
Kenneth Scarratt, *GIA, Bangkok* (ken.scarratt@gia.edu)

TUCSON 2015

Once again, buyers and sellers from all over the world converged on a corner of the American Southwest for the annual Tucson gem shows. Many broad trends continued from 2014: Consuming markets are hungry for fine colored gems, and demand still outstrips supply, causing prices for some gems to reach new highs. As more buyers from Asia compete for new production of rough gemstones, the secondary market is becoming more important for domestic dealers. Many recycled gems and jewelry pieces were returning to the market through estate sales, or directly from owners lured by all-time high prices. Some sellers were showing items that had been held in inventory for years or even decades (figure 1). These included fine corundum, Imperial topaz, red spinel, and aquamarine. We noted that many of these "recirculated" goods were exceptional gems, superior to newly mined production. Many vendors are unable to source new production at prices their clientele are prepared to pay.

Cultured pearls of every type were in high demand—especially from the Chinese market. The same was true of rubellite and "watermelon" tourmaline, tsavorite, and spinel, especially red to pink material from Mahenge, Tanzania.

Overall, we observed several clear trends:

- Many gem-quality stones were cut in nontraditional shapes such as cabochons, fantasy cuts, carvings (figure 2), and even slices.
- Many jewelry pieces had an organic, natural feel. Similarly, non-round pearls—particularly large baroque shapes—were also everywhere. The freeform shapes of many opals also fit well with natural-shape trends for jewelry, lending themselves to carved flowers, animals, and abstract pieces.
- Designers were seeking out unusual colors for standard gems: fancy-color sapphires, colored diamonds, tourmalines, spinel, garnets, zoisite, zircon, and beryl (morganite was very much in demand).
- Many vendors told us they left their "traditional" inventory items at home, as they can sell those at any time. The Tucson crowd demands the unusual (figure 3), so vendors brought nontraditional items and were reportedly selling them at a good pace.
- Even though red-brown "Marsala" was named the Pantone color of the year for 2015, it did not appear to be an overall favorite, with the most observed colors being bright blues, greens, and pinks.
- The largest crowds observed at the wholesale shows were gathered at the booths selling nontraditional gem materials such as cabochons, druzy, tourmalinated and rutilated quartz (again, see fig-

Figure 1. Many sellers at Tucson were displaying very large, fine, or unusual gems that had been held in inventory for years. Photo by Duncan Pay/GIA; courtesy of Noor Gems Japan Ltd.

Editors' note: Interested contributors should send information and illustrations to Stuart Overlin at soverlin@gia.edu or GIA, The Robert Mouawad Campus, 5345 Armada Drive, Carlsbad, CA 92008.

Gems & Gemology, Vol. 51, No. 1, pp. 68–110, http://dx.doi.org/10.5741/GEMS.51.1.68.

Figure 2. Rutilated quartz was a popular material at the 2015 Tucson gem shows. These examples were carved by German artist Alexander Kreis. Photo by Eric Welch/GIA; courtesy of Sonja Kreis.

Figure 3. All throughout central Tucson and along the Interstate 10 corridor, tents sprang up around hotels and other venues to host buyers and sellers from all over the globe. Photo by Duncan Pay/GIA.

ure 2), and crystal slices—material typically used in "craft" jewelry.

- Opal (figure 4) was prominent: There was an abundance of Ethiopian hydrophane opal, Australian opal, Mexican fire opal, and material from the U.S. Recent finds in Ethiopia have generated a buzz for all types, according to several vendors.

Foot traffic at the main AGTA and GJX shows appeared down from 2014, but most merchants reported brisk sales, especially of very fine or unique items. In fact, many vendors mentioned that this was their best show in recent years. Eric Braunwart of Columbia Gem House (Vancouver, Washington) said he had forgotten what a "good year was like" until this show.

Alexander Wild (Wild & Petsch Lapidaries, Kirschweiler, Germany) provided a broad-brush market update from his firm's perspective. Rough prices for many gems continued on an upward trajectory, he reported. Just a few years ago, fine-color, high-clarity rubellite tourmaline sold at wholesale for $300 to $350 per carat. These numbers reflected the asking price for superb quality, with perhaps just a few tiny inclusions. In 2015, prices for equivalent material are almost triple that figure.

As in the previous year, sourcing rough gems remains a problem, although it is by no means impossible for established companies with good connections in source

Figure 4. Opals of all kinds were prominent at this year's shows. The freeform shapes of these Mexican fire opals lend themselves to one-of-a-kind pieces. Photo by Eric Welch; courtesy of Opalos & Artesanias Mexicanas.

Figure 5. The Cruzeiro mine, the Miranda Group, and KGK work together to bring Brazil's bicolor and rubellite tourmaline to the market in China. The Cruzeiro mine provides the rough to the Miranda Group, which cuts the material. Photo by Andrew Lucas; courtesy of Miranda Group Co. Ltd.

countries, such as Wild & Petsch. The company is able to source quality rough, though prices are definitely higher for many goods. Since mid-2014, prices for many other commodities such as oil and copper have fallen. But gemstone rough prices continue to rise, largely due to demand from China. In Wild's opinion, such high prices are unsustainable. He wondered how long this would continue, asking rhetorically, "Is this a gem bubble?"

Asked what was in demand, he answered that it was the gemstones Wild & Petsch is known for: fine tourmaline and beryl. With their African connections, they secured a nice production of Paraíba-type copper-bearing tourmaline from Mozambique, along with good parcels of aquamarine. As a result, they were able to offer their clientele this material at what Wild considered very fair market prices. In contrast, supply of rubellite and pink tourmaline rough is quite difficult, and most of his supply has been coming from Nigeria. Brazilian rubellite is basically unavailable.

Figure 6. Rough tourmaline crystals are sliced or sawn by the Miranda Group in Hong Kong, then faceted and polished at their factory in Shenzhen. Photo by Andrew Lucas; courtesy of Miranda Group Co. Ltd.

Figure 7. Fine Brazilian rubellite tourmaline at the Miranda Group's factory in Shenzhen—most of these cut stones are larger than 10 ct. The factory needs to receive 100 kilos of rough per month to meet production goals of 25,000 to 30,000 carats. KGK markets and sells the cut stones and also mounts them into jewelry for sale, primarily in China. Photo by Andrew Lucas; courtesy of Miranda Group Co. Ltd.

[*Editor's note*: In a 2014 visit to Brazil's Cruzeiro mine in Minas Gerais State, a GIA team witnessed recovery of large facet-grade rubellite crystals (figure 5), which were all put aside for exclusive sale to a consortium—composed of the Miranda Group and KGK—that fashions the material at its own factory in Shenzhen, China, for the Chinese market (figures 6 and 7). Only blue to green production was available for sale to local and export markets.]

Adjusting to price fluctuations has always been part of life for colored stone merchants, Wild conceded, but not sudden, successive increases to levels that are three, four, or five times higher than the market was previously accustomed to (see www.gia.edu/gia-news-research-miranda-journey-of-rubellite-tourmaline).

Wild offered the possibility that at some point a single market will be satisfied—even one as large as China's. When that happens, suppliers will have to find other markets for these goods. Wild believes the North American and European markets are more sophisticated in terms of pricing—especially for cut goods—than China's current market. There is also the possibility that any political upheavals there could cause rough prices for certain gems to go down sharply, he said. And that could spell trouble for some miners who base their operations on today's historically high rough gem prices.

Wild said business at the 2015 show had been better than the year before. He reckoned business was a third above 2014, with some big-ticket items—including a fine aquamarine suite—spoken for prior to the show. He confirmed our impression that traffic was down slightly from last year—possibly due to fewer Asian buyers or the winter travel difficulties on the U.S. East Coast.

Wild intimated that many clients came with specific requirements in mind, particularly aquamarine or Paraíba-

Figure 8. A group of Paraíba tourmalines from Brazil's Rio Grande do Norte state. From the top: a 6.28 ct cushion, a 1.73 ct triangular brilliant, a 5.28 ct oval, three smaller ovals totaling 3.50 carats, and a 0.97 ct triangular brilliant. Photo by Robert Weldon/GIA; courtesy of Brazil Paraíba mine.

type tourmaline, and selection was good for these gems at this year's show. He mentioned they had even sold a few collectors' pieces, including a beautiful large green step-cut beryl that measured more than 200 ct. That was a surprise to him, because such items have proven more difficult to sell the last few years.

"Everyone is searching for good things," Wild concluded. "For the most part, we get what we need." Asked if the trend is still toward finer, more unique pieces, Wild responded, "Absolutely. I think quality still comes first. A lot of the trends from last year still apply, and we're still waiting to see if there's going to be any deflation in pricing for some goods."

Once again, *G&G* greatly appreciates the assistance of the many friends who shared material and information with us this year, with special thanks to the American Gem Trade Association for providing photography studio space during the AGTA show. Dr. Tao Hsu, Andy Lucas, Donna Beaton, Pedro Padua, and Dr. Jennifer Stone-Sundberg contributed to these reports.

New production of copper-bearing tourmaline from Rio Grande do Norte, Brazil. At the GJX show, Sebastian and Ananda Ferreira (Brazil Paraíba mine, Parelhas, Brazil) showed us examples of new production from their MTB mine, which a GIA team visited in April 2014. The seven principal stones we saw were a 6.28 ct square cushion, a 1.73 ct triangular brilliant, a 5.28 ct oval, three small ovals totaling 3.50 carats, and a smaller 0.97 ct triangular brilliant (figure 8).

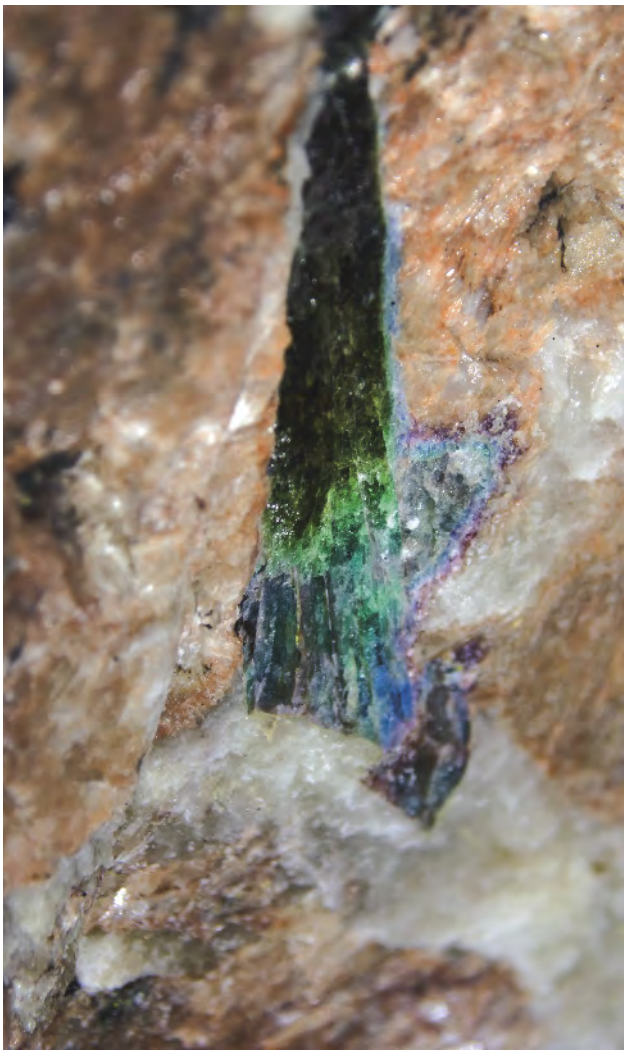

Figure 9. Discovered in early 2014, this spray of copper-bearing tourmaline was a harbinger of new production at the MTB mine in Rio Grande do Norte. Photo by Duncan Pay/GIA.

The MTB mine is located at the northern edge of a ridge of low, rounded hills that curve to the south and west from Rio Grande do Norte toward the original copper-bearing tourmaline discoveries by Heitor Barbosa at Mina da Batalha in the state of Paraíba. The geology is very similar to the Batalha occurrences, except that the feldspars in the MTB mine's pegmatites are not decomposed.

These gems represent the first new production from the mine in several years. At the time of GIA's visit, the operation was reprocessing ore from previous mining for melee-sized rough. This produces strongly colored precision-cut gems, much in demand for the watch industry. When GIA visited the mine, miners had recently extended the workings downward and been rewarded with sprays of what appeared to be copper-bearing tourmaline in the wall rock (figure 9).

Figure 10. This exceptional 9.22 ct emerald is from Belmont's underground mine. Photo by Robert Weldon/GIA; courtesy of the Belmont mine.

The new production that furnished the cut gems seen in figure 8 came a few weeks after the GIA team's departure. For more on the MTB mine, please see www.gia.edu/gia-news-research-an-overview-of-2014-gia-brazil-expedition.

Duncan Pay
GIA, Carlsbad

New production of Brazilian emerald from Minas Gerais. At the GJX show, Marcello Ribeiro (Belmont Mine, Itabira, Brazil) showed us production from Belmont's underground mine, including one especially fine 9.22 ct stone (figure 10). As a GIA team visited Belmont in April 2014, it was interesting to see the gems from this relatively new part of the mining operation for sale at the show.

Originally the site of a cattle ranch, Belmont yielded its first emeralds in 1978 (H.A. Hänni et al., "The emeralds of the Belmont Mine, Minas Gerais, Brazil," *Journal of Gemmology*, Vol. 20, Nos. 7–8, 1987, pp. 446–457). Since then, the mine has expanded to include both open-pit and underground operations with a highly sophisticated recovery plant. Mining is supported by a comprehensive geological survey program. To date, more than 15 km (9.3 miles) of 3.8 cm (1.5 inch) diameter cores have been drilled. Geological surveys indicated that a 300-meter-thick schist layer—with emerald potential—underlies much of the property, including the recovery plant. Core sampling defined the extent and depth of the emerald ore body and proved the viability of an underground mine at Belmont. Sampling the underlying rocks also helped plan the mine's mechanical structure by showing which layers would be capable of supporting underground tunnels.

The underground mine is accessed via a 666-meter ramp that allows removal of up to 30 to 40 truckloads of ore per day using large commercial trucks (figure 11). At the time of our visit, approximately 10 to 15 truckloads per day (about 200 tonnes) were being taken to the recovery plant. The underground workings deliver a ratio of one tonne of ore to one tonne of waste. Each tonne of ore yields about two grams of rough emerald. On average, those two grams of rough produce two carats of faceted emeralds. By contrast, the ratio for the current open pit is only one tonne of ore per 11 tonnes mined. The rest is overburden or waste. There is clearly the capacity for many more years of productive mining at Belmont.

During the same April 2014 trip, GIA field gemologists visited the Montebello mine, near Nova Era. At this year's GJX show, Sergio Martins (Stone World, São Paulo) showed us new production from that mine (figure 12). These gems were in the 2–4 ct range, bright with strong color and good luster.

Figure 11. A full-size truck navigates the tunnels of Belmont's underground mine. From the outset, the operators determined this would be a high-capacity, ramp-style mine. Photo by Duncan Pay/GIA; courtesy of the Belmont mine.

Figure 12. This array of gems in the 2–4 ct range from the Montebello mine shows the bright, vivid appearance of high-quality emeralds from Nova Era. Photo by Robert Weldon/GIA; courtesy of the Montebello mine.

The Montebello mine is adjacent to the independent miners' village of Capoeirana, about 6 km (3.7 miles) from Nova Era. Capoeirana is about 26.5 km (16.5 miles) east of Itabira. Unlike the larger mechanized operation at Belmont, the area around Capoeirana hosts a variety of small-scale mining activities by these independent miners, known as *garimpeiros*. The Montebello mine is perhaps the largest, employing 15 of them.

Emeralds were first discovered near here in 1988 (D. Epstein, "The Capoeirana emerald deposit near Nova Era, Minas Gerais, Brazil," Fall 1989 *G&G*, pp. 150–158; www.gia.edu/gems-gemology/fall-1989-brazil-emeralds-epstein). The exploration that led to a mining boom in nearby Capoeirana was triggered by the discovery of emerald at Belmont. Production has dwindled in Nova Era, due in part to the 2008 global economic recession and the greater depths—often more than 100 meters—required to reach the emerald mineralization (A. Lucas, "Brazil's emerald industry," Spring 2012 *G&G*, pp. 73–77; www.gia.edu/gems-gemology/spring-2012-brazil-emerald-lucas). Emerald mineralization in the surrounding area appears to start in Nova Era and finish at the Belmont mine. Between them is another—currently unworked—mine, called Piteiras, which Martins used to operate. Mining stopped there due to ownership disputes that the parties hope will be resolved shortly.

At Montebello, the main elevator shaft descends 130 meters. At the time of GIA's visit, miners had sunk a new vertical shaft about 40 meters below the level of the existing main shaft (figure 13). It follows a new vein that dips steeply underground. Neighbors in an adjacent mine have already found a productive vein at about that level. When the miners sunk their shaft, they located a seven-meter-thick seam of soft black schist underlain by granite. Emeralds occur in the boundary where the quartz meets the schist. The dark color of the schist and the presence of quartz are good indicators for emeralds and pale beryl crystals. From this new 40-meter shaft, they are driving a new horizontal tunnel out into the schist. The miners plan to expand the shaft and install a second elevator. The miners added that Montebello's stones appear to increase in size and color with depth.

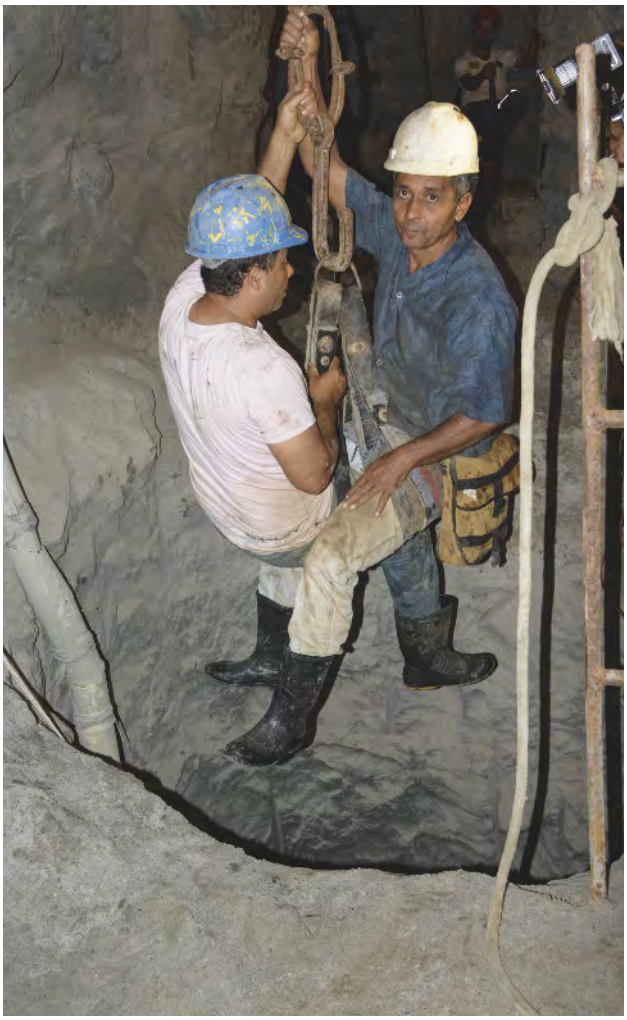

Figure 13. At Montebello, the miners have sunk a new shaft to follow a promising vein of emerald-bearing schist to deeper levels in the mine. The base of the new shaft is 170 meters below the surface. Photo by Andy Lucas/GIA; courtesy of the Montebello mine.

Duncan Pay

Exceptional red spinels and fine aquamarine. At the GJX show, Axel Henn (Henn GmbH, Idar-Oberstein, Germany) showed a superbly colored 61.29 ct Tanzanian red spinel measuring 36.49 × 18.44 × 13.55 mm (figure 14), along with two pear-shaped gems cut from similar rough. Red spinels of this size, color, and quality are exceptionally rare. Indeed, stones of such deep, rich color larger than 50 ct are almost unheard of.

According to Henn, this gem was from a find of three exceptionally large spinel crystals (one larger than 50 kg) recovered from a dried riverbed in the mid-2000s. Henn heard of the discovery through a local Tanzanian contact.

Figure 14. Superb Tanzanian red spinel marquise of 61.29 ct. Photo courtesy of Henn Gems.

Figure 15. Among the many fine aquamarines at Axel Henn's booth, the standout was this 450.08 ct square step-cut gem. Photo by Duncan Pay/GIA; courtesy of Henn Gems.

The crystals needed to be hammered and trimmed, but they still produced cuttable rough of significant size, including a suite of gems totaling 174.58 carats. In his opinion, the 61.29 ct marquise is the finest of the lot.

This is likely the same discovery as the widely reported 2007 recovery of four giant spinel crystals weighing 52, 28, 20, and 5.7 kg from a zone in the Ipanko ruby and spinel mining area known as the "Joel Box." Reported as having a "vibrant orangy, pinkish red color," the largest crystal was broken up for transportation away from the mining area. The outside portions of crystals had some superb cuttable material, but the cores were mostly lower quality. Although the eventual yield was said to be as low as 3%, the crystals had the potential to produce many thousands of carats of cut gems, including significant pieces of over 50 ct. The 61.29 ct marquise is likely part of this yield.

Henn also displayed a superb 450.08 ct rectangular (corners-on) step-cut aquamarine (figure 15). This gem possessed the coveted pure blue "Santa Maria" color, with no hint of green or yellow (this name refers to a mine near Santa Maria de Itabira in Minas Gerais, Brazil). The gem was of stunning clarity—this cutting style is very revealing of any imperfections—and was fashioned from rough recovered in 1927. Henn said he purchased the rough from an "old gemstone family," and it had been "kept in the basement" for generations.

Duncan Pay

Fine tsavorite and spinel. Bruce Bridges (Tsavorite USA Inc., Tucson) said that fine stones often return to his inventory after years in a collector's possession. At the AGTA show, he showcased a vivid, top-quality 12.46 ct cushion-cut tsavorite fashioned some 15 years earlier, which made its way back into the market in the last two years (figure 16). As tsavorite rough has a high value, gems are typically cut to maximize weight. Rough is typically recovered as long, thin asymmetrical fragments that lend themselves to pear, marquise, and trilliant shapes. This example's unusual square cushion shape, large size, color, and clarity make it a notable and rare gemstone.

After seeing the wealth and variety of gems on display at the Tucson gem shows, it might be easy to come away with the impression that fine colored stones are not particularly rare. Yet the truly magnificent stones are extremely rare and often have a memorable provenance. One such gem is the 18.21 ct triangular cut red spinel Bruce Bridges showed us at his AGTA booth (figure 17). According to Bridges, this magnificent gem was cut in 2007 in Bangkok from rough recovered in one astounding find in Tanzania's Ipanko mining area that yielded several giant spinel crystals, one of which weighed in at over 50 kg. A number of other dealers at this year's show, including Axel

Figure 16. This spectacular 12.46 ct tsavorite recently returned to Bruce Bridges's inventory after being in a collector's possession for many years. Photo by Robert Weldon/GIA; courtesy of Bridges Tsavorite.

Figure 17. This 18.21 ct Tanzanian red spinel was fashioned from material recovered from one of four enormous multi-kilogram crystals reputedly found in the Ipanko ruby and spinel mining area near Mahenge, Tanzania. Photo by Robert Weldon/GIA; courtesy of Bridges Tsavorite.

Figure 18. This unheated 8.56 ct intense pink sapphire represents the very best of recent production from Madagascar. Photo by Robert Weldon/GIA; courtesy of B&B Fine Gems.

Henn, also displayed fine gems from this one extraordinary discovery.

Donna Beaton
GIA, New York

Fine corundum, demantoid garnet. At the AGTA show, Dave Bindra (B&B Fine Gems, Los Angeles) showed us some exceptional corundum, especially fine untreated yellow and pink sapphires.

The first standout piece Bindra showed us was an 8.56 ct unheated, intense pink sapphire of extremely high clarity from Madagascar. Under the lights of our photo studio, it showed an intense pink hue (figure 18). A gem of this quality might expect to realize a wholesale price in the region of $10,000 to $15,000 per carat. Bindra noted that Madagascar is producing some superb fancy sapphire, including pink, violet, and "padparadscha" colors.

Although this pink gem represented recent production, Bindra explained that the secondary market has become an extremely important source for many dealers now that competition for freshly mined goods is so intense, particularly from buyers serving Asian markets. These recirculated gems coming back onto the market offer a way for dealers to procure stones that often surpass current production in size and quality, or are simply unobtainable today. As an example, Bindra cited an 89.55 ct unheated golden sapphire from Sri Lanka (figure 19), remarking that he had not seen material of this color emerge from the ground in Sri Lanka for more than 10 years. Originally this gem was somewhat larger, over 100 ct. Modern cutting reduced the weight slightly but produced a dramatic improvement in color and brilliance. Bindra described this gem's appearance and stature as "world class." As such, it would likely command a wholesale price in excess of $3,000 per carat.

Bindra next showed us a blend of new production and recirculated stones: a graduated suite of 12 perfectly matched Russian demantoid garnet round brilliants. Each gem contained a classic "horsetail" inclusion. Weighing in at 20 carats total, the suite took Bindra four years to complete. He described it as a special item, with the stones from the secondary market selected and recut to perfectly match the newer gems.

For Bindra, Mozambique is the future of ruby production. He illustrated this with three fine heated gems from the Montepuez deposit weighing 7.05, 7.92, and 9.35 ct (figure 20). Although all three stones represented beautiful, clean material, he considered the 7.92 ct gem the finest, due to its superior brilliance and intense red hue. Due to the ongoing trade embargo with Myanmar, classic "Burmese" ruby is unobtainable for U.S. dealers. Fine Mozambique rubies like these in the 7–9 ct range are in high demand and exceptionally rare. Gems larger than 4 or 5 ct are increasingly hard to find, Bindra pointed out.

Figure 19. This exceptional unheated 89.55 ct golden sapphire from Sri Lanka is an example of a recirculated stone. Photo by Robert Weldon/GIA; courtesy of B&B Fine Gems.

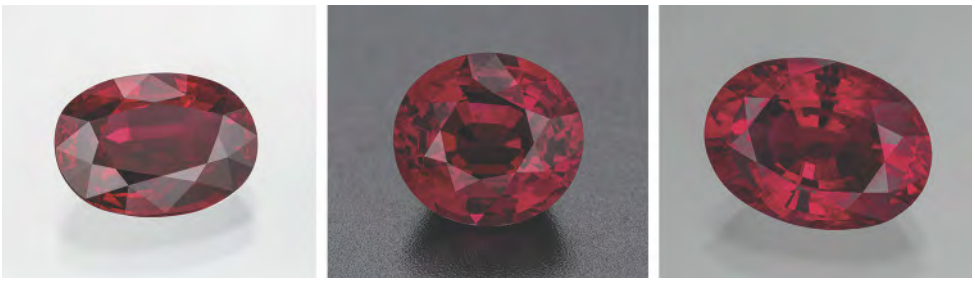

Figure 20. Left to right: These heated rubies from Mozambique weigh 7.05, 7.92, and 9.35 ct. Photos by Robert Weldon/GIA; courtesy of B&B Fine Gems.

Unlike Myanmar, Mozambique does not carry the stigma of human rights abuses. The heat treatment of these rubies is not an issue with consumers, either. As Bindra explained, the market for top natural unheated ruby has now reached such rarified levels that buyers are very receptive to high-quality heated rubies. (The current auction record is held by an unheated 8.62 ct Graff ruby, of Burmese origin, which sold for $8,372,094—or $994,040 per carat—at a Sotheby's Geneva auction in September 2014.) Purchasing such expensive stones is a stretch even for the top 1% of consumers. By contrast, stones like the three Bindra showed us wholesale in the region of $35,000 to $50,000 per carat. He said gems like these are "quite consumable" and can be the centerpieces of wearable jewelry, meaning they will occasionally be seen outside of safe deposit boxes.

Bindra faces the same issue as many other colored stone dealers in Tucson: scarcity of new rough production due to intense competition between the U.S. market and buyers purchasing for Chinese consumers. This is the major driver for dealers looking for alternative sources of gems such as recirculated goods, he said.

The new wealth in China has created a different dynamic. For more than 50 years, American and European consumers have been the main buyers of fine gemstones, he explained. Now these established markets have competition, and Bindra and many of his colleagues in the business supply gems to these competitors as well. Besides China, other cultures—India, for instance—have a rich jewelry heritage, and consuming gems is ingrained. This trend is not going to change, so there will be more wealthy consumers in emerging markets that desire colored gems, and current producers will struggle to meet demand.

In terms of demand at the show, Bindra reported that rubies and unheated sapphires were quite strong. There was demand for anything rare and exotic, goods that the average consumer would not find elsewhere. He also saw renewed demand for emerald. In the past, he noted a "certain favoritism" toward Colombian emerald, but increased supplies of quality gems from Zambia have made it a much more popular source and established the "Zambian brand" in people's minds.

Duncan Pay

High-end colored gems. At GJX, Constantin Wild (W. Constantin Wild & Co., Idar-Oberstein, Germany) showed us a remarkable multicolored suite composed of 12 gems from all over the world. The total weight was 290 carats, with each gem weighing approximately 25 ct and measuring 19–20 mm. The suite included aquamarine and an unheated purple copper-bearing tourmaline from Mozambique; rubellite, yellow beryl, green tourmaline, and Imperial topaz from Brazil; peridot and kunzite from Pakistan; mandarin (spessartine) garnet from Nigeria; tanzanite from Tanzania; green sphene from Sri Lanka; and "canary" tourmaline from Zambia (figure 21).

Figure 21. Constantin Wild displays a unique 290 carat multicolored gem suite. Photo by Duncan Pay/GIA.

Figure 22. 26.18 ct and 19.83 ct "canary" tourmalines from Zambia. Photos by Duncan Pay/GIA; courtesy of Constantin Wild.

Wild specifically highlighted canary tourmaline (figure 22). He remarked that its intensity of color is reminiscent of Paraíba tourmaline. Found intermittently in the 1980s and marketed since the early 2000s, this typically yellow-green material is rich in manganese (up to 9.18 wt.% MnO). Wild had two significant oval-cut gems of 19.83 and 26.18 ct, both unheated. For more information on this unique gem, see www.gia.edu/gems-gemology/winter-2007-yellow-tourmaline-zambia-laurs.

Another standout at Wild's booth was a superb suite of rubellite tourmaline totaling 339.42 carats (figure 23). Wild called it a suite "from two continents," as it contained both South American and African gems. The suite featured a spectacular cushion-cut 77.16 ct Nigerian rubellite centerpiece from new production, measuring 28.30 × 24.87 mm, framed by nine perfectly matched Brazilian rubellites from previous inventory weighing 262.26 carats.

Besides his higher-end single gems and suites, Wild also displayed some mixed-color sets, which he described as more "fashion-oriented" combinations (figure 24). Intended as concepts for jewelry designers, they included color combinations such as opal with pink tourmaline and morganite beryl with red tourmaline, tanzanite, tsavorite,

Figure 23. This superb 339.42 carat suite of 10 rubellite tourmalines contains Brazilian gems with a Nigerian center stone. The gems in the suite range from 39.61 to 77.16 carats (center stone). Photo by Duncan Pay/GIA; courtesy of Constantin Wild.

and treated blue topaz, along with more unusual arrangements: demantoid and "Mali" garnet with fire opal, or yellow beryl and mandarin garnet.

Another trend was the use of facet-grade rough for cabochons. These were often of large size and superb color. Of particular note were a 104.83 ct tanzanite and a 140.95 ct kunzite spodumene (figure 25).

Duncan Pay

Tsavorite garnet and Mahenge red spinel. At GJX, Daniel Assaf (The Tsavorite Factory, New York City; figure 26) explained the current market situation for tsavorite garnet, Tanzanian red to pink spinel, and yellow danburite. According to Assaf, the recent recession and the ensuing disruption in supply had less of an impact on his business

Figure 24. Constantin Wild's selection of mixed-color sets for jewelry designers included some interesting combinations. Photo by Duncan Pay/GIA; courtesy of Constantin Wild.

Figure 25. Left: A 140.83 ct tanzanite cabochon with superb color and clarity. Right: Kunzite is rarely seen in cabochon cuts. The color and clarity of this 140.95 ct example make it noteworthy. Photos by Duncan Pay/GIA; courtesy of Constantin Wild.

than increasing demand from China. For him, current rough scarcity and high prices relate more to the growth in the Chinese jewelry market, which 5 to 10 years ago was a fraction of its size today.

Assaf explained that both tsavorite and spinel are rare stones, and even minor changes in the market might have a considerable impact. If just a fraction of one percent of Chinese consumers becomes interested in tsavorite, this has a measurable consequence for supply, especially if production in mining areas is static or even showing slight declines. According to Assaf, the biggest tsavorite purchasers at the source in Arusha, Tanzania, are Sri Lankans buying for the Chinese domestic market. These buyers are prepared to pay very high prices for tsavorite rough.

To illustrate the sporadic nature of current supply, Assaf cited a bright, light-toned green grossular garnet. This material has become popular and is sold as "Merelani mint" garnet. It is usually recovered as a byproduct of tanzanite mining. Every so often, he related, miners find a productive pocket and buyers fly in within a couple of weeks.

According to Assaf, the stones on the tray in front of us (figure 27) were from the latest small pocket and had been in the ground just a few months earlier. After the initial flurry of buying activity, Assaf said, it might be another year or two before a similar discovery. In the meantime, the miners might bring buyers the occasional stone—at much higher prices.

In Assaf's opinion, today's tsavorite rough prices in Arusha are almost "out of control." In effect, there is a disconnect between the Arusha prices and the prices in Tucson, which will likely take several years to readjust.

His company stops buying before the Tucson show because the clientele here will not pay the high asking prices. He cited an instance several weeks earlier in which buyers were offering him top-quality rough for approximately $10,000 per stone, in sizes sufficient to cut 3 ct finished gems. A stone cut from this rough would have a per-carat price well above what the market at the Tucson show would pay. Besides the high asking price, Assaf said there is a significant element of risk in buying rough: "You never know what kind of unpleasant surprises you might find."

He pointed out that there are places in the world where such high prices are accepted—China and possibly parts of Europe—which is why the few fine rough tsavorites that become available every month are snatched up. Assaf had just heard of a 7-gram piece of tsavorite—perhaps suitable for a 10 ct finished gem—that sold for $200,000 in Arusha.

Assaf showed us two examples of the finest tsavorite col-

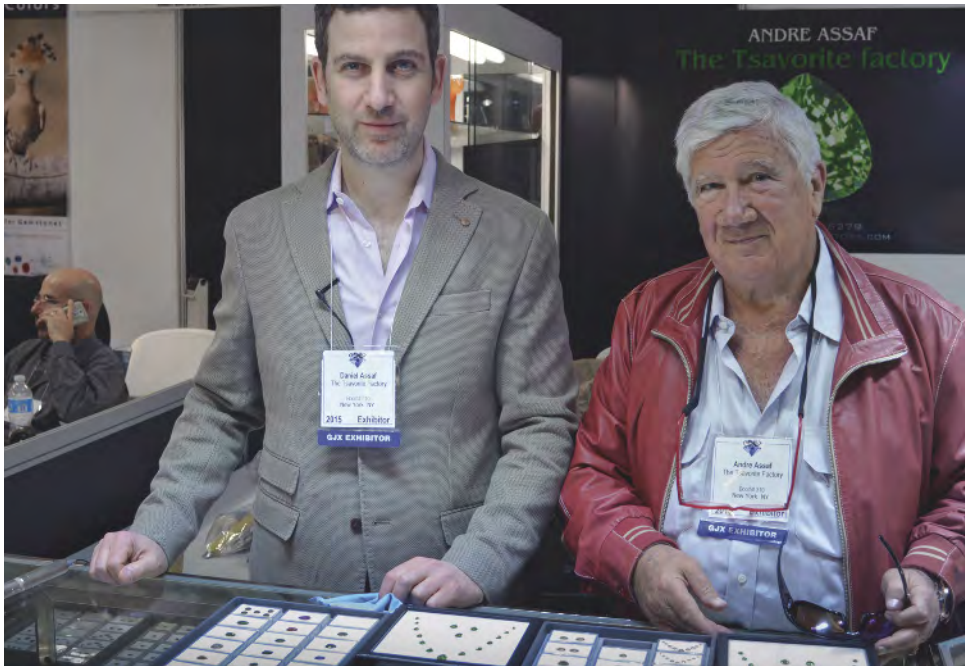

Figure 26. Daniel and Andre Assaf of the Tsavorite Factory explained the current market for tsavorite. Photo by Duncan Pay/GIA.

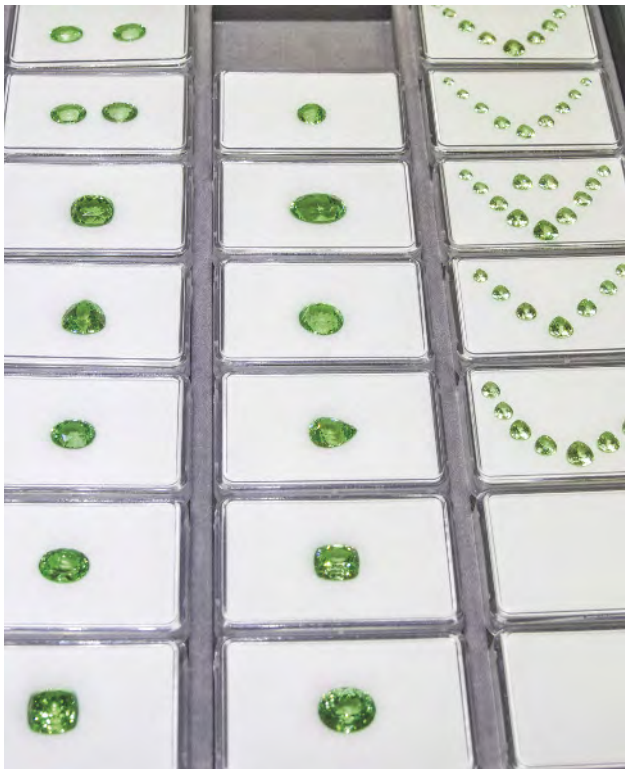

Figure 27. These light-toned Tanzanian grossular garnets—termed "Merelani mint"—were mined just a few months prior to the Tucson show. Photo by Duncan Pay/GIA; courtesy of Tsavorite Factory.

ors. In his opinion, both are of equal merit (figure 28, left). Some clients love the deeper, darker color, while others prefer a brighter, lighter-toned green. In either case, he said, the most important consideration is to have a blue color component rather than a yellow one. As long as the gem is not overly dark, and has a bluish cast to the green, it is a quality stone. If it is pale but still has a bluish component to the green, he would classify it as a "mint" garnet.

We asked Assaf how recent Chinese demand has affected tsavorite prices. He said that for sizes under 2 ct, prices have increased as much as 30–40%. The impact has been most dramatic in larger stones: For gems larger than 3 ct, prices have tripled. He felt that prices for large tsavorites have gone up in relation to emerald and other gems due to scarcity of supply and high demand.

To emphasize the point, Assaf chose a suite of three tsavorite pear shapes totaling 37.79 carats (figure 28, right). Each gem was above 10 ct and of the highest clarity, so they constituted exceptionally rare material. Aside from these standouts, Assaf admitted he had few stones of such size—large stones are typically a Tsavorite Factory specialty—due to the prohibitively high price of rough. He lamented that with today's stratospheric prices, he would have to pay around $200,000 to obtain another 7-gram piece to cut another 10 ct gem. And very few clients—likely none at this show—would accept the resultant high per-carat prices for the finished gem. That leaves two possibilities: Either the prices will adjust in Arusha, or they will become accepted in the U.S.

Assaf recounted that some of the same market factors apply to red spinel. His company does not carry spinel from Myanmar, focusing instead on Tanzanian material. This year, he said, a specific color people were calling "Mahenge"—deep pink with a touch of orange, almost like a padparadscha color—was in extremely high demand (figure 29). Assaf had sold all of his "Mahenge" spinel but none of the other colors. While these lavenders, blues, and mauves are quite beautiful and competitively priced at around 10% of the pinks, the red to pink spinels are what his clients seek. Assaf also mentioned that buyers looking for something unusual picked yellow danburite from Tanzania, and that this gem had sold quite well for him at the show (Summer 2008 GNI, pp. 169–171).

Duncan Pay

Figure 28. Left: Some prefer tsavorite garnets with a brighter color, while others prefer a darker appearance. The stone on the left weighs 9.50 ct. Right: This suite of three pear-shaped tsavorites totals 37.79 carats. The approximate asking price for such fine gems would be about $15,000 per carat. Photos by Duncan Pay/GIA; courtesy of Tsavorite Factory.

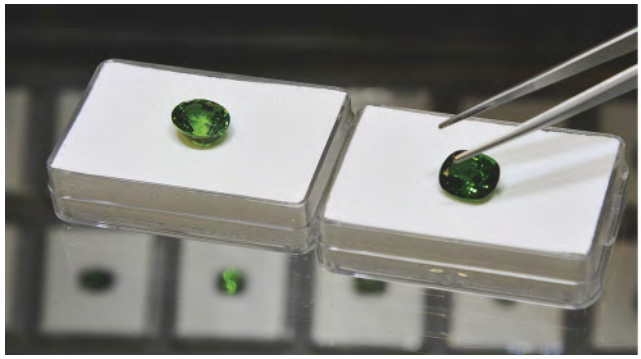

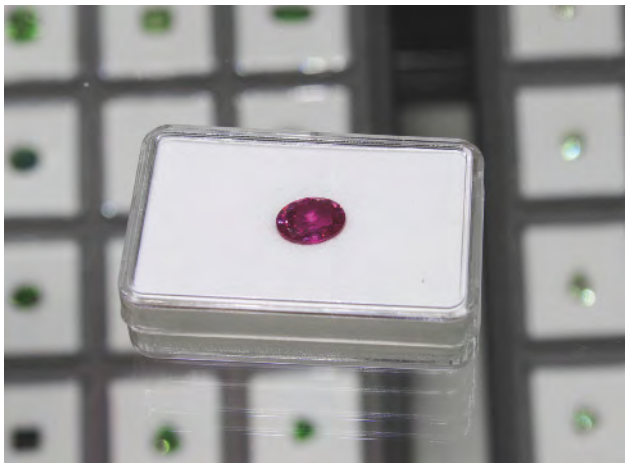

Figure 29. An example of "Mahenge" spinel from Tanzania. This was one of the few examples left at Daniel Assaf's booth at the time of our interview. Photo by Duncan Pay/GIA; courtesy of Tsavorite Factory.

Figure 30. Fashioned by lapidary Jean-Noel Soni, this 35.50 ct mixed-cut sunstone is reportedly from a mine on Eagle Butte, in Oregon's remote Harney Basin. Photo by Robert Weldon/GIA; courtesy of Suncrystal Mining.

Oregon sunstone update. At the GJX Show, Nirinjan Khalsa (Suncrystal Mining, Lake and Harney Counties, Oregon) showed us a remarkable 35.50 ct rich orangy red Oregon sunstone fashioned into a modern mixed-cut cushion by lapidary Jean-Noel Soni (Top Notch Faceting). This stone (figure 30) resembled a fine ruby under the showcase lights and was one of the most exquisite examples we had seen.

At Khalsa's request, we followed up with Soni after the show. He told us the original rough weighed 198.82 ct. As is typical with Oregon sunstone, the rough contained spots of strong red or green color in the cores of otherwise yellow or near-colorless crystals. This crystal had two color spots, so he divided it, and this gem was the first of two he intended to cut. Rather than using CAD software to design his gems' faceting styles, Soni treats each rough as unique and individual, cutting to maximize color and luster. He explained that the pavilion had to be deep, due to sunstone's relatively low RI (1.563–1.572). This produced a 63.00 ct preform, from which he faceted the 35.50 ct gem we saw. The asking price for this gem—reportedly from one of the mines on Little Eagle Butte (in Harney Basin, near Plush, Oregon)—was in the region of $60,000.

Also at the GJX show, Don Buford and Mark Shore (Dust Devil Mining, Plush, Oregon) gave an update on their operations. They said 2014 was a good year at Dust Devil. They uncovered a former dried creek bed where the basalt was extensively decomposed, which has allowed easier recovery of the sunstones. Buford hopes to have the mine's optical sorter operational for the 2015 mining season.

Shore showed us an exceptional 156.00 ct "watermelon" sunstone from recent production (figure 31). The stone has a red center surrounded by a greenish "rind." Shore has made arrangements to have it carved by Dalan Hargrave, winner of multiple AGTA Spectrum Awards.

At the 22nd Street show, Terry Clarke, co-owner of the Dust Devil mine, explained a recent initiative to maintain the integrity of natural, untreated Oregon sunstone and promote it to retailers and consumers as a rare and desirable "all-American" gemstone. Called the Oregon Sunstone Miners Association (OSMA), the organization includes most of the miners with working claims or mines in Lake and Harney Counties (figure 32). OSMA also offers an associate membership for sellers of loose gems or jewelry. Anyone purchasing sunstone from an OSMA member can be assured they are getting the natural, untreated Oregon product. The intention is to expand the marketplace for this unique gem and maintain stability and consumer confidence in the event of an influx of treated material from another source. The association's website is www.oregonsunstonema.com.

At the AGTA show, John Woodmark (Desert Sun Mining & Gems, Depoe Bay, Oregon) provided an update of his

Figure 31. This 156.00 ct rough sunstone belongs to the Dust Devil mine's Mark Shore and will likely become a fine carving. Photo by Duncan Pay/GIA; courtesy of Mark Shore.

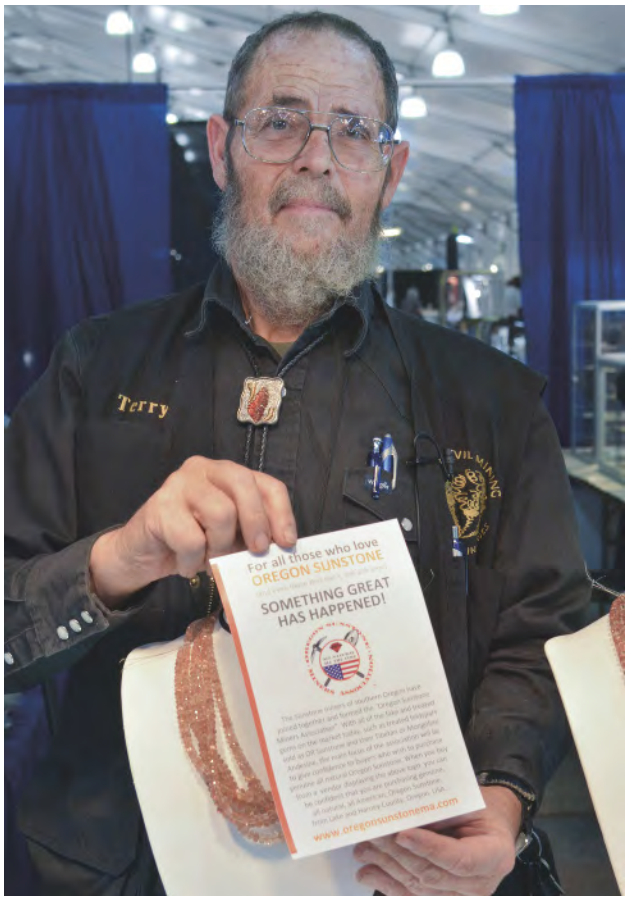

Figure 32. Dust Devil Mining's Terry Clarke holds a flyer promoting the Oregon Sunstone Miners' Association. Photo by Duncan Pay/GIA; courtesy of Dust Devil Mining.

operations at the Ponderosa mine and summarized the current market for his goods. He showed us a striking 2.77 ct "spinel red" gem from recent production (figure 33).

According to Woodmark, 2014 saw heightened interest in Oregon sunstone. He received requests for rough from clients in Australia and for finished stones from Brazil and Europe (principally the UK and Germany). At this particular show, Woodmark said he had received many more inquiries from domestic jewelers for samples and information, all following customer requests due to growing public awareness of the gem. He cited a TV shopping channel's recent promotion of production from the Sunstone Butte mine and the growing reach of his Internet business. For more information on the Sunstone Butte mine, see www.gia.edu/gia-news-research-butte-sunstone.

Woodmark observed that Internet merchandising, often by TV jewelry shopping channels, has been transformative for low-volume, one-of-a-kind products like Oregon sunstone. Web marketing frees traditional TV merchandisers from the production costs of on-air hosts and studios, and allows the cost-effective presentation of a spectrum of Oregon sunstone from "bargain parcels" to unique designer

Figure 33. This 2.77 ct "spinel red" sunstone, measuring 10.5 × 8 mm, is from Oregon's Ponderosa mine. Photo by Robert Weldon/GIA; courtesy of Desert Sun Mining & Gems.

cuts costing several thousands of dollars per piece. According to Woodmark, one buyer for a major TV jewelry retailer at the Tucson shows said that Internet business was now 40% of the company's total sales volume.

Woodmark estimated the total volume of fashioned Oregon sunstone on the market in 2014 was approximately 70,000 carats. By his calculations, that would be sufficient to supply one large U.S. retail jewelry chain with 10 carats per store per month over the course of a year. If demand picks up in 2015, that volume will not meet the industry's needs. Woodmark reported that business was up 25% on the previous year's show, which was up one-third on the year before.

In the 2014 mining season, Woodmark employed up to five pickers working the screens. He worked the mine for a total of 20 days and produced almost 2,000 kg of rough in all grades. Woodmark plans to work for 40 days in 2015 and expects to recover 4,000 to 5,000 kg of rough. To start the upcoming mining season, Woodmark will bring in heavier machinery and extend the pit back into the hillside. He will also bring in a bulldozer with a ripper to tear up the pit floor and start moving downward, too. Late 2014 saw recovery of larger rough, some pieces up to 70 grams (figure 34). In addition, the pit's "red zone," with a higher proportion of red-cored rough (up to 20%), remained productive. Woodmark expected the trend of bigger, better stones to continue as the miners work deeper into the deposit. This is similar to the situation at Sunstone Butte, he remarked.

Anticipating higher demand, he also planned to cut more frequently in 2015. Rather than cutting two to three times per year, he will cut 2,000 to 4,000 kg per month (new production plus stockpiled rough), depending on his needs. As 4,000 kg equates to approximately 2,000 carats of finished stones, Woodmark expected his production to significantly increase market availability of Oregon sunstone in 2015.

Like all the Oregon sunstone mines, Ponderosa pro-

Figure 34. The 2014 season saw some larger rough sunstone from Ponderosa mine in the 20–70 gram range. As operations go deeper, stone size seems to increase. Photo by Duncan Pay/GIA; courtesy of Desert Sun Mining & Gems.

duces a substantial quantity of yellow and near-colorless labradorite—material with little or no pink or red and no visible coppery reflections. One of the things Woodmark has learned at this show is the importance of cutting style and quality on a gem's perceived value. He sold 2 kg of yellow rough to another vendor at the AGTA show—Ken Ivey (Ivey Gemstones, Prescott, Arizona)—and was astonished at the result.

Ivey's use of concave cutting styles (figure 35) presented the feldspar's bright yellow color far more effectively than conventional cuts. With conventional cutting, Woodmark struggled to get a few tens of dollars per carat for yellow goods. With only a modest investment in extra cutting costs for concave faceting—perhaps twice the expenditure—the same material can sell for up to five times as much. As the yellow rough sells for a couple hundred dollars per kilogram, this is a potentially significant value addition in the finished product.

Another encouraging trend Woodmark sees is that designers and jewelers are mixing calibrated sunstones of different shapes and colors in the same jewelry piece. The casting is standardized, but because every combination is unique there is no longer the need to match them. Volume business with sunstone jewelry has always been hampered by the perception that every stone in a piece has to match and every piece must be uniform.

In Woodmark's opinion, even home shopping channels like QVC are moving away from that concept, in essence marketing the uniqueness of the gem rather than a uniformity it can never provide. He cited a piece for which he supplied 3.0, 4.0, and 5.0 mm calibrated gems. One was a top-quality red sunstone, and the others were paler pink. In this way, the manufacturer does not have to match the stones and can use larger volumes.

Duncan Pay

Figure 35. The concave cutting style used on these Oregon feldspars accentuates their yellow color and raises the market value of the material. Photo by Duncan Pay/GIA; courtesy of Ivey Gemstones.

Figure 36. Noor Gems showcased afghanite from Badakhshan Province, Afghanistan. Photo by Duncan Pay/GIA; courtesy of Noor Gems Japan Ltd.

Large and unusual gems. The inventory of Noor Gems Japan Ltd. at the GJX show was characterized by large and unusual gems, including a fine selection of rare blue and pink gemstones: afghanite, hauynite, hemimorphite, and pezzottaite. Bright blue afghanite (figure 36), which the company has been selling for three years, was available in gem quality in the 0.3–1.5 ct range, priced at approximately $500–$700 per carat. It has been especially popular with Noor's Japanese clientele. Afghanite is a relatively soft stone for jewelry, with a hardness 5.5 to 6, best suited for pendants and earrings. While near-colorless material can be found in Italy and Germany, the recent production of blue afghanite is from Badakhshan Province, Afghanistan.

Figure 37. Another attraction at the Noor Gems booth was pinkish purple copper-bearing tourmaline from Mozambique, which they labeled as "Paraíba." Photo by Duncan Pay/GIA; courtesy of Noor Gems.

Figure 38. Marketed as "ginger" garnet, these four garnets range from 8.33 to 35.54 ct. Photo by Robert Weldon/GIA; courtesy of Advanced Quality.

Mehraj Uddin exhibited two large topaz of exceptional pink to red color (6.38 and 12.08 ct). As with virtually all pink topaz, he acknowledged that these fine stones were heat treated. Debuting at Noor's GJX booth was pinkish purple copper-bearing tourmaline from Mozambique (figure 37).

For some large and exceptional gemstones, such as a 254.50 ct peridot cabochon from Pakistan, Uddin admitted they hold on to these stones for 10 or 20 years. The company is reluctant to sell them because of the difficulty in replacing such inventory. They will only sell when they feel the market is high.

Donna Beaton

Ginger garnet, "fancy" tanzanite. Kobi Sevdermish (Advanced Quality, Ramat Gan, Israel) showed us large fine "ginger" garnets and discussed the cutting of natural-color tanzanite crystals. The garnets are from a new find in Tanzania, discovered in late 2014. In large sizes, the stones have a pleasing "open" pinkish orange or orangy red hue (figure 38). By "open," Sevdermish meant the tone is not too dark, remaining lively and relatively bright even in sizes above 30 ct. He noted that many red garnets cut in large sizes have a tendency to become very dark, and this material avoids that pitfall. If fashioned correctly, it "pops." Along with the virtues of lighter tones and relatively large sizes, it possesses high clarity.

Supply has been limited—Sevdermish had only seen a few parcels of larger rough suitable for cutting gems up to 40 ct—and some of this material was of lower clarity. Standard gemological testing revealed an RI of 1.74 and an SG in the range of "Malaya" garnet (3.78–3.85).

As in 2014, Sevdermish reported that "natural-color" tanzanite remained a very successful item for Advanced Quality. He showed us a selection of unheated gems in a range of subtle secondary colors (greens and pinks) behind the predominant "typical" blue to purple tanzanite colors (figure 39). Sales have been strong in Europe and particularly Asia. According to Sevdermish, this is because no two

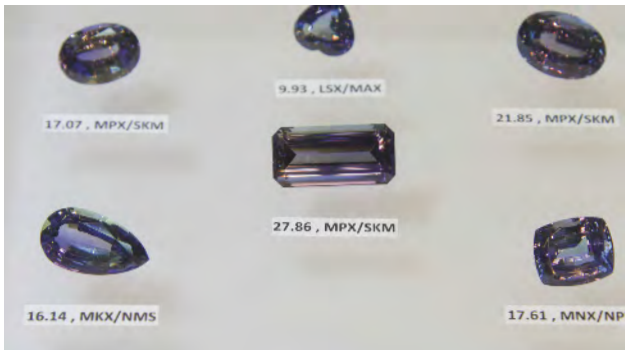

Figure 39. A selection of reportedly natural-color, unheated tanzanites ranging from 9.93 to 27.86 ct. Photo by Duncan Pay/GIA; courtesy of Advanced Quality.

are exactly alike. To demonstrate, he showed us a large suite of mixed fancy colors (figure 40).

He explained that rough of "odd" colors—unheated pinks and greens—did turn up over the years, but in the last year and a half, material from Block B of the tanzanite mining area has provided some "magnificent" natural colors: lavender, cognac or golden colors, and very rare pink and yellow and green.

Sevdermish noted that buying suitable tanzanite rough in these colors is a painstaking business, even though the company has cultivated connections in Africa that locate this material for them. Some purchases take time, he said, and require him to extend buying trips to obtain a few special, unique pieces. He added that it takes persistence to negotiate with miners and their representatives. And if no other buyers outbid you, you succeed. Sevdermish said that many of the stones at his booth were cut about a week and a half earlier.

Advanced Quality documents, through video recording and photography, each rough piece as it goes through the planning, sawing, and faceting process—in essence, the mine-to-market story of each significant gem. In this way, Sevdermish asserted the company can show—to the best of its knowledge—the unheated nature of its gems to clients. Many of the stones promoted as "unheated" in the market are actually the products of less-than-successful heating, he explained.

Just a couple of weeks earlier, he managed to obtain a few large pieces of rough with unique light yellow colors, one of which yielded a 27.59 ct antique cut (figure 41). The gem came out predominantly greenish yellow, but with flashes of lilac pink, which is what Sevdermish initially expected from the rough. The company debated whether to cut the original rough, as it was such a spectacular piece, but ultimately decided to fashion it because the crystal was not quite perfect enough to be a specimen.

Sevdermish described buying and cutting rough as a lottery. Certain gems—some spinels or even regular tanzanite—are more or less predictable. But with others, especially the rough for this "fancy-color" tanzanite, the results are less foreseeable. The rough for the 27.59 ct gem promised a "kaleidoscope of colors" blending pink, yellow, and green, so Sevdermish expected to see an interplay of colors inside the fashioned gem. Instead, he was dismayed to find the gem was colorless. Fortunately, Sev-

Figure 40. Kobi Sevdermish of Advanced Color shows off natural-color tanzanite, including a remarkable multicolor necklace of almost 170 carats total. Photo by Duncan Pay/GIA.

Figure 41. This 27.59 ct unheated, natural-color zoisite or "fancy" tanzanite shows a subtle tint of lilac pink against a greenish yellow bodycolor. Photo by Robert Weldon/GIA; courtesy of Advanced Quality.

dermish reported, the hoped-for greenish yellow color returned after the gem had "rested" for two days in its parcel paper.

Duncan Pay

Gem artistry in smaller sizes. At GJX, we caught up with gem artist Alexander Kreis (Sonja Kreis Unique Jewelry, Niederworresbach, Germany). It is a family business, with his father buying the rough, his mother designing the jewelry, and Alexander cutting the gems. Kreis had placed their best Oregon sunstone and their largest rutilated quartz pieces prominently in the booth to achieve a "wow" effect. Immediately beneath those signature pieces, Kreis had positioned more accessible gems that customers could use to make more affordable jewelry items. Although smaller than his trademark pieces, these were invested with the same precision and beauty. He produces pairs that would be ideal for earrings or even men's cufflinks. Kreis spoke about three of these more accessible lines, involving tourmaline, citrine, and blue topaz.

For Kreis, green and pink tourmaline symbolize the colors of the rainforest, so their design evokes the vivid foliage and blooms of that environment. The curves provide a fluid elegance, and the cuts on the underside capture the veins and structure of tropical leaves.

Among Kreis's new product designs for this year are citrines cut in a more angular style, with very detailed carvings on the back representing sunrays (figure 42). To Kreis, citrine's color represents the heat of the sun, while the carvings channel its intense slanted rays.

In striking contrast, another new design he called "frozen topaz" (figure 43) uses the icy hue of treated blue topaz to evoke arctic waters. The carving in the center is smoothly polished; the light rays, which are reflected from the polished carving, produce pinpoints of light on the gem's frosted sides. The design and the material combine to produce an icy brilliance. As the wearer moves the gem, Kreis said, it produces "a harmony of light points dancing through the stone."

Duncan Pay

Figure 42. Gemstone artist Alexander Kreis holds a sun carving, one of his new designs in citrine. Photo by Duncan Pay/GIA; courtesy of Sonja Kreis.

Figure 43. In these examples of "frozen topaz," the smooth carvings contrast with the frosted textures and lend an icy brilliance to the finished gems. Photo by Duncan Pay/GIA; courtesy of Sonja Kreis.

Figure 44. This edge-on view of the "wheel of light" reveals its construction. Photo by Duncan Pay/GIA; courtesy of Nature's Geometry.

Figure 45. Seen end-on, the larger disk displays the spectrum as concentric colors. Photo by Duncan Pay/GIA, courtesy of Nature's Geometry.

Larger optic disks. At the 2014 GJX show, Brian Cook (Nature's Geometry, Graton, California) showed us innovative optical disks made of colorless quartz featuring a drilled tube containing pieces of brightly colored gem and mineral rough. The tube is subsequently sealed with clear quartz. When the disk is viewed face up, the insert's reflections permeate the disk with bright color.

For this year's show, Cook's "wheel of light" design evolved into larger sizes with more intriguing reflective effects. Seen front-on, the new disks produced concentric colored reflections. The first we saw measured approximately 4 cm (1.57 in.) in diameter and featured Brazilian emerald, Paraíba tourmaline, and haüyne insets (haüyne is a brittle sodium calcium sulfate that provides rich blues). One innovative feature is that the viewer could see different colors depending on the viewing direction. From various directions the disk was suffused with bands of rich green, electric blue, or royal blue color.

According to Cook, this new product takes the color and amplifies it. There is a chamber within the quartz, which he polishes before inserting the colors he wants. Because no faceting is involved, all the colors are blended together. Cook said his passion for Paraíba tourmaline was the starting point.

Cook unwrapped a larger disk, approximately 8 cm (3.15 in.) in diameter. Viewed edge-on, the chamber's pattern of colored rough gems and minerals was revealed (figure 44). Cook had arranged a complete spectrum of rainbow colors in sequence: ruby, spessartine garnet, a gold nugget, Paraíba tourmaline, and haüyne (figure 45).

Cook also showed us a smaller optic disk set in a handmade platinum pendant set with diamond and melee-size Paraíba tourmaline from the Brazil Paraíba mine in Parelhas, Rio Grande do Norte. This piece combined the unusual optic effects of the center, which featured more Paraíba tourmaline and haüyne, with a conventional suite, which besides the pendant included a pair of earrings set with similar optic disks.

Duncan Pay

Figure 46. This unique 303 carat "Snow White" tourmaline suite was reportedly carved in Idar-Oberstein in the 1970s. Photo by Duncan Pay/GIA; courtesy Jan Goodman Co.

Unusual carved tourmaline suite. Jan Goodman (Beverly Hills, California), had an exquisite 303 carat suite of carved, particolored tourmaline depicting Snow White and the Seven Dwarfs (figure 46). In most depictions of the dwarfs in a line, the lead figure is "Doc" carrying a lantern. In this series, in a nod to the jewelry industry, the lead dwarf is depicted carrying a beaded necklace. Goodman recalls that the set was carved in Idar-Oberstein in the 1970s and came to him mounted in the presentation case. The suite had been in his personal collection for more than 30 years. Goodman told us "demand and price are finally in such a place as to justify parting" with it.

Donna Beaton

Figure 47. A carved agate and leaf pendant featuring diamond and tsavorite accents. Photo by Robert Weldon/GIA; courtesy of Jeff Bilgore, LLC.

Figure 48. A platinum pendant featuring 13 natural colored diamonds (6.31 carats total) with an 18K yellow gold and platinum chain featuring 36 oval fancy color diamonds (4.23 carats total). Photo by Robert Weldon/GIA; courtesy of Jeff Bilgore, LLC.

Gemstones and jewelry inspired by nature. Jeff Bilgore has 18 AGTA Spectrum Awards to his credit in both the cutting and design categories. His booth in the AGTA GemFair featured two pieces that departed from the norm of colored stones: an exquisitely carved leaf brooch of moss agate, highlighted with diamonds (figure 47), and a platinum pendant panel and chain featuring natural-color fancy diamonds that appeared to float within the frame (figure 48). The cut-corner rectangular panel, reminiscent of a classic Cartier design, featured 11 natural colored diamonds (5.68 carats total, all with GIA reports confirming Fancy, Fancy Vivid, or Fancy Intense hue), paired with a chain featuring 36 additional oval fancy colored diamonds (4.23 carats total).

After viewing the selection of carefully curated gemstones, one becomes aware of the entwined themes of art and nature. Bilgore espouses the principle of biophilia, the belief that humans intuitively respond positively to nature. Rather than viewing gemstones as inanimate objects, Bilgore sees them as part of nature, and he displays many of the gemstones and jewelry pieces with a tiny easel featuring an associated image (figure 49). A 5.69 ct Australian crystal opal, exhibiting play-of-color in all hues, was displayed with an image of the aurora borealis. Some of the other images are Bilgore's own photos, taken in his garden or while hiking. In a further nod to nature, the design of the colored diamond panel pendant was inspired by the Golden Mean and the Fibonacci series, mathematical relationships often found in nature and incorporated into man-made creations as diverse as music and architecture.

Donna Beaton

Rare stones in demand. For Brad Wilson and John Bradshaw (Coast-to-Coast Rare Stones International, Kingston, Ontario), their inventory of corundum and other familiar

Figure 49. A 5.69 ct Australian crystal opal is accompanied by an image of the aurora borealis on a tiny easel. Photo by Towfiq Ahmed; courtesy of Jeff Bilgore, LLC.

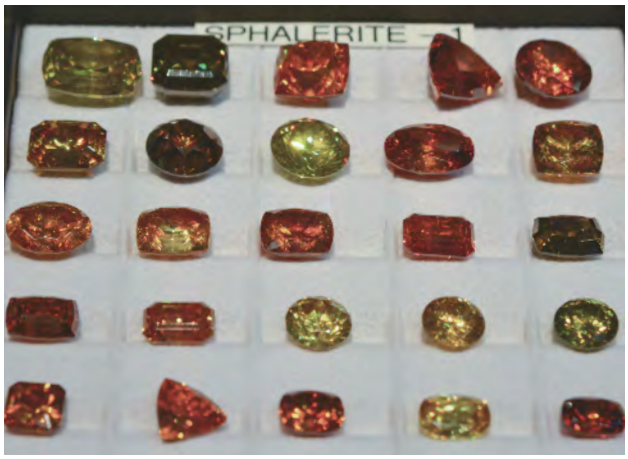

Figure 50. Brightly colored sphalerite is one of the most popular "unusual" gems sold by Coast-to-Coast. Photo by Duncan Pay/GIA; courtesy of Coast-to-Coast Rare Stones International.

gemstones never makes the trip to Tucson. Instead, their showcases are filled with rarities such as afghanite, bastnaesite, beryllonite, clinohumite, celestite, hambergite, magnesite, montebrasite, pargasite, sphalerite, violane, and zincite. These stones often are soft and near-colorless and have cleavage, making them less desirable for jewelry. But for a collector or a designer looking for the unusual who understands how to work with such challenging stones in jewelry, Coast-to-Coast at GJX is a worthwhile destination.

Some of the lesser-known stones available at Coast-to-Coast included datolite, cobaltocalcite, faceted aragonite, and tenebrescent scapolite. Fluorescent opal was a noteworthy new find. Under ordinary interior lighting, this opal is near colorless to very pale yellow. It can fluoresce bright green in response to the small UV component in ordinary daylight. Placed under an ultraviolet light or 405 nm laser, the fluorescent effect is spectacular.

With unfamiliar collectors' stones, colorful varieties usually sell best. Wilson's more popular items for this show included sphene, sphalerite (figure 50), and apatite. He told us that other stones rise and fall in popularity. One example is tugtupite, a rosy-pink mineral, usually found in aggregate form, that exhibits both interesting fluorescence and tenebrescence. It sold out on the first day in previous shows, according to Wilson, but in 2015 only a few had sold by the third day.

Donna Beaton

Color-change garnets from Tanzania. At the Riverpark Inn (Pueblo) show, Todd Wacks (Tucson Todd's Gems, Tucson and Vista, California) showed us interesting color-change or color-shift garnets from Tanzania (figure 51). According to Wacks, they were mined in Morogoro, Tanzania, back in 1988, and documented the same year (see C.M. Stockton, "Pastel pyropes," Summer 1988 *G&G*, pp. 104–106). The material resembled rhodolite rough and contained fine needle-like inclusions—most likely rutile.

The gems were pinkish purple in daylight and showed a color change from intense pink in warm incandescent light to purple—almost like a fine amethyst—in cool LED light. Wacks said the larger stones display the most pronounced color change. Very similar color change phenomena have been reported for other purple "pastel pyropes" from Tanzania, Sri Lanka, and Madagascar.

The rough had been stuck in a safe deposit box for years, he said, because most potential buyers assumed it was rhodolite, saw the inclusions, and lost interest. Wacks recently acquired the 2–4 kg of rough, cut a few pieces, and discovered the color change. He has been promoting the gem since then.

He sent samples to Dr. George Rossman (California Institute of Technology, Pasadena), San Diego gemologist Kirk Feral, and GIA. According to Wacks, the gems are approximately 80% pyrope, 10% spessartine, and 10% almandine, with an RI of 1.736. (This material will be the subject of a more detailed paper in the Summer 2015 *G&G*.)

Sharing booth space with Wacks was colleague and jewelry designer Mary van der Aa (vdAaco, Vista, California). She produces jewelry designs for many of the gems he cuts, including pastel pyropes and pink tourmalines from some

Figure 51. This 7.61 ct "pastel pyrope" shows a strong pink color in warm incandescent light and a strong purple in cool LED light. Photos by Duncan Pay/GIA; courtesy of Tucson Todd's Gems.

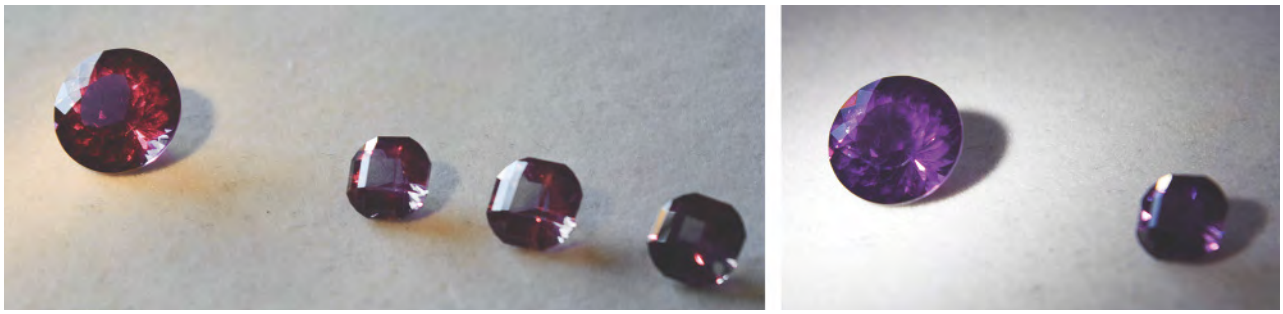

Figure 52. This hand-fabricated 14K rose gold and yellow gold pendant by Mary van der Aa features a 6 ct "hot pink" tourmaline from the Stewart mine, cut by Todd Wacks. Photo by Duncan Pay/GIA; courtesy of vdAaco.

of the mines in San Diego County (figure 52). Her jewelry also features stones cut by renowned gem artist Meg Berry.

Duncan Pay

Bold color combinations. For retailers and designers overwhelmed by the endless rows of gemstones lined up in trays, inspiration could be found at the booth of Stephen M. Avery (Lakewood, Colorado). Avery presented "statement"-sized gemstones in suites of bold color combinations (figure 53). His company has mainly sourced African stones but is now traveling to Asia to add brightly colored sapphire and spinel to its design palette. Avery, an expert cutter as well as buyer, fashioned all the gemstones in his inventory. The combination of craftsmanship and creative inspiration appeared to have paid off, as he reported the company's best show ever.

Donna Beaton

Chrysocolla in quartz. The Rare Earth Mining Company (Trumbull, Connecticut) booth at the AGTA show displayed a specialized inventory of unique and rare materials available as finished gemstones, mineral specimens, and fossils. Curt Heher, Rare Earth's president of sales, reported more than 300 companies placing orders in finished stones alone: "We enjoyed our biggest Tucson show in 40 years."

We obtained two cabochons of blue-spotted clear and near-colorless quartz (figure 54) that were reminiscent of "K2 stone" or "Raindrop azurite" seen in previous years (Spring 2012 GNI, pp. 55–56). Heher's father bought the rough, which was crystallized around blue stalactites, at auction in the 1980s. It remained in storage until recently. The material was reportedly mined in Globe, Arizona, in the 1970s.

Gemological examination of the 19.16 and 52.96 ct cabochons revealed an RI of 1.54 to 1.55 in most areas, but

Figure 53. Top: This vibrant 2.08 ct oval pink sapphire flanked by a pair of warm-hued spessartine garnets totaling 3.41 carats strikes a tropical note. Bottom: This bold pendant and earring suite features three marquise-shaped tanzanites totaling 6.73 carats, with modified trilliant rubellite tourmalines of 14.20 carats total. Photos courtesy of Stephen M. Avery.

approximately 1.5 in the blue area, and a 1.46 spot reading in transparent areas. Specific gravity ranged from 2.36 to 2.47. The fluorescence reaction to long-wave UV was weak white in fractures and the transparent areas. Raman analysis confirmed that the blue material was chrysocolla, the transparent to whitish areas were quartz, and the transparent cryptocrystalline areas were chalcedony. Raman analysis also indicated the presence of a hardened glassy polymer (polymethyl methacrylate). FTIR also confirmed the polymer, corroborating the stabilization that Heher indicated

Figure 54. 52.96 ct and 19.16 ct chrysocolla in quartz, obtained from Rare Earth Mining Company at the AGTA show. Photos by Jian Xin (Jae) Liao.

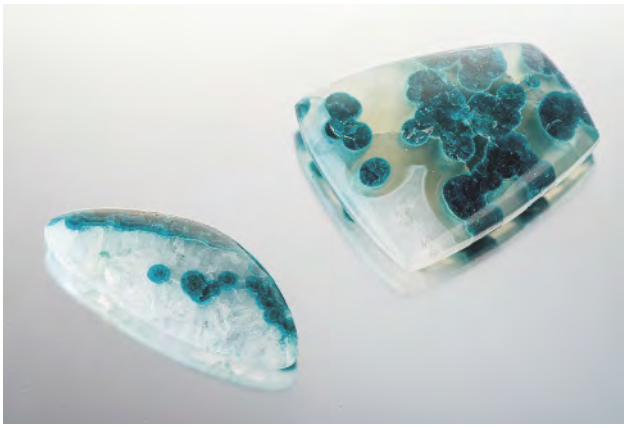

was needed to prevent crumbling or fracturing during the cutting and polishing process. The treatment conclusion on a GIA report would be "impregnated" or possibly "composite" if the polymer occupied significant volume or surface area.

Chrysocolla in quartz is not uncommon, but it is rare to see such defined stalactites resulting in a distinct orbicular pattern. This material often remains as mineral specimens rather than being cut for jewelry purposes.

Donna Beaton and Akhil Sehgal

PEARLS

Cultured pearl market update. At the 2014 AGTA show, Fran Mastoloni (Mastoloni Pearls, New York City) provided a market summary from his own business perspective. He emphasized surging demand in the Chinese domestic market for all cultured pearl types, plus the need to introduce innovative styles and pearl combinations in contemporary jewelry. Since then, overall supply of fine cultured pearls of every type has become even more challenging.

This year, Mastoloni reported that Chinese demand for Philippine golden cultured pearls continues unabated, and the domestic market there is absorbing nearly all available production, effectively pricing them out of the North American market. Although never a high-turnover item in the U.S., any such pearls sold in the American market will likely come from suppliers' existing inventory. And once sold, they will not be replaceable given current market prices. Mastoloni predicted an eventual downward correction, once the Asian market's appetite for golden pearls is sated.

Supply of quality Tahitian cultured pearls (figure 55) is also becoming problematic. Mastoloni said the Tahitian government has ceased support of pearl farmers, with a resulting decline in colors, sizes, and overall product quality.

Figure 55. Mastoloni described this fine 16.4–16.7 mm Tahitian cultured pearl with natural color and luster as his "new favorite pearl." He added that top-quality examples like this are increasingly hard to find. Photo by Duncan Pay/GIA; courtesy of Mastoloni Pearls.

Figure 56. Top-quality Australian South Sea baroque cultured pearls 15.5 × 19.0 mm and larger grace this spectacular necklace. Photo by Duncan Pay/GIA; courtesy of Mastoloni Pearls.

Exceptional pearls are particularly scarce. He was very concerned about pearl production over the next 10 years. Prior to 2008, he said, Tahitian pearl farmers were very conscientious about quality. Today, in Mastoloni's words, "Farmers are producing to turn over."

[*Editor's note*: On October 1, 2008, the Tahitian government abolished the pearl export tax, which had largely supported the GIE Perles de Tahiti industry association. This removed the funding for the promotion of Tahitian cultured pearls, leading to GIE Perles de Tahiti's collapse in 2012. The 2008 global economic downturn drastically curtailed pearl sales and stressed many Tahitian pearl farmers (see A. Müller, "A brief analysis of the global seawater cultured pearl industry," European Gemmological Symposium, Bern, Switzerland, June 5, 2009, pp. 7–10). Since the collapse of GIE Perles de Tahiti, producers have increasingly looked to China as a promising export market, which is also likely to affect availability for U.S. and European markets.]

Mastoloni noted that white South Sea cultured pearls remain the standard by which fine pearls are judged. Although fine quality is still difficult to find, supply is good. He showed us a spectacular Australian South Sea necklace composed of white to pink 15.5 to 19 mm-plus baroque pearls with excellent luster and unblemished surface (figure 56). Weighing in at an "extraordinary" 46.1 momme

Figure 57. Left: Long necklaces are in style. This "Wave" necklace features multicolored Tahitian cultured pearls ranging from 7 to over 14 mm. Right: This close-up of the necklace shows its repeating color and size patterns in a succession of "waves." Photos by Duncan Pay/GIA; courtesy of Mastoloni Pearls.

(172.88 grams), this necklace took more than two years to complete. There is always the temptation to keep improving a piece, to make it "bigger and better." As an example, he showed us a large baroque specimen that measured 23.3 × 28.6 mm and weighed 4 momme (15 grams), with superb luster, that he would like to make the centerpiece of the necklace. Prices for baroque cultured pearls are stable with moderate demand, he noted, but sourcing high-quality goods is somewhat difficult.

Mastoloni said fine akoya cultured pearls are also in high demand. Once again, he faces competition from Chinese buyers purchasing for their domestic market. According to Mastoloni, pearl farmers in China are no longer concentrating on smaller round pearls. They are not producing enough 5, 6, or 7 mm diameter goods in sufficient quality, in either akoya or freshwater types, to satisfy demand. The result is increased competition, with Chinese buyers competing at the source in Japan for akoya. This demand is driven by the emerging wealth of Chinese consumers. Their purchasing power and the sheer quantity of consumers in the Chinese domestic market is fueling unprecedented demand. They are looking for better quality, and fine Japanese akoya pearls meet that need.

In terms of trends, Mastoloni noted that "long is in." Double- and triple-length necklaces from 32 to more than 50 inches are very popular, he said. He has also noticed that basic necklaces are making a comeback, and more retailers are asking him to supply "regular" necklaces for their inventory. Mastoloni showed us a double-length necklace that made clever use of soft-colored round Tahitian cultured pearls in a variety of sizes. He called it the "Wave" necklace (figure 57). "Swells" graduating from 7 to over 14 mm form waves in repeating color patterns along the length of this necklace (approximately 36 inches), creating a layered look. The repeating size and color patterns lend a sense of movement and drama.

Duncan Pay

Chinese freshwater pearl culturing, overall market summary. Also at the AGTA show, Jack Lynch (Sea Hunt Pearls, San Francisco) offered his perspective as a pearl entrepreneur (figure 58). Over the years he has introduced many trends in cultured pearls and pearl culturing techniques to

Figure 58. Jack Lynch of Sea Hunt Pearls displays strands of baroque bead-nucleated Chinese freshwater cultured pearls at his AGTA booth. Photo by Duncan Pay/GIA.

Figure 59. This spectacular strand of Chinese freshwater cultured pearls is graduated from 15.4 to 19.3 mm. Lynch described it as the best of four such strands available when he purchased it from his supplier. Photo by Duncan Pay/GIA; courtesy of Sea Hunt Pearls.

the market, including soufflé pearls: large baroque Chinese freshwater cultured pearls with fine luster, interesting colors, and light heft (Spring 2010 GNI, pp. 61–63, www.gia.edu/gems-gemology/spring-2010-gem-news-international).

Lynch's reputation for introducing new products and styles leads to the same question at his Tucson booth every year: "What's new in the pearl business?" Typically the question centers on freshwater cultured pearls from China. This year, he noted, the emphasis of Chinese pearl culturing innovation was on size. As evidence, Lynch showed us a remarkable necklace composed of round freshwater cultured pearls graduating from 15.4 to 19.3 mm (figure 59). He had never seen a necklace of this size and quality, with beautifully matched, top-quality round pearls. His supplier only had four available, and this necklace was the finest.

Rather than producing baroque pearls, like the soufflé, the drive is now toward bead nucleation and large, spherical pearls. As producers initially sell by weight, there is a financial imperative to produce bigger pearls.

Although producers are ultimately striving for quality, quantity is still the most important factor. Lynch felt that the goal of Chinese freshwater pearl culturing has always been the production of "large white round pearls" and that success to date has been limited, with extremely small volumes of fine-quality product available. Certainly, Lynch knows of no more than a handful of examples like the necklace he showed us at his AGTA booth.

Lynch was uncertain which kind of nuclei or culturing process is used for these larger spherical pearls, but he said the results speak for themselves. He believed it might be similar to the proprietary process used by Chinese producer Grace Pearl for its "Edison" pearls. In this method, genetically selected mussels are implanted using tiny beads instead of mollusk tissue. "Edison" is a backhanded tribute to American inventor Thomas Edison.

Lynch noted that producers are continually hybridizing the mussels used for cultivation, and that they remain very tight-lipped about their methods. Without drilling, sawing, or X-raying the pearls, it is difficult to fully understand the processes or growth methods used.

He mentioned that some of the top producers in China have become increasingly "bullish" about their products, comparing them very favorably with the best South Sea cultured pearls. Because the Chinese domestic market is so strong, its consumers are prepared to pay higher prices than consumers in countries like the U.S. The producers are, in effect, pricing their products out of these markets. According to Lynch, the message from these producers is that the traditional stature of their product vis-à-vis other pearl types must change. In the meantime, they will not consider lowering their prices to satisfy traditional export markets in the U.S. and Europe.

We noticed he had a comprehensive selection of baroque freshwater cultured pearls. Lynch said that while there is moderate market demand for baroque pearls, much of the production originates from cultivators striving for spherical pearls, because "that's where the money is." In his opinion, much of the current Chinese production is similar to "Kasumiga pearls" with textured skins that display very strong orient over natural colors (figure 60).

Known as "ripple" pearls for their textured surface, they are highly regarded for their prismatic effects, near-metallic luster, and organic shapes. As a strand wholesales for just a few hundred dollars, they present a "big look" for a modest outlay. For example, a very rough estimate on the

Figure 60. These 16 × 13 mm bead-nucleated baroque Chinese freshwater cultured pearls have impressive heft along with striking orient and warm natural colors. Photo by Duncan Pay/GIA; courtesy of Sea Hunt Pearls.

Figure 61. These slightly larger, higher-quality baroque cultured pearls have smoother skins than those in figure 60. As a consequence, they are priced two to three times higher. Natural-color goods are in the foreground, while the white pearls have been bleached for a more uniform appearance. Photo by Duncan Pay/GIA; courtesy of Sea Hunt Pearls.

15.4–19.3 mm round necklace shown in figure 59 would be $10,000 per strand, whereas these baroque multicolor necklaces cost just a few hundred dollars per strand.

Lynch's higher-quality baroque Chinese freshwater pearls are larger and have smoother skins (figure 61), so the price rises accordingly. The next examples he showed us cost two to three times more. According to Lynch, they are very fashion-forward and still represent a tremendous value for the size.

The higher-quality baroque strands Lynch showed us were also bead nucleated, but the bead had been positioned more conventionally, in the gonad of the mollusk. This technique produces a different type of pearl, known in the trade as a "fireball" (D. Fiske and J. Shepherd, "Continuity and change in Chinese freshwater pearl culture," Summer 2007 *G&G*, pp. 138–145, www.gia.edu/gems-gemology/summer-2007-continuity-change-chinese-freshwater-pearl-culture-fiske).

All the peach to pink colors in these strands are natural, Lynch told us. Bleaching produces the white product. Unlike the soufflé pearls, which are typically hollow after being drilled, these bead-nucleated pearls have impressive heft. They sell very well, according to Lynch, and no two necklaces are quite the same due to the uniqueness of every pearl. As an aside, he told us that the weight of the pearls he shipped to the show was around 489 pounds (about 221 kg), much of that consisting of bead-nucleated freshwater cultured pearls.

Next, he showed us some tissue-nucleated (non-beaded) round freshwater cultured pearls (figure 62). These 5–6 mm spherical pearls were impressively uniform with high luster and crisp reflections from smooth skins, making them an excellent substitute for an akoya strand. Finding this sort of quality is very difficult these days, Lynch told us. These also cost a few hundred dollars per strand.

Although Lynch carries a wide stock of Chinese freshwater pearls, most of his resources go into purchasing Tahitian, South Sea, and akoya cultured pearl products. All in all, he said, supply of every top-quality cultured pearl type is very limited, and competition for available product is very high. The increase in Chinese consumption has drastically affected supply for U.S. and European wholesalers. Fortunately, Lynch told us with a sense of relief, he has been a "pearl hoarder" for many years, so he has a significant inventory to draw upon.

Lynch suggested that the Chinese domestic market does not know what the market value of many products might be elsewhere. The Chinese have a different mindset

Figure 62. These tissue-nucleated Chinese freshwater cultured strands resemble fine akoya cultured pearls. Photo by Duncan Pay/GIA; courtesy of Sea Hunt Pearls.

Figure 63. Fine Tahitian and South Sea cultured pearl singles and pairs are in high demand with designers for one-of-a-kind custom jewelry pieces. Photo by Duncan Pay/GIA; courtesy of Sea Hunt Pearls.

than consumers in the West, he told us, citing a fashion example: "You'll pay more for couture items in Shanghai than in Paris… If it's expensive, it's better." Although many commentators insist the Chinese economy is slowing down and no longer enjoying double-digit percentage growth, Lynch said that the emergence of a large middle class that wants all the trappings of wealth is driving up the market prices for gems and pearls. He noted that the tChinese like to display their wealth, and jewelry is an obvious way to do that.

Asked what was selling this year, Lynch explained how his business has changed. He used to sell more volume at the Tucson show, especially freshwater items wholesaling for $300 to $600 apiece. Today he handles fewer transactions, but the average transaction has increased dramatically. Lynch's perception is that spending habits have changed as the middle class in the U.S. has shrunk. He finds fewer consumers looking for $1,000 items. Instead, he sees purchasers from a higher income bracket looking for a $20,000 or $30,000 piece.

Lynch now sells far more round white South Sea and Tahitian goods, along with fine single pearls and pairs (figure 63). The first piece he showed us was a superb, exceptionally large round South Sea cultured pearl of 18.2 mm (figure 64). Lynch said he buys with designers in mind, as items like this are far more affordable than a strand and make excellent centerpieces for custom jewelry pieces. The price for such a piece would be approximately $6,000, whereas a necklace of this quality would cost many tens of thousands of dollars.

Finally, Lynch pulled out a uniquely shaped Tahitian baroque cultured pearl (figure 65). Its flattened shape would allow it to sit especially well as a pendant. At 19.7 mm, it was large. Even though the pearl was very baroque, its color was exceptional. This piece had the style and substance to really make a statement at a reasonable price (a couple of thousand dollars).

Duncan Pay

CONFERENCE REPORTS

GILC 2015. The International Colored Gemstone Association (ICA) sponsored the invitation-only GILC (Gemstone Industry & Laboratory Conference) on February 2, during the Tucson gem shows. Participants represented primarily gemological laboratories, educational institutions, gemstone buyers and wholesalers, and retailers (figure 66).

Shane McClure of GIA began with an update on the activities of the Laboratory Manual Harmonization Com-

Figure 64. This superb spherical South Sea cultured pearl measures 18.2 mm in diameter and weighs 8.25 grams. Photo by Duncan Pay/GIA; courtesy of Sea Hunt Pearls.

Figure 65. This 19.7 mm Tahitian Sea cultured pearl weighs 2.45 momme (9.19 grams). It would make a fine centerpiece for an item of custom jewelry. Duncan Pay/GIA; courtesy of Sea Hunt Pearls.

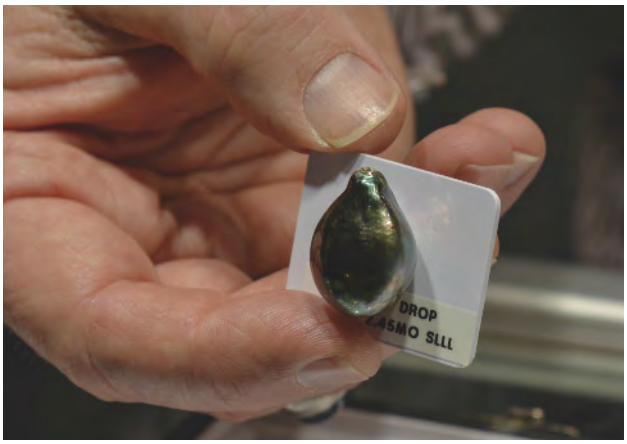

Figure 66. Laboratory representatives at the GILC in Tucson spoke on a wide range of topics related to colored gems, including nomenclature, treatment, and clarity enhancement. Photo by Duncan Pay/GIA.

mittee (LMHC). The LMHC establishes consistent nomenclature among international lab reports but does not address standardization of criteria and testing procedures. The committee consists of seven international gemological laboratories, whose representatives meet three times per year by teleconference or in person. Information sheets that are under development include hydrophane opal, along with "pigeon's blood" and "royal blue" designations for corundum. Topics under discussion include light sources, tanzanite/zoisite nomenclature, and the problem of stones being treated soon after a laboratory report is issued.

McClure also presented additional color designations for ruby that will be featured on GIA reports. He noted that "pigeon's blood" would designate vivid red color on rubies with high fluorescence and low iron content, as typified by high-quality Burmese rubies. "Scarlet" and "crimson" would be used for fine-colored iron-bearing rubies with low fluorescence, in the slightly orangy to slightly purplish ranges, respectively. "Deep red" will be used for rubies of darker tone. There appeared to be different opinions among the participants about the definition of pigeon's blood, and no clear agreement about the proposed new terms. This provoked a lively discussion as to whether "romantic" terminology belonged on lab reports, and whether the use of advantageous vocabulary was a move by some labs to gain market share.

Chris Smith of AGL spoke on the detection of low-temperature heat treatment of corundum. Smith defined "low temperature" as less than 1300°C, a treatment range where rutile (including silk) would still remain intact. The treatment has a long history and is still used to improve the color of pink, red, yellow, and orangy corundum, typically by removing purplish or bluish components. Characterization of non-rutile mineral inclusions and IR spectroscopy are keys to detecting the treatment.

Gabriel Angarita, ICA ambassador to Colombia and president of the Emerald Exporters Association, gave a presentation on residues in emeralds caused by the cutting process. He presented visual evidence that "dust" from the emeralds, laps, or abrasive powders can enter fractures during cutting and polishing, and he was concerned that they might be interpreted as clarity enhancement residues. It emerged during the discussion that although the stones might not have been intentionally clarity enhanced, the lubricating oil used in the cutting process, or the wax or nail polish used on rough to seal the fractures from dust, could be the source of the clarity enhancement being detected by gemological laboratories.

In the open session forum, participants pointed out that confidence in lab reports was waning for two reasons: (1) the inconsistency in country-of-origin and treatment determinations, and (2) the increasing prevalence of stones being altered or treated after receiving a favorable report (for instance, the re-oiling of emeralds).

The issue of hydrophane opal was revisited, with a call for nomenclature and comments, and perhaps a standardized method of assessing and communicating the degree of absorption and its impact on durability and color stability.

While trade in elephant ivory is prohibited in the U.S., the trade in extinct mammoth ivory has been severely restricted in New York and New Jersey, and on eBay. Nomenclature to distinguish the two types needs to be developed, along with awareness of treatments to disguise modern ivory as mammoth or antique to circumvent restrictions.

Another issue raised was the treatment of spinel, once considered a gemstone that was not treated. Participants confirmed the routine heating of spinel from Myanmar and Tanzania, as well as the colored (red) oiling of both spinel and corundum in Mogok. While microscopic examination does little to detect heating, photoluminescence and Raman spectroscopy are useful.

Donna Beaton

International Diamond School. In late January 2015, nearly 100 scientists (figure 67) gathered in the northern Italian town of Brixen to attend the Second International Diamond

Figure 67. Attendees from countries including Australia, Botswana, Russia, Brazil, and the United States learned the latest tools and techniques for diamond research at the Second International Diamond School. Photo by Fabrizio Nestola.

School (IDS). The program, titled "The Nature of Diamonds and Their Use in Earth's Study," was designed so that attendees from varied educational and professional levels could learn from leaders in the field of natural diamond research.

The school successfully blended student and professional perspectives, as well as the cross-disciplinary nature of the participants and speakers. Over four days, IDS attendees from a wide range of backgrounds—including experimental researchers, petrologists, mineralogists, crystallographers, isotope geochemists, and diamond industry experts—were treated to a wide scope of lectures and workshops. Presentations provided insight into diamond exploration, advanced research-level analysis, diamond morphology, inclusion chemistry, and geologic occurrences.

George H. Read (Shore Gold Inc., Vancouver) presented a recent history of diamond exploration, culminating with his company's new Canadian diamond mine: Star-Orion in Saskatchewan, a $2.5 billion project. He provided context on production history, sources, and trading centers. He outlined future diamond mining projects in Botswana, Canada, Lesotho, and India, concluding that the small number of viable projects might signify a shortfall in rough supply. The complexity and financial risks involved with bringing new diamond mines online was made evident.

Bruce Kjarsgaard (Geological Survey of Canada, Ottawa) reviewed kimberlite eruptive models based on 1970s and 1980s research in South Africa. He explained the revision of these models after new kimberlite discoveries in the 2000s in Canada's Slave craton. He defined kimberlite as a strongly homogenized and "mixed-up" hybrid rock, representing a blend of crystallization out of the magma with country rock, that is often highly variable from place to place. In a second presentation Kjarsgaard examined the major techniques used for exploration for diamondiferous kimberlites, focusing on the Canadian experience and its applicability to glaciated shield areas such as Canada, Russia, the northern United States, and Finland. These techniques have been remarkably successful, partly because of the solid scientific research behind them.

Jeff Harris (University of Glasgow, UK) reviewed the characteristics of lithospheric diamonds based on his experience as a De Beers research director and his access to an unparalleled proportion of run-of-mine diamonds. He showed how different pipes produce distinct diamond size ranges and morphologies. He covered the age relationships between inclusions and host diamond, inclusion chemistry, formation pressures and temperatures, fluid inclusion chemistry, and the abundance of different carbon and nitrogen isotopes in diamond.

Michael Walter (University of Bristol, UK) discussed the super-deep carbon geodynamics of Earth's mantle along with information provided by analysis of lower-mantle fluids found as inclusions in "superdeep" (sublithospheric) diamonds from Brazil's Juina field. He explained how new thinking over the past five to six years has provided a model for diamond formation by subduction of carbonate-bearing hydrated oceanic crust in the transition zone of the mantle at depths of 440 to 600 km.

Paolo Nimis (University of Padua, Italy) discussed thermobarometry, a technique that uses mineral phase diagrams to discover the original formation conditions (pressure, temperature, and therefore depth) of rocks in the mantle. He also related the possibility of applying similar techniques to inclusions in diamonds to help determine their formation conditions. His talk explored the accuracy and precision of the different thermobarometers and where future improvements are likely to occur.

Ross Angel (University of Padua) discussed elastic barometry for inclusions in diamonds. This new field uses Raman shift or X-ray diffraction (lattice distortion) to measure decompression effects on the surrounding diamond crystal caused by inclusions formed at high pressure to estimate pressure of diamond formation.

Fabrizio Nestola (University of Padua) explained the ad-

vanced X-ray diffraction methods used in their laboratory, which permit very rapid crystal orientation and data collection. This work has shown that some olivine inclusions cannot be syngenetic, as they share no preferred orientation with the host diamond.

Graham Pearson (University of Alberta, Canada) overviewed the petrology and geochemistry of cratonic mantle roots. He explained the effects of melt depletion (removal of clinopyroxene and orthopyroxene) to produce very magnesium-rich melts in the sub-continental mantle, which removes rhenium (Re) to "freeze in" the osmium (Os) isotopic system to allow radiometric dating. This gives very different mean Re/Os model ages for "on-craton" (>2.5 billion years) and "off-craton" (<2.0 billion) mantle xenoliths (potential diamond host rocks) for the Kaapvaal craton, which underlies southern Africa.

Steven Shirey (Carnegie Institution of Washington) reviewed the topic of age-dating diamonds, beginning with work in the 1980s using rare-earth element ratios in silicate mineral inclusions within the diamonds. He covered rhenium/osmium dating techniques devised in the late 1990s and perfected in the 2000s, finishing with recent Re/Os dating work on zoned diamonds from Yakutia, which showed two-billion-year-old cores surrounded by younger rims of one billion years.

Oded Navon (Hebrew University of Jerusalem) presented on silicic and low-magnesium carbonatitic fluids in fibrous diamonds and their relationship to fluids in gem-quality diamonds. He explained how new work on inclusions along the twin planes of otherwise gem-quality diamonds—macles—revealed fluids of very similar compositions. One can generalize from previous studies of fibrous diamond that most diamonds form under similar growth conditions most of the time.

Thomas Deining (WITec Instruments Corp., Ulm, Germany) introduced WITec's confocal Raman spectrometer system and described its ability to map three-dimensional fields of features at very high resolution. This instrument is ideally suited to looking into diamond, and his talk set the stage for the Raman workshops the following day.

Maya Kopylova (University of British Columbia) discussed fluid inclusions and volatiles in monocrystalline, octahedral diamonds, with a focus on nitrogen (N_2) and carbon dioxide (CO_2). She related this new work to previous studies on fibrous diamonds, showing it has wider relevance than previously thought.

Wuyi Wang (GIA, New York) covered diamond treatment and synthesis. He introduced the various causes of color in natural diamonds and explained how combinations of irradiation and high-pressure, high-temperature (HPHT) treatment might alter or remove color. He also reviewed improvements in synthetic diamond size and quality due to advances in HPHT and chemical vapor deposition (CVD) synthesis technology.

Frank Brenker (Goethe University, Frankfurt) outlined the latest findings on ultra-high pressure mineral phases in diamonds. Much of this work is nanostructural in nature and requires removing exceptionally thin wafers of diamond by focused ion beam lithography, a technique borrowed from the electronics industry. Brenker dealt specifically with the idea that some of the inclusion minerals thought to have grown in the lower mantle (e.g., Mg perovskite and ferropericlase) might actually have formed at the shallower depths of the mantle transition zone or even the upper mantle.

Dan Frost (University of Bayreuth, Germany) presented on the experimental petrology of the mantle, using state-of-the-art multi-anvil presses capable of achieving pressures of 250,000 bar at 1,800°C. This work demonstrates the possibility that at certain temperatures and pressures, a system may exist where carbon dioxide (CO_2) and methane (CH_4) produce carbon (C) plus water (H_2O). He presented this as a new model for diamond formation in the deep mantle.

Pierre Cartigny (Institut de Physique du Globe de Paris) showed how carbon and nitrogen isotopes are used to characterize the fluid sources and fractionations that can occur with diamond growth. One of his long-standing conclusions is that even though subduction of C and N can occur and is thought to be a major process for introducing fluids into the mantle, the signatures of subduction are not as clear as one would expect. The possible isotopic changes that can occur between the diamond and its host fluid during diamond growth need much further study.

Andy Davy (Rio Tinto Plc., Bristol, UK) drew upon his experience as a consulting geologist to discuss the role of engineers and natural diamond scientists in evaluating diamond deposits. His talk covered the exploration and evaluation of prospective deposits, improvements in recovery methods to prevent diamond breakage, and assessing the performance of deposits through time. He left the audience with a realistic picture of the complications in establishing diamond grade, price, and hence the viability of any given diamond project. He further showed how exceedingly rare good diamond-producing kimberlites are.

The school was a fantastic opportunity for attendees to learn about diamond exploration, advanced research-level analysis, diamond morphology, inclusion chemistry, and geologic occurrences in a way that will inspire their future studies and career choices. GIA's contribution directly benefited these up-and-coming research scientists by reducing the attendance fees for the conference, permitting many students to attend who otherwise would have been unable to do so.

IDS was organized by Fabrizio Nestola, Graham Pearson, and Steven Shirey, under the auspices of the Diamonds and Mantle Geodynamics of Carbon (DMGC) consortium, part of the Deep Carbon Observatory (DCO). The school was sponsored by GIA, the DCO, the Italian Society of Mineralogy and Petrology (SIMP), and the University of Padua. The IDS website is at www.indimedea.eu/diamond_school_2015.htm.

Steven Shirey
Carnegie Institution of Washington
Washington, DC

REGULAR FEATURES

COLORED STONES AND ORGANIC MATERIALS

A remarkably large amblygonite-montebrasite carving. Recently the Gem Testing Laboratory in Jaipur had an opportunity to examine an unusually large yellow, semitransparent to translucent carving (figure 68). This 1,871 g (9,355 ct) piece measuring approximately 18.50 × 15.10 × 7.30 cm was fashioned after Lord Mahavira, one of the ancient Indian sages who established the tenets of Jain Dharma. Initial observations suggested beryl due to the color, medium heft, and cloudy liquid inclusions visible to the unaided eye. Gemological testing ruled out that possibility, however. Spot RI was approximately 1.61, with a small but distinct birefringence blink, while hydrostatic specific gravity measured 3.00. The carving was inert to UV radiation.

Examination with a hand loupe revealed reflective liquid films (figure 69, left), fingerprints composed of phase droplets, elongated phase/short tubes oriented in one direction, aligned in planes intersecting at approximately 65/115° angles (figure 69, center). Also present were parallel reflective films that appeared to be incipient cleavage (figure 69, right). The overall inclusion pattern was typical of gems found in pegmatitic bodies such as beryl, tourmaline, and topaz.

The carving was identified as amblygonite-montebrasite by Raman spectroscopy in the 200–2000 cm^{-1} region, which revealed distinct peaks at ~297, 425, 481, 600, 643, 797, 1011, 1058, 1107, and 1186 cm^{-1} (figure 70). Amblygonite and montebrasite are both lithium phosphates with a common chemical formula of (Li, Na)$AlPO_4$(F, OH), forming an isomorphous series between F-rich amblygonite and OH-rich montebrasite. The two minerals can be colorless, yellow, or green. High-quality crystals are prized by collectors but rarely seen in the gem trade (R. Webster, *Gems: Their Sources, Descriptions and Identification*, 5th ed., rev. tby P.G. Read, Butterworth-Heinemann, Oxford, UK). The amblygonite and montebrasite end members can be differentiated on the basis of peaks at ~600 and 1060 cm^{-1} and a peak at ~3370 cm^{-1}. With an increasing percentage of fluorine, the 600 cm^{-1} peak shifts from 599 to 604 cm^{-1} while the 1060 cm^{-1} peak shifts from 1056 to 1066 cm^{-1} (B. Rondeau et al, "A Raman investigation of the amblygonite-montebrasite series," *The Canadian Mineralogist*, Vol. 44,

Figure 68. This 1,871 g amblygonite-montebrasite carving (18.50 × 15.10 × 7.30 cm) is unusual for its size and transparency. Photo by Gagan Choudhary.

Figure 69. Examination of the carving with a hand loupe revealed reflective liquid films (left), elongated phase/short tubes oriented in one direction and aligned in planes intersecting each other at approximately 65/115° (center), and parallel reflective films that appeared to be incipient cleavage (right). Photos by Gagan Choudhary; image width 25 mm.

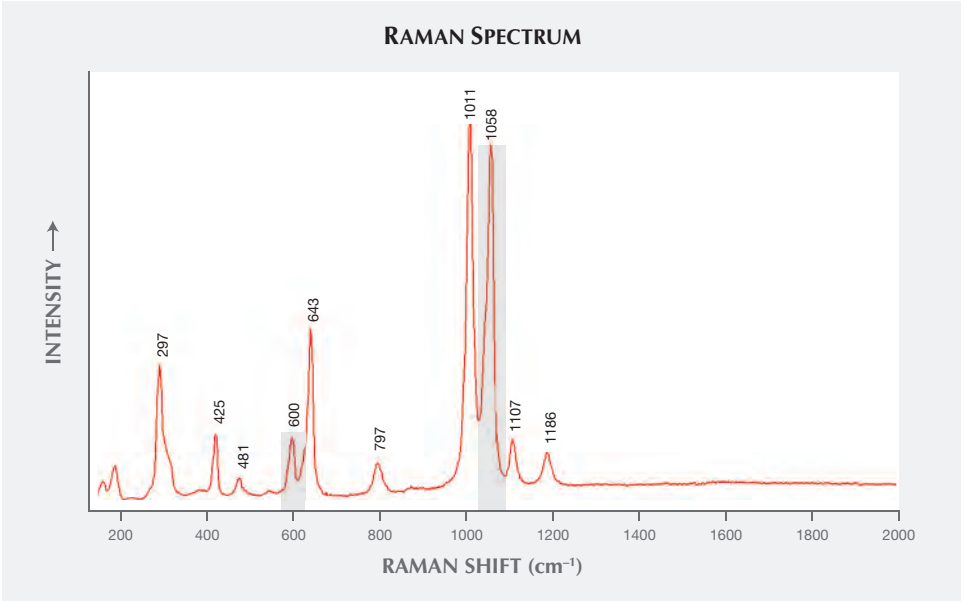

Figure 70. The carving's Raman spectrum showed major peaks at around 297, 425, 481, 600, 643, 797, 1011, 1058, 1107, and 1186 cm^{-1}. The peaks at approximately 600 and 1058 cm^{-1} suggest an intermediate member of the amblygonite-montebrasite series.

No. 5, pp. 1109–1117). According to the RRUFF database, however, the peak for montebrasite is at 1047 cm^{-1} while amblygonite's is at 1060 cm^{-1}. This is possibly due to different instrument settings. Although the ~3370 cm^{-1} peak was not studied here, the 600 and 1058 cm^{-1} peaks in this carving suggested that it belongs to an intermediate state in the amblygonite-montebrasite series.

Amblygonite-montebrasite is known from many localities, especially the United States and Brazil, but the client did not know the source of the carving. A few faceted samples have been examined at this laboratory, but the carving documented here was exceptional for its large size and transparency, despite its brittleness and tendency to crack.

Gagan Choudhary (gagan@gjepcindia.com)
Gem Testing Laboratory, Jaipur, India

Amethyst from Morocco: An update. Most major sources of fine amethyst are located in Africa. Yet African amethysts on the market, especially Zambian material, tend to be dark and difficult to find in sizes larger than 10 ct. Since the late 1980s, there have been additional discoveries in Malawi, Tanzania, Namibia, Nigeria, and the Democratic Republic of Congo. The most recent African source is Morocco (see Spring 2009 GNI, pp. 62–63), which has produced gem-quality amethyst with an appealing purple color and sizes larger than 10 ct.

GIA's Bangkok laboratory recently examined several parcels of gem-quality Moroccan amethyst (figure 71) received from Tom Banker, a colored stone dealer. Gemological properties obtained from the crystals and faceted stones were similar to those reported in the 2009 GNI entry.

Figure 71. These Moroccan amethyst crystals, which weigh 2.87 and 6.24 grams, display an attractive purple zoning conforming to the rhombohedral faces. Photo by Nuttaphol Kitdee.

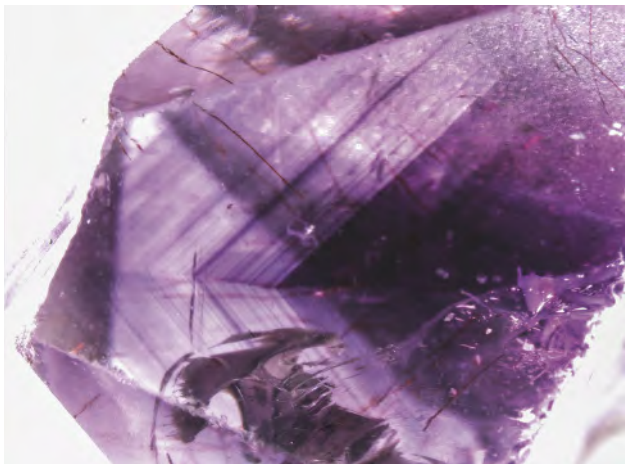

Figure 72. A closer view of the amethyst shows alternating bands of darker and lighter purple color zoning. Photo by Charuwan Khowpong; magnified 10×.

Common characteristic internal features were intense color zoning conforming to the rhombohedral faces (figure 72), reddish brown needle-like hematite inclusions (figure 73, left), and fingerprints consisting of two- and three-phase inclusions (figure 73, center). Dolomite and anhydrite inclusions were also found (figure 73, right).

A thin wafer with a thickness of 1.28 mm was prepared for FTIR and UV-Vis-NIR spectroscopy. The wafer plane was oriented parallel to the c-axis. The FTIR spectra were recorded using a Thermo Nicolet 6700 spectrometer with a resolution of 4 cm^{-1} and 200 scans, while the UV-Vis spectra were collected using a Hitachi U-2910 spectrometer at 1.5 nm slit width and 100 nm/min scan speed, integrated with a polarizer accessory controlled by Thorlabs APT.

FTIR spectroscopy revealed typical features of amethyst. The absorption peaks at 3585 and 3613 cm^{-1} were related to vibrations caused by Al substitutions. The absorption shoulder at 3595 cm^{-1} is common in natural quartz and rarely seen in synthetic quartz. The cause of this feature remains unknown (S. Karampelas et al., "Infrared spectroscopy of natural vs. synthetic amethyst: An update," Fall 2011 *G&G*, pp. 196–201). Areas of dark, medium, and light purple zoning had very similar FTIR patterns.

Amethyst owes its purple color to color centers associated with Fe^{2+} or Fe^{3+} impurities (A.J. Cohen, "New data on the cause of smoky and amethystine color in quartz," *The Mineralogical Record*, Vol. 20, No. 5, 1989, pp. 365–367). The UV-Vis-NIR absorption spectra showed bands in the visible range at 545 nm caused by Fe^{4+} charge transfer (E.H.M. Nunes, "Spectroscopic study of natural quartz samples," *Radiation Physics and Chemistry*, Vol. 90, 2013, pp. 79–86; E. Neumann, "Mechanism of thermal conversion of color and color centers by heat treatment of amethyst," *Neues Jahrbuch für Mineralogie, Monatshefte*, 1984, No. 6, pp. 272–282). The complexity of absorption bands in the ultraviolet region is related to the presence of Fe^{3+} in more than one environment in the α-quartz structure (F. Hassan and A.J. Cohen, "Biaxial color centers in amethyst quartz," *American Mineralogist*, Vol. 59, Nos. 7–8, 1974, pp. 709–718).

Further chemical analysis using advanced techniques such as EDXRF and ICP-MS will be conducted to summarize the characteristic chemical profile of the Moroccan material.

Ratima Suthiyuth
GIA, Bangkok

Dumortierite in rock crystal quartz. Dumortierite, which commonly occurs as a blue borosilicate mineral, is of gemological interest when present in quartzite, making an attractive blue ornamental material. Recently examined by GIA's Carlsbad laboratory were several examples of dumortierite inclusions in rock crystal quartz (figure 74) provided by Luciana Barbosa (Asheville, North Carolina). According to Mrs. Barbosa, the material is reported to be from the Brazilian state of Bahia, in the Serra do Espinhaço Range near the Vaca Morta quarry.

Much of the material examined by the authors showed phantom planes and clusters of acicular needles with a vibrant blue coloration (figure 75). Polarized light revealed

Figure 73. Microscopic examination of the Moroccan amethyst samples revealed reddish brown hematite (left), two-phase inclusions (center), and dolomite crystals (right). Photomicrographs by Charuwan Khowpong; magnified 50×, 5×, and 80×.

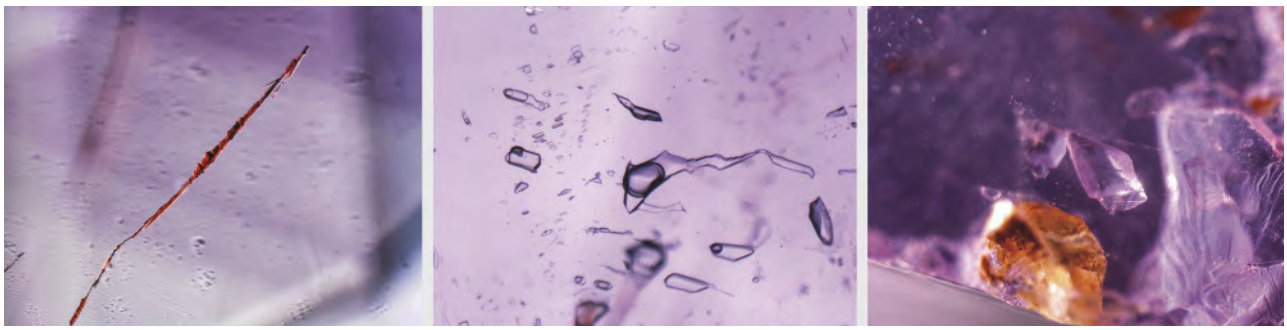

Figure 74. This group of rock crystal quartz from Brazil shows vibrant blue dumortierite inclusions. The largest rough crystal weighs 139.79 ct, and the faceted stone weighs 15.47 ct. Photo by Kevin Schumacher.

very strong blue to colorless pleochroism in the blue mineral inclusions. Raman analysis confirmed the identity of the needles as dumortierite. Also observed in one sample were colorless acicular crystals on a phantom plane, which were also identified by Raman as dumortierite (figure 76).

Blue color in dumortierite has previously been reported to be caused mainly by Fe^{2+}-Ti^{4+} charge-transfer (see http://minerals.gps.caltech.edu/FILES/Visible/dumortierite/Index.htm). The chemical composition of the blue and colorless dumortierite inclusions was analyzed by LA-ICP-MS to look for any prominent differences that might explain the variance in observed color. The most significant difference was in the magnesium content, which was almost 10 times higher in the colorless dumortierite inclusions (1070 ppma, compared to 127 ppma Mg in the blue dumortierite). While more research is needed to fully understand the role this higher magnesium content has on color, the authors speculate that the titanium preferentially charge-compensates with magnesium instead of iron. If there is not enough excess titanium relative to magnesium, it may not be possible for titanium to pair with divalent iron, and this would prevent the formation of blue color.

Figure 75. Clusters of vibrant blue acicular dumortierite were observed in this rock crystal quartz. Note that some dumortierite crystals are brownish due to epigenetic mineral staining along the interface of the quartz host and the dumortierite inclusions. Photomicrograph by Nathan Renfro; horizontal field of view 7.38 mm.

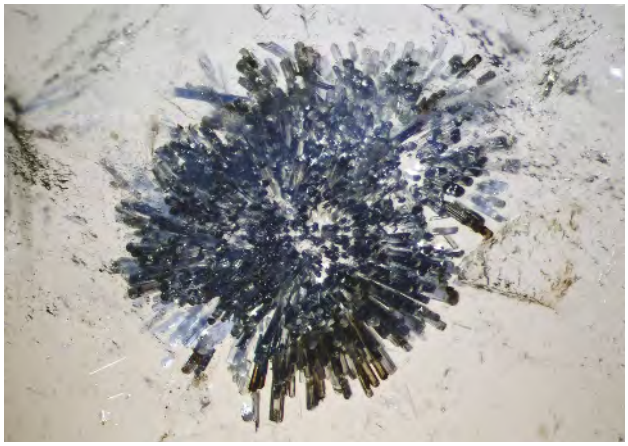

Figure 76. Unusual pale blue to colorless needles of dumortierite were also observed in the rock crystal quartz. Photomicrograph by Nathan Renfro; horizontal field of view 2.24 mm.

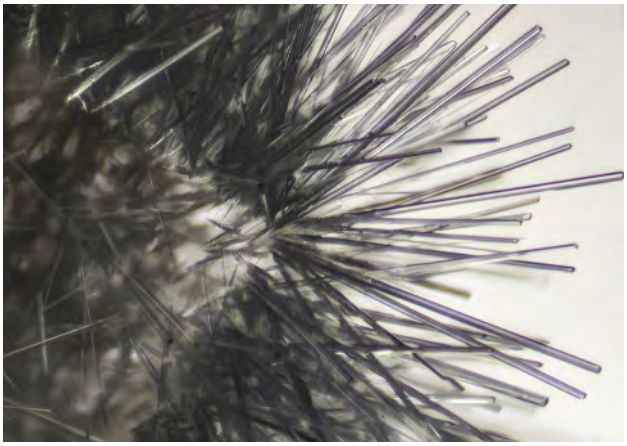

These are the first examples of prismatic blue and colorless dumortierite inclusions in rock crystal quartz we have encountered.

Nathan Renfro, Ziyin Sun, and John Koivula
GIA, Carlsbad

Jadeite with high albite content. With high prices and demand from Chinese consumers for jadeite jade (or *fei cui*), correctly identifying samples is a major challenge for gemological laboratories. Jadeite's complex mineral composition and its nature as a rock rather than a mineral further complicate this problem. While jadeite is the main mineral in jadeite jade, other pyroxene minerals such as kosmochlor, omphacite, amphibole-group minerals, plagioclase (especially albite), and even some iron oxides may also be present. Recently, the National Gold & Diamond Testing Center (NGDTC) lab tested 29 bangles submitted as jadeite jade (figure 77). The results again raised the issue of nomenclature.

The samples could be separated into two groups, one group with finer texture and color (shown on the left in figure 77). Standard gemological tests were applied to all of the samples, and the surface features were observed using a standard gemological microscope. The samples showed the characteristic 437 nm line with a handheld spectroscope. Ten randomly chosen spot RI readings were recorded on each bangle, and the results offered interesting insights. Two different readings of 1.52 and 1.66 were observed, indicating the presence of two major components. The SG ranged from 2.99 to 3.34, while the referenced SG for jadeite jade is 3.34 (+0.06–0.09). The low SG indicates a significant amount of light minerals in these samples. Another observation was that the group of lesser luster and color (shown on the right in figure 77) tended to have lower SG than the higher-quality samples. Overall, most of the samples were inert to UV, though six showed weak to moderate unevenly distributed bluish fluorescence. Under 30× magnification and brightfield illumination, two major mineral groups with contrasting color, crystal shape, and luster were revealed (figure 78).

Figure 77. These 29 bangles were submitted to NGDTC by a wholesaler as jadeite jade. The bangles in the left column are slightly finer and of better color. Photo by Li Jianjun.

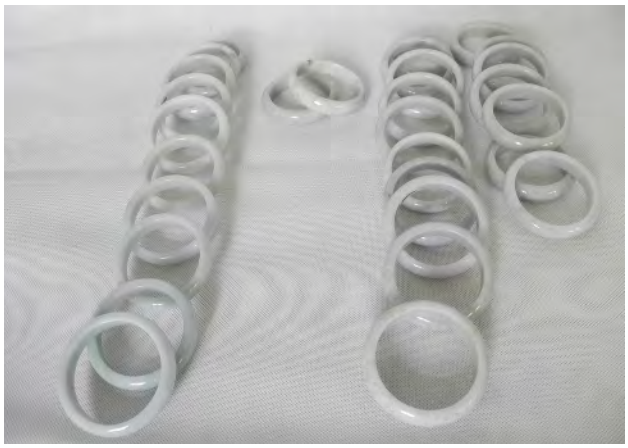

Figure 78. Two groups of minerals were observed on the surface of this sample under brightfield illumination. One group is composed of the pale whitish subhedral to euhedral grains, the other of the creamy minerals in between. Photomicrograph by Li Jianjun; magnified 30×.

Transmission infrared spectra collected from the positions that fluoresced weakly to moderately showed no polymer-related features. To confirm the composition of the two major minerals, we collected micro-infrared reflectance spectra from them (figure 79). The spectrum of the pale whitish mineral indicated jadeite, with the presence of the featured 1050 and 744 cm^{-1} bands in addition to the four bands between 400 and 600 cm^{-1}. The IR spectrum of the creamy mineral matched that of albite, with the characteristic peak at 1040 cm^{-1} band assigned to the Si-O stretching vibration in the SiO_4 tetrahedral structure. The multiple peaks in the 800–700 cm^{-1} region can also help to distinguish albite from jadeite.

The spot RI readings around 1.52 were consistent with albite's published RI of 1.528–1.542. The SG of albite is 2.60–2.65, considerably lower than that of jadeite. The presence of albite as a major mineral component in this material could account for the much lower SG in most of the samples. Although albite is one of the common minerals in jadeite jade, the amount is usually very minor and cannot be easily detected by standard gemological tests. Because the lab could not destroy the samples, no quantitative data were achieved.

Identifying these materials is not easy, especially when the concentration of certain components cannot be quantitatively determined and there is no trade standard on the boundaries for the different varieties. This study serves as a reminder that in addition to the omphacite issue, the high concentration of albite in some goods is a potential problem facing laboratories. To better protect consumers, the NGDTC recommends a clear statement regarding the pres-

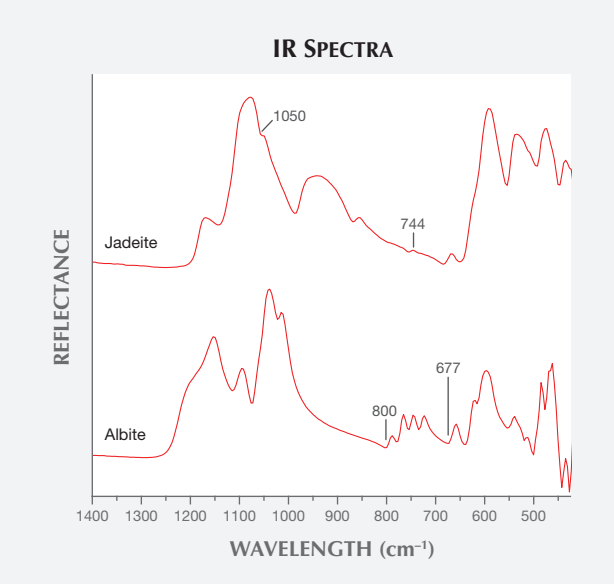

Figure 79. IR reflectance spectra collected from the two main minerals in the samples identified one as jadeite and the other one as albite.

ence of albite on laboratory reports once the albite is identified by the standard gemological test especially according to refractive index, even by the FTIR spectrometer.

Li Jianjun, Luo Yuanfei, Liu Xiaowei, Yu Xiaoyan, Li Guihua, Fan Chengxing, and Ye Hong
National Gold & Diamond Testing Center, Jinan City, China

Moldavites: natural or fake? Tectites are members of a large group of impact glasses, formed by the collision of a meteorite on the Earth's surface and the subsequent melting of surrounding rocks. The most famous tectites used as gemstones are moldavites from southern Bohemia in the Czech Republic. These were formed by a meteorite's impact in the Ries crater in southern Germany 14.7 million years ago, about 500 km from their occurrence (V. Bouška, *Moldavites: The Czech Tektites*, Stylizace, Prague, 1994). Moldavites are popular for their pleasant green color, enigmatic origin, and interesting etched texture. They are used in jewelry, in either faceted or natural form. The price of moldavite has risen in the last few years, and as a logical consequence imitations have become more widespread.

In fact, moldavite imitations are nothing new. Faceted moldavites were very popular in Czech jewelry during the second half of the 19th century, often with Czech garnets (chrome pyropes) or small river pearls. Their use diminished in the beginning of the 20th century when imitations made from green bottle glass began to appear. Nevertheless, the author's recent study of five moldavite sets (bracelet, brooch, and earrings) from the second half of the 19th century in the collection of the Museum of Decorative Arts in Prague revealed an unexpected result. Only one

Figure 80. Glass in a silver brooch, hallmark from 1866. Private collection, photo by Jaroslav Hyršl.

set contained moldavites—a donation to the museum by Olga Havlova, the first wife of Vaclav Havel, the late Czech author and statesman. All of the stones in the other four sets proved to be glass imitations. This means that glass imitations have been around decades longer than previously thought (figure 80).

Fortunately, the identification of faceted moldavite is simple. Besides their flow texture and abundant bubbles (almost always much more abundant than in an artificial glass), moldavites contain "wires" of lechatelierite, a high-temperature form of SiO_2. Lechatelierite is very easy to see with a loupe due to its lower RI.

The identification of moldavite with a natural-looking surface is much more difficult. Rumors of moldavite imitations from China have been circulating among Czech dealers for many years, but only recently has the author been able to study some examples (see figure 81). Two large moldavite imitations were seen in a high-end jew-

Figure 81. Two moldavites from southern Bohemia, Czech Republic (top row) and two recent imitations from China (bottom row). The natural specimen on the top right measures 44 mm across. Photo by Jaroslav Hyršl.

Figure 82. One of two huge moldavite fakes seen in Hanoi. Photo by Jaroslav Hyršl.

elry shop in Hanoi during the 2013 International Gemmological Conference (figure 82). Their size was astonishing, because very few real moldavites weigh more than 100 g. Their shape was also too perfect, making them easy to recognize.

Chinese producers are now manufacturing small stones weighing just a few grams that are very realistic. The surface feature of natural moldavite is caused by natural etching, and an almost identical feature can be created artificially, likely in hydrofluoric acid. If the stone in question has a polished surface, the presence or lack of lechatelierite "wires" (figure 83, top and bottom) is the best diagnostic tool, along with refractive index (table 1). For rough, immersion in water or especially oil with a similar RI is very helpful to reveal lechatelierite. Imitation moldavite also has a different density, UV-Vis absorption spectrum (figure 84), and fluorescence (again, see table 1). The color of natural moldavites is caused by very low concentration of iron; all other tectites are more Fe-rich and therefore black. Fluorescence is particularly helpful because it may be used on large mixed lots. Some imitations are not fluorescent, however. One imitation seen by the author several years ago was not fluorescent, but its very high specific gravity of 3.60 immediately ruled out natural moldavite.

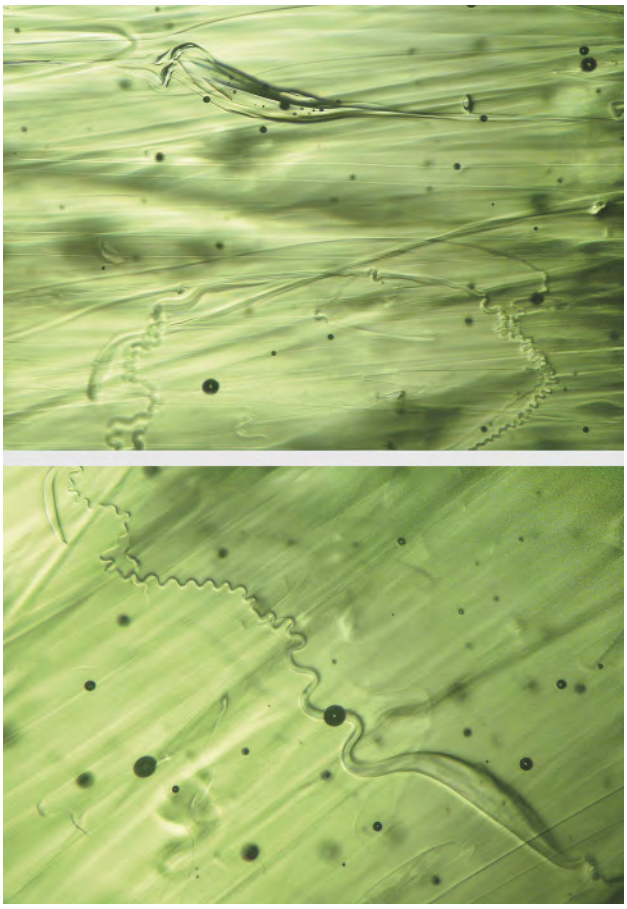

Figure 83. Typical bubbles and inclusions of lechatelierite in natural moldavite; image width 5 mm. Photomicrograph by Jaroslav Hyršl.

Jaroslav Hyršl (hyrsl@hotmail.com)
Prague

Iridescent scapolite. GIA's Carlsbad laboratory recently examined two cabochons from L. Allen Brown (All That Glitters, Methuen, Massachusetts) that exhibited prominent

TABLE 1. Characteristics of natural and imitation moldavite.

	Moldavite	Chinese imitations	19th-century glass imitations
Color	Light green to brown	Light green	Light green
RI	1.490 (1.480–1.510)	1.520	1.545–1.580
Density	2.35 (2.27–2.46)	2.52–2.53	n.a.
Fluorescence	Inert in UV	Chalky in short-wave UV	Inert in UV
Absorption spectrum	Minimum at 550 nm	Maxima at 460 and 640	n.a.

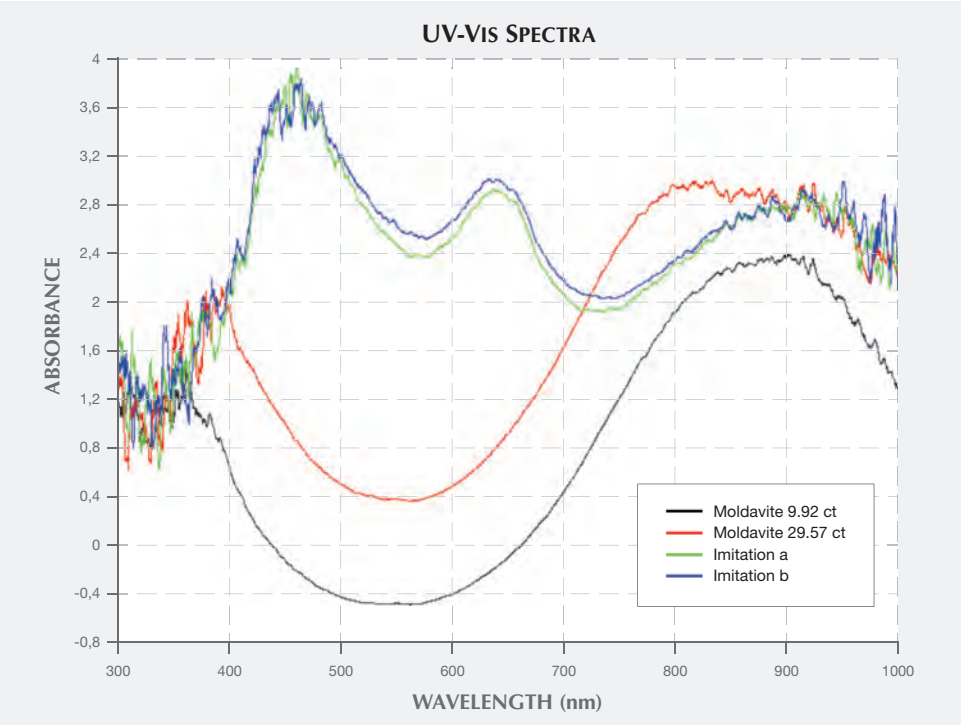

Figure 84. Absorption spectra of natural moldavite (black and red lines) and imitations (green and blue lines).

iridescence in reflected light (figure 85). Standard gemological testing of the 7.30 and 32.22 ct specimens revealed a spot RI of 1.55 and a hydrostatic specific gravity of 2.67. Fluorescence was inert to long- and short-wave UV light. The stones also showed a very weak reaction to a strong magnet.

Under magnification, the most distinctive internal characteristic was the presence of dark brown exsolution stringers of a secondary mineral. Larger tabular dark brown crystals were also observed (figure 86, left). Under reflected light, these exsolution stringers proved to be the source of the iridescent colors (figure 86, right). Similar material has been reported to occur in India, by G. Choudhary (Spring 2013 GNI, pp. 58–59), but the identity of the phenomenon causing inclusions was not determined.

Raman spectroscopy confirmed that the stones were scapolite. To identify the color causing inclusions, the smaller stone was selected for destructive testing. Windows were polished to expose some of the inclusions to the

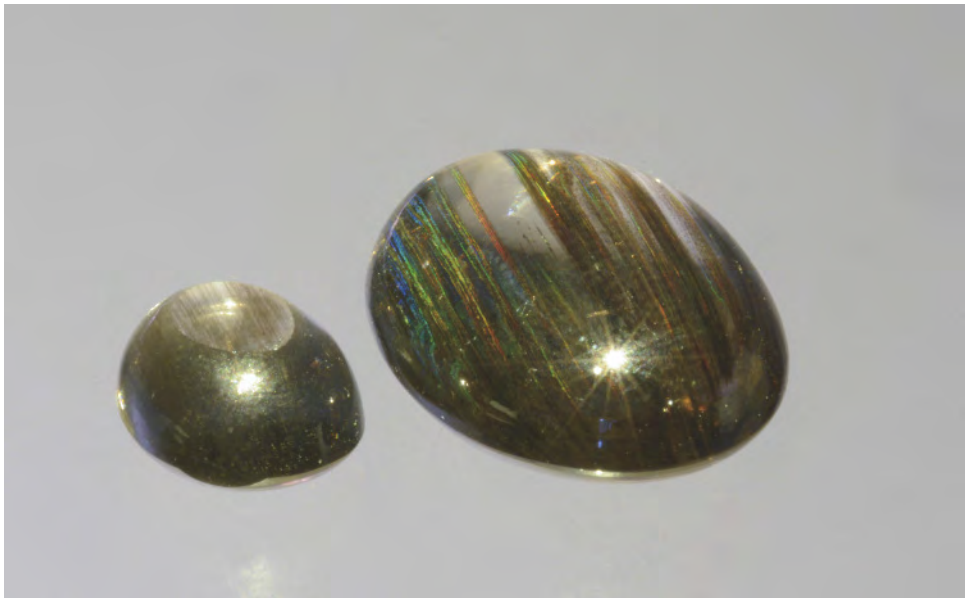

Figure 85. These two scapolite cabochons (7.30 and 30.22 ct) displayed prominent iridescence in reflected light. Photo by Don Mengason.

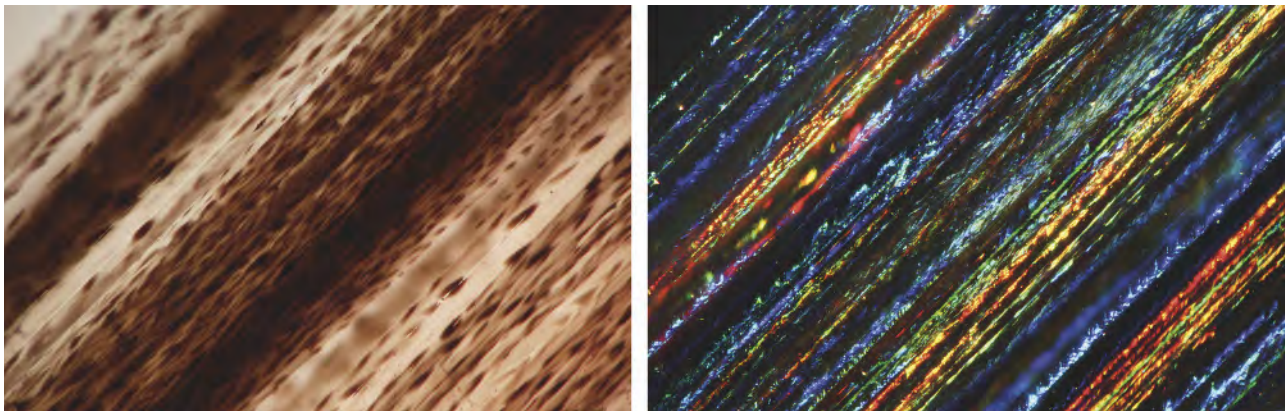

Figure 86. Dark brown exsolution stringers of magnetite (left), also viewed with oblique fiber-optic illumination (right), were the source of iridescence in this scapolite. Photomicrographs by Nathan Renfro; field of view 4.37 mm.

surface of the stone. The exposed surface of the inclusion showed a metallic luster (figure 87), which was identified as magnetite by Raman spectroscopy, and was explanatory of the magnetic reaction observed.

Laser ablation–inductively coupled plasma–mass spectrometry (LA-ICP-MS) analysis was used to further support the identity of the inclusions. While the exposure of the inclusions on the stone's surface was too small for a clean analysis without a contribution from the scapolite host, the results showed a significant increase in iron as the laser ablated through the brown inclusion and decreased afterward.

Scapolite occurs in a number of rock types as a product of regional metamorphism or metasomatism. The close association of magnetite with scapolite has been noted before, particularly in some skarn deposits and some hydrothermally altered volcanic formations (J.A. Naranjo et al., "Subvolcanic contact metasomatism at El Laco Volcanic Complex, Central Andes," *Andean Geology*, Vol. 37, 2010, pp. 110–120). Choudhary reported similar material, but the inclusions that caused the iridescence were not identified. This scapolite with iridescence, also known in the trade as rainbow scapolite, is a very interesting example of a phenomenal gemstone.

Ziyin Sun, Nathan Renfro, and Aaron C. Palke
GIA, Carlsbad

Figure 87. Under reflected light, the exposed surface of the inclusion showed a metallic luster. Photomicrograph by Ziyin Sun; field of view 0.25 mm.

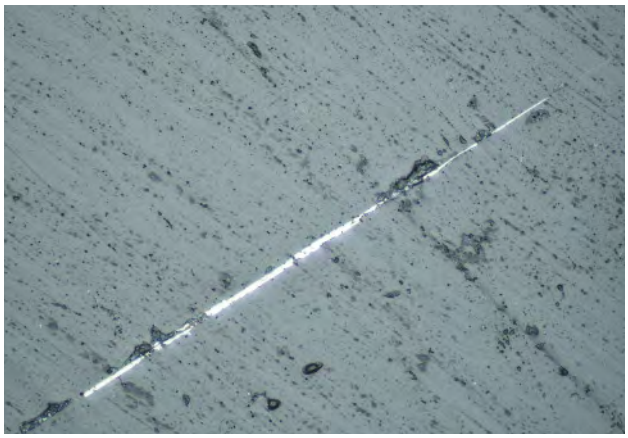

Attractive composite quartz beads. The Gem Testing Laboratory in Jaipur recently received a 145.70 carat string of attractive blue and golden brown spherical beads (figure 88) measuring approximately 7.91–8.48 mm in diameter. The beads were readily identified as artificial by their appearance, which consisted of metallic golden brown veining and concentrations of blue color against a whiter body. Further tests were performed to identify the blue areas.

The measured RI was approximately 1.54. The beads displayed a patchy chalky blue reaction to short-wave UV

Figure 88. This string weighing 145.70 carats consists of attractive blue and golden brown beads measuring approximately 7.91–8.48 mm in diameter. The beads were identified as composites fashioned from pieces of dyed quartzite held in a polymer matrix. Photo by Gagan Choudhary.

Figure 89. Color concentrations of blue dye were easily visible along the fractures against a white background, while the golden brown areas were composed of copper-zinc based fine flakes. Also note the greenish polymer along the edge of the golden brown and blue areas. Photomicrograph by Gagan Choudhary; magnified 48×.

and were inert to long-wave UV. Their Chelsea filter reaction was red, and under the desk-model spectroscope they displayed a band at approximately 650 nm. Under magnification, the blue areas displayed fluid inclusions that gave the beads a cloudy effect. In addition, the abundant fractures showed the presence of dye (figure 89) that was responsible for the beads' blue color. Such features are commonly observed in dyed quartzite, but these were not sufficient to prove its identity. The golden brown areas, which consisted of fine flakes (again, see figure 89) held in a soft polymer, were later identified by EDXRF spectroscopy as copper and zinc composites. Similar composites in which the components are held together in a polymer matrix have been known in the trade for several years now (see G. Choudhary, "A new type of composite turquoise," Summer 2010 *G&G*, pp. 106–113). Also present were thick layers of polymer along the edges of the blue and golden brown areas, which appeared green due to the overlap of the blue dye with the golden flakes. Raman spectroscopy confirmed that these blue portions were quartz.

Recognizing these beads as composites was straightforward, but identification of the components required Raman and EDXRF spectroscopy. Although these beads were obviously created to offer something fancy and attractive to consumers at a low price, clear and complete disclosure remains imperative.

Gagan Choudhary (gagan@gjepcindia.com)
Gem Testing Laboratory, Jaipur, India

SYNTHETICS AND SIMULANTS

CVD synthetic diamond with unstable color centers. The Indian Gemological Institute – Gem Testing Laboratory, New Delhi recently examined a 1.42 ct (7.06–7.08 × 4.49 mm) round brilliant. Viewed perpendicular to the pavilion facets with its table down, the sample displayed a grayish yellow color, but a slight rotation changed the color to pinkish. On viewing the specimen parallel to the direction of the growth planes, the sample appeared grayish yellow; viewing perpendicular to these same planes, the sample appeared pinkish.

Infrared spectroscopy showed features typical for type IIa diamond. Magnification revealed no internal features except for a feather on the girdle and the two growth planes, which appeared textured. There are very fine pinpoint-like inclusions lying just along the planes (figure 90, left). These planes of pinpoints were also visible from the table (figure 90, right). Examined in the DiamondView

Figure 90. Left: These growth planes were observed in a CVD synthetic diamond; fine pinpoints were found along the growth planes. Photomicrograph by Meenakshi Chauhan; magnified 30x. Right: Pinpoints along the growth plane were also visible from the table. Photomicrograph by Meenakshi Chauhan; magnified 10×.

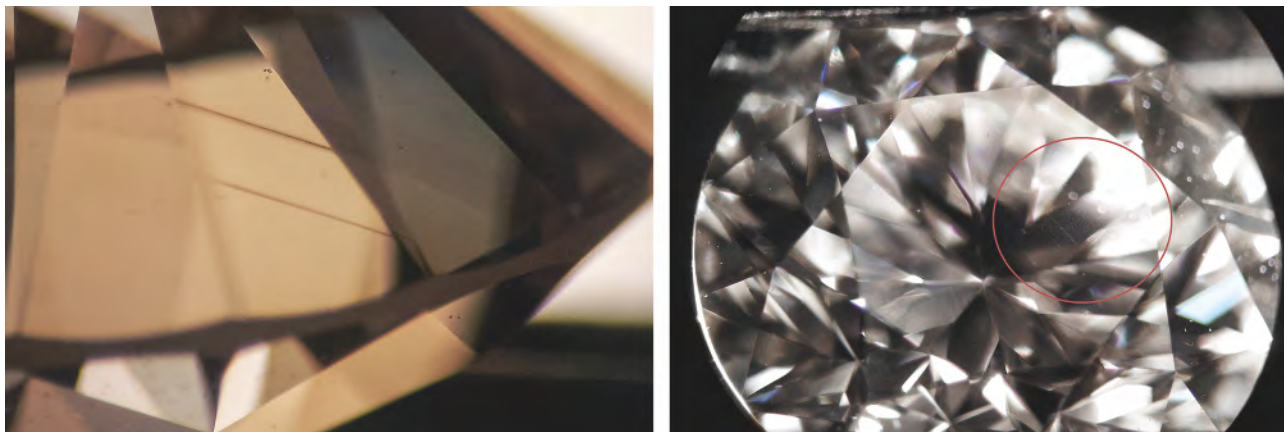

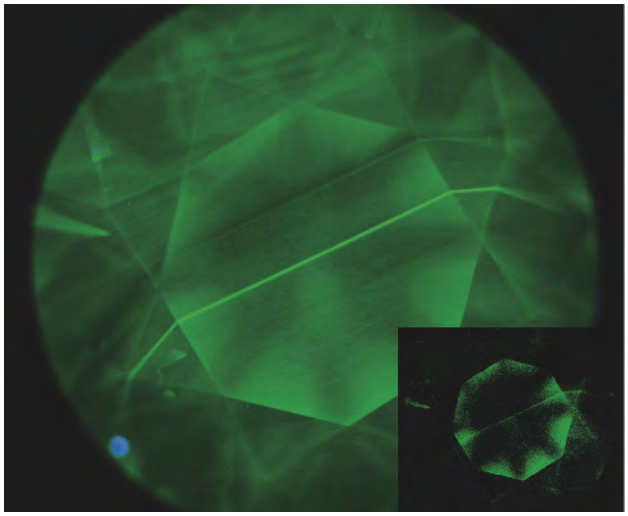

Figure 91. In the DiamondView, the 1.42 ct round showed striations typical of CVD growth. Notice the two parallel planes fluorescing stronger than the bulk of the crystal. The sample also showed moderate phosphorescence (inset), another indication of CVD growth. Images by Meenakshi Chauhan.

(using less than 225 nm short-wave UV radiation) to reveal its growth patterns, the round brilliant showed parallel striations indicative of CVD growth (figure 91). It also exhibited moderate phosphorescence under the UV lamp for approximately 20–25 seconds. (figure 91, inset), confirming synthesis by a CVD process.

Upon removal from the DiamondView after approximately two minutes of exposure time, it showed a distinct grayish blue color. After exposure to a 100-watt halogen bulb for about three minutes, the synthetic diamond regained its initial color (figure 92).

This process was repeated, and the sample turned a grayish blue color after a single minute of exposure to the short-wave UV radiation of the DiamondView and regained its initial color in approximately one minute under the halogen light.

UV exposure produced unstable color centers in this CVD synthetic diamond, which gave it a grayish blue color. Heat removed the color centers, restoring the CVD synthetic diamond to its initial grayish yellow color.

Meenakshi Chauhan (meenakshi@gjepcindia.com)
Indian Gemological Institute – Gem Testing Laboratory

INSTRUMENTS AND TECHNIQUES

The Foldscope and its gemological applications. The Prakash Lab of Stanford University, a small team of graduate students led by bioengineering professor Manu Prakash, has created a portable paper microscope called the Foldscope. Originally conceived for disease detection in remote areas, it was later expanded for educational use. The concept of the Foldscope won a $100,000 grant from the Gates Foundation in 2012 and a $50,000 first prize from the 2014 Moore Foundation Science Play and Research Kit Competition, which challenges participants to reinvent scientific tools of the past to attract a new generation of scholars. Speaking at the annual TED Conference in March 2014, Dr. Prakash announced that the concept was prototyped, functional, and could be manufactured for less than $1 each.

Submissions were accepted for a beta test group (now closed) named the "10,000 Microscope Project." The goal was to get a Foldscope in the hands of 10,000 users worldwide, in medical and non-medical fields. The project requested users who understood microscopy and agreed to write detailed scientific studies based on their own research, to be collected and published to show the variety of potential uses. Seeing a major application in field gemology, this author requested and received a Foldscope.

Beta testers received Foldscope components and instructions in December 2014. The body is made of a mate-

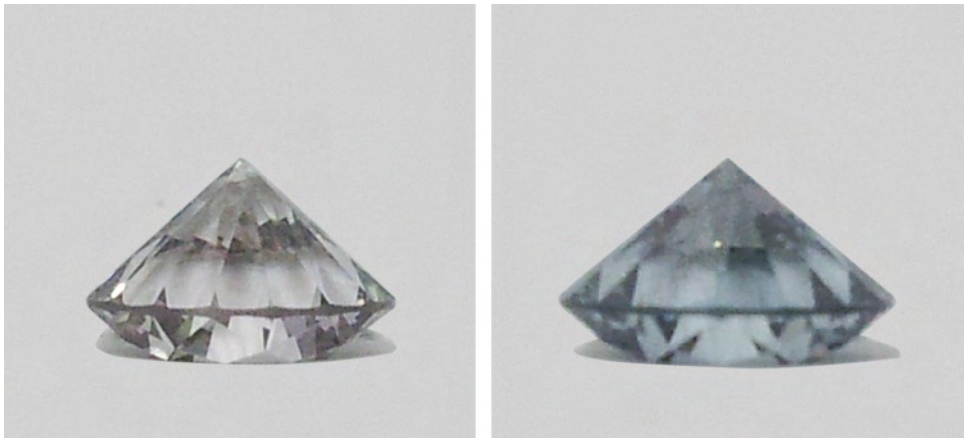

Figure 92. The CVD synthetic diamond before (left) and after exposure (right) to the short-wave UV radiation of the DiamondView. Photos by Meenakshi Chauhan.

Figure 93. A fully assembled Foldscope measures approximately 7 × 2.5 in. A toggled LED light source is tucked into tabs on the back, and the bottom center slit accommodates standard glass microscope slides. Photo by Kate Pleatman.

rial more like plastic than paper, to prevent tearing. Pieces are punched out of perforated sheets and assembled like origami (figure 93). The kit also contained interchangeable low-magnification (140×) and high-magnification (400×) lenses, a 3V LED toggled light source, and a surprise: a coupler to connect to a cell phone for photomicrography. Due to its complexity, assembling the Foldscope may take an hour or two. The device was ingeniously constructed, but would it work with gems?

Stones between 1 and 3 mm could be mounted onto glass slides for study. Larger stones were held with gem tweezers in the slide opening, to test whether the Foldscope would work with loose stones as well. Stones that were transparent and relatively small produced impressive results. The use of a binder clip to hold the slide or tweezers in place freed the hands to manipulate the focus more precisely. Focusing was the biggest obstacle, and late in the research the author inadvertently scratched a lens while trying to focus on a 1 mm corundum culet.

It was possible to clearly distinguish between natural and synthetic stones, because the magnification levels were exceptional (figures 94–96). Yet the small fixed size of the slide opening made it difficult to use with loose stones in tweezers, and gems more than 8 mm in depth could not pass enough light to view. Opaque material was not visible at all.

Research details, photos, and feedback were sent to the Prakash Lab, along with design recommendations for making the device more ideal for gemological use. Suggestions included protection for the lens to prevent scratching

Figure 94. This photomicrograph of synthetic opal, taken using the high-magnification lens (400×), shows the characteristic cellular mosaic appearance. Photomicrograph by Kate Pleatman.

Figure 95. These fluid inclusions in quartz were taken using the Foldscope's low-magnification lens (140×). Photomicrograph by Kate Pleatman.

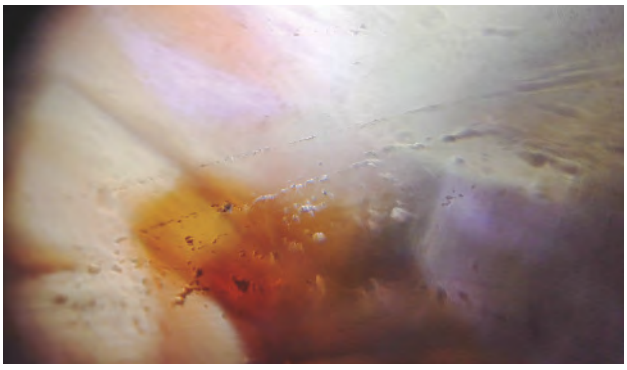

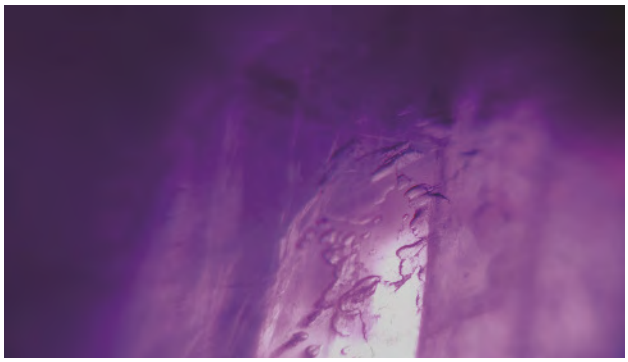

Figure 96. These liquid inclusions in ruby are seen using the low-magnification lens (140×). Photomicrograph by Kate Pleatman.

and a larger gap for examining non-slide materials such as loose stones held with tweezers. An optional three- or four-inch fiber-optic light attachment would offer illumination from any angle, even for mounted stones. The Foldscope team has been very attentive to the feedback, although they have not committed to any alterations. Time will tell if the suggested modifications are feasible. No public release date or final price for the existing version has been announced. For more on this tool, visit www.foldscope.com.

Kate Pleatman
Facets & Frosting
Cincinnati, Ohio

Sri Lankan heat treater Master Simon displays his copy of the Fall 2014 G&G. *The issue's cover featured him heating a star ruby using an old-fashioned blowpipe technique. Photo by Vincent Pardieu.*

For More on Tucson 2015

Explore the emerging trends, unique pieces, and production updates from this year's gem shows. GIA's coverage from Tucson provides an exclusive look at the gem and jewelry industry through video interviews and photo galleries.

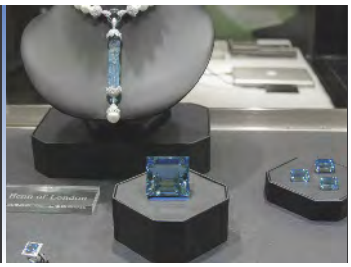

Visit www.gia.edu/gems-gemology/spring-2015-gemnews-tucson-2015-overview, or scan the QR code on the right.